REGENERATION AND PLASTICITY OF DESCENDING MOTOR PATHWAYS FOLLOWING SPINAL CORD INJURY

by

Brett Jason Hilton

B.A., The University of British Columbia, 2010

B.Sc., The University of British Columbia, 2010

A THESIS SUBMITTED IN PARTIAL FULFILLMENT OF

THE REQUIREMENTS OF THE DEGREE OF

DOCTOR OF PHILOSOPHY

in

THE FACULTY OF GRADUATE AND POSTDOCTORAL STUDIES

(Zoology)

THE UNIVERSITY OF BRITISH COLUMBIA

(Vancouver)

December 2016

Abstract

Spinal cord injury (SCI) results in paralysis due in part to the inability of central nervous system (CNS) axons to regenerate following their transection. However, after anatomically incomplete SCI, partial spontaneous recovery can often occur. I studied the regeneration and plasticity of descending pathways involved in forelimb motor function following SCI to better understand the mechanisms underlying axon regeneration failure and spontaneous motor recovery.

In Chapter 2, I developed an injury model in adult mice that results in complete axotomy of the rubrospinal tract and sustained deficits in forelimb motor function. I found that when a left dorsolateral funiculus crush injury was instigated at vertebral level C4, there were sustained deficits in left forelimb function while when the same injury was instigated at vertebral level C6, there was spontaneous recovery in left forelimb function to baseline levels.

In Chapter 3, I used the injury model developed in Chapter 2 in conditional PTEN KO mice to test the hypotheses that 1) PTEN deletion promotes rubrospinal axonal regeneration following SCI and 2) Aging significantly diminishes the regenerative capacity of PTEN deleted rubrospinal neurons. I found that when PTEN was deleted within rubrospinal neurons in 4 week old mice, there was significant rostral axon growth and regeneration past the lesion site to ~1 mm relative to controls. However, when PTEN was deleted within rubrospinal neurons in 7-8 month old mice, while rostral axon growth occurred, there was no caudal regeneration. Thus, there is an age-dependent decline in regeneration of CNS neurons.

In Chapter 4, I used optogenetic and chemogenetic tools to assess motor cortical plasticity in adult mice. I found that following ablation of the dorsal corticospinal tract, the motor cortex is able to re-establish output to the limbs and the minor dorsolateral corticospinal tract representing 3% of direct spinal cord transmission is able to partially mediate spontaneous recovery.

Taken together, these data demonstrate an age-related decline in axon regeneration in the adult mammalian CNS and show that a minor corticospinal pathway is necessary for spontaneous recovery following SCI.

Preface

The majority of the work presented in this dissertation has been peer-reviewed and accepted by internationally recognized scientific journals.

The work presented in chapter 2 has been published as: **Hilton BJ**, Assinck P, Duncan G, Lo S, Lu D, Tetzlaff W. (2013). Dorsolateral funiculus lesioning of the mouse cervical spinal cord at C4 but not at C6 results in sustained forelimb motor deficits. **Journal of Neurotrauma** 30(12), 1070-1083.

In Chapter 2, I conducted or supervised all of the animal work in this study including all the behavioural assessments and histological assessments. I performed the stereotaxic tracing surgeries, data analysis, wrote the manuscript, and oversaw experiments design. Peggy Assinck performed a blinded assessment of mice on the cylinder task. Greg Duncan performed a blinded assessment of mice on the CatWalk task. Stephanie Lo performed a blinded assessment of mice on the Horizontal Ladder task. Daniel Lu helped cryosection spinal cord tissue. Wolfram Tetzlaff supervised this project, performed dorsolateral funiculus crush injuries, edited the manuscript, and helped with experimental design.

The work presented in chapter 3 has been published as: Geoffroy G*, **Hilton BJ***, Tetzlaff W, Zheng B. (2016). Evidence for an Age-Dependent Decline in Axon Regeneration in the Adult Mammalian Central Nervous System. Cell Reports 15 (2), 238-246. *co-first author.

In Chapter 3, I conducted or supervised all of the animal work in this study including all histological assessments. I performed stereotaxic viral injections, fluorescence microscopy, data analysis, co-wrote the manuscript, and oversaw experimental design. Wolfram Tetzlaff

supervised the project, performed dorsolateral funiculus crush injuries, edited the manuscript, and helped with experimental design. Cedric Geoffroy and Binhai Zheng performed work contributing to the manuscript that is not part of this thesis. This work was conducted with the approval of the University of British Columbia Animal Care Committee.

The work presented in chapter 4 has been published as:

Hilton BJ, Anenberg E, Harrison TC, Boyd JD, Murphy TH, Tetzlaff W (2016) Re Establishment of Cortical Motor Output Maps and Spontaneous Functional Recovery via Spared Dorsolaterally Projecting Corticospinal Neurons after Dorsal Column Spinal Cord Injury in Adult Mice. **The Journal of Neuroscience** 36 (14): 4080-4092.

In Chapter 4, I conducted all of the animal work in this study. I performed cortical chronic window implantations, dorsal column spinal cord injuries, and optogenetic motor mapping. I performed the data analysis on optogenetic motor maps, wrote most of the manuscript, and oversaw experimental design. Eitan Anenberg and Thomas Harrison provided consultation on analyzing optogenetic motor mapping data. Jamie D. Boyd wrote new data analysis software to analyze the optogenetic motor mapping data. Timothy H. Murphy supervised the optogenetic mapping experiments and co-wrote the manuscript. Wolfram Tetzlaff supervised the behavioural/pharmacogenetic experiments and co-wrote the manuscript.

Certificate of approval:

The animal studies presented in this thesis were performed with ethics approval from the University of British Columbia Animal Care Committee (certificates #A09-0741 and A12-0120) and the University of British Columbia Biosafety Committee (certificate #B15-0004).

Table of Contents

List of Figures

List of Abbreviations

4E-BP - Eukaryotic translation initiation factor 4E-binding protein

AAV - Adeno-associated virus

Aldh1L1 - aldehyde dehydrogenase 1 family member L1

AMP - Adenosine monophosphate

BDA – Biotinylated dextran amine

CBP - CREB binding protein

ChAT – Choline acetltransferase

ChR2 – Channelrhodopsin 2

CNO – Clozapine *N*-oxide

CNS - Central nervous system

CREB - cyclic AMP response element-binding protein

CS-56 - Chondroitin sulphate 56

CSPG - Chondroitin sulphate proteoglycan

CST - corticospinal tract

DLF - Dorsolateral funiculus

DNA - Deoxyribonucleic acid

DREADD - Designer receptor exclusively activated by designer drugs

EC - Euriochrome Cyanine

FL - Forelimb

GFAP - Glial fibrillary acidic protein

GFP – Green fluorescent protein

GSK3 - Glycogen synthase kinase 3

HM4Di - human muscarinic M4 Gi-coupled DREADD

HL - Hindlimb

ICMS – Intracortical microstimulation

IGF – Insulin growth factor

JAK - Janus kinase

KLF - krüppel-like factor

M1 – Primary motor cortex

MAG - Myelin-associated glycoprotein

MAI - Myelin associated inhibitor

mTOR – Mechanistic target of rapamycin

NeuN - Neuronal nuclei

NG2 - neural/glial antigen 2

NgR1 - Nogo receptor 1

OMgp - Oligodendrocyte myelin glycoprotein

P53 – phosphoprotein p53

PBS – Phosphate buffered saline

PCAF - p300/CBP-associated factor

PI3K - Phosphatidylinositol-4,5-biphosphate 3 kinase

PKCy – Protein kinase C gamma

PNS - Peripheral nervous system

PTPσ - Protein tyrosine phosphatase sigma

PTEN - Phosphatase and tensin homolog deleted on chromosome ten

RGC - Retinal ganglion cell

RST – Rubrospinal tract

S6K1 - Ribosomal protein S6 kinase beta-1

SCI - Spinal cord injury

Sox9 - Sex determining region Y box 9

STAT - Signal Transducer and Activator of Transcription

Thy1 - Thymocyte differentiation antigen 1

YFP – Yellow fluorescent protein

Acknowledgments

First and foremost, I would like to thank my supervisor and mentor, Professor Wolfram Tetzlaff. I can't thank Wolf enough for providing such a great learning environment for me to conduct my PhD in. The Tetzlaff Lab has been a place where I've been able to explore my own ideas and to develop as an independent scientist. Wolf's door was always open to me, and his passion, integrity, and intellect will continue to provide a model for me throughout the rest of my career.

Second I would like to extend my heartfelt thanks to Professor Timothy Murphy who allowed me the great opportunity to perform a series of experiments using optogenetic motor mapping in his laboratory and provided key intellectual mentorship to me throughout my PhD. Dr. Murphy took a chance in allowing me to work in his lab and I am very grateful as it provided an introduction to optogenetics and allowed me to see how a different (and highly productive) neuroscience lab operates first-hand. In this regard, I would like to acknowledge the contributions of Eitan Anenberg, Dr. Thomas Harrison, and Dr. Gergely Silasi, the motor mappers, who provided much help with my project and great feedback on my work.

I would also like to thank Dr. Cedric Geoffroy and Professor Binhai Zheng from the University of California – San Diego, who proved to be excellent collaborators for the work presented in Chapter 3. Our interactions enriched my understanding of intrinsic axon regeneration a great deal and the process of writing the PTEN manuscript with them was a tremendous learning experience.

Thank you also to my other two committee members, Professors Tim O'Connor and Matt Ramer. In addition to providing great feedback on my work during my committee meetings, these two provided help in other ways. Professor Ramer contributed particularly early on during my PhD with his insights during a weekly journal club. Professor O'Connor proved to be my favorite lecturer during NRSC 500 and upper level CELL courses. I learnt a great deal about teaching from him. Thank you both for being part of this.

The Tetzlaff Lab has been an excellent environment for me to train. This has occurred in no small part due to the citizens of our lab. Thank you especially to Greg Duncan and Peggy Assinck. Through the highs and lows of the PhD program, these two were wonderful colleagues and friends. You're both excellent scientists and part of the joy of science for me in the years ahead will be to see what important contributions you'll both surely make. Dr. Jason Plemel and Dr. Joseph Sparling were senior graduate students when I started who have provided much guidance for me. Thank you both for your time and mentorship. Thank you also to the graduate students in the lab for the discussions and ideas: Doug Brown, Sohrab Manesh, Simon Bedard, Aaron Moulson, and Nathan Holmes. Thank you to the great support staff in the Tetzlaff lab without whom this work would not have been possible: Nicole Janzen, Jie Liu, Yuan Jiang, and Clarrie Lam. I'd also like to thank the undergraduates who have helped me with these projects: Daniel Lu, Shahrzhad Khahait, Namrta Vashisht, and Stephanie Lo.

I would like to thank my parents, Jane and John Hilton, and my brother, Shane, for their love and support throughout the years. It wasn't always obvious that this day would come, but they have supported me steadfastly throughout the years and always been a phone call away. I would also like to thank Thea Van Rossum, who has been a rock for me throughout this PhD and without whom I doubt this would have been possible.

Finally, I would like to thank the funding agencies that supported this work (The Canadian Institutes of Health Research, Wings for Life Foundation, and International Spinal Research Trust) and the individuals with spinal cord injuries that these agencies represent. I believe that treatments for spinal cord injury are just around the corner, and I hope that the work described here turns out to contribute meaningfully to the development of these treatments.

Chapter 1. General introduction

1.1 Introduction overview

The spinal cord is a region of the CNS that extends from the medulla oblongata of the brain stem to the lumbar region of the vertebral column (Kandel et al., 2000). It is a key site of transmission of neural signals from the brain to the rest of the body and vice-versa, and in this regard, a central conduit for descending pathways from the brain that control movement and sensory pathways to the brain that transmit all peripheral sensation below the neck(Kandel et al., 2000). Following damage or injury to the adult mammalian CNS, limited recovery typically occurs (y Cajal, 1928). A major reason for this is that the adult mammalian CNS is unable to effectively regenerate lost neurons and axons (y Cajal, 1928). As such, spinal cord injury (SCI) typically results in life-long deficits in motor and sensory function below the level of injury (Curt et al., 2008; Steeves et al., 2011). While considerable advances in the surgical and medical management of SCI have been made, to date, no therapeutic intervention that effectively restores lost neurologic function has been developed.

The central focus of this thesis is the regeneration and plasticity of descending motor pathways following SCI. Descending motor pathways harbour cell bodies in many different regions of the brain, including the cortex, midbrain, and brain stem (Kandel et al., 2000). These neurons project axons to the spinal cord and play a major role in the orchestration of movement by controlling the activity of premotor spinal interneuronal networks or by

synapsing directly onto motor neurons (Kandel et al., 2000). Following SCI, axon regeneration failure of descending motor pathways is a key contributor to sustained paralysis of muscles controlled by circuits below the level of injury. However, despite this failure, some recovery of neural control of movement can occur when SCI is anatomically incomplete (i.e. when the spinal cord is not completely severed). This recovery process is poorly understood but believed to rely at least in part on the reorganization or plasticity of spared or uninjured pathways. Thus, in addition to studying axon regeneration of descending motor pathways, I also focused on this form of plasticity in Chapter 4.

This introduction reviews the major topics pertinent to Chapters 2, 3, and 4. I begin by describing a definition of axonal regeneration and its experimental evidence. Then, I overview the major mechanisms of axon regeneration failure in the adult mammalian CNS, with a particular focus on the role of PTEN/mTOR as the deletion of PTEN in rubrospinal neurons was used to study rubrospinal axon regeneration in Chapter 3. I then describe the general organization of the adult mammalian motor system with a focus on the orchestration of forelimb movement and the descending motor pathways that are a focus of this thesis, the corticospinal and rubrospinal tracts. I describe what is known about plasticity in these descending pathways following SCI. Then, I provide a brief overview of optogenetic and pharmacogenetic techniques that were central methodologies employed in this thesis. At the end, I provide an experimental overview and a statement of the major hypotheses that drove this work.

1.2 Axon regeneration failure in the adult mammalian CNS

1.2.1 A definition of axon regeneration

As denoted previously, axon regeneration failure is a principal mechanism underlying sustained paralysis following SCI. A tremendous amount of research is being performed and has been performed detailing the mechanisms underlying this regeneration failure and strategies that might be conducive to promoting regeneration following SCI. But what is axon regeneration anyway? In this thesis, I will use the term axon regeneration to denote axon outgrowth from a neuron that has had its axon transected, which is consistent with the definitions described by Steward, Zheng, Tuszynski, and Geoffroy (Steward et al., 2003; Tuszynski and Steward, 2012; Geoffroy and Zheng, 2014). This definition stands in contrast to "axon sprouting", which is axonal outgrowth from uninjured neurons in response to injury (Tuszynski and Steward, 2012). Methodologically distinguishing between regenerating and sprouting axons is important, because while regeneration failure is the norm in the adult mammalian CNS, axon sprouting associated with partial spontaneous recovery of function can occur (Weidner et al., 2001; Bareyre et al., 2004; Ballermann et al., 2006; Courtine et al., 2008; Takeoka et al., 2014). Demonstrating that regeneration has occurred requires either a) the utility of an injury model that completely transects a pathway of axons, and/or b) the use of a technology that permits the re-construction of an axon back to its point of transection, such as three-dimensional imaging of unsectioned tissue (Ertürk et al., 2012; Chung et al., 2013) or in vivo imaging of live axons (Laskowski and Bradke, 2013; Gomis-Rüth et al., 2014; Lorenzana et al., 2015). If an injury model does not completely transect a pathway of

axons, or the axon cannot be re-constructed back to its point of transection, it remains possible that sprouting, and not regeneration, has occurred, based on the possibility that the axon has been "spared" from injury (Steward et al., 2003). Demonstrating regeneration, as opposed to sprouting, of rubrospinal axons following SCI, was the principal motivating factor behind the development of the dorsolateral funiculus crush injury model in Chapter 2 and its application in Chapter 3. In cases where it is unclear whether "regeneration" or "sprouting" has occurred, I use the term "axon growth" as an umbrella term encompassing both.

Although axon regeneration failure in the adult mammalian CNS is extremely complex, conceptually, researchers have divided the mechanisms of this failure into two broad categories: mechanisms that are extrinsic to the axon, and those that are intrinsic.

1.2.2 Extrinsic mechanisms of axon regeneration failure

Extrinsic mechanisms of axonal regeneration failure can be broadly defined as those arising "outside" the neuron or its axon. This includes substrate deficiencies in the injured spinal cord as well as the presence of cells or expression of molecules that inhibit regeneration from occurring. The concept that extrinsic inhibition of axon growth is a primary facture underlying regeneration failure derives originally from F. Tello and Santiago Ramon y Cajal, who found that central axons could grow into predegenerated peripheral nerve segments (y Cajal, 1928). This idea was famously revisited by Aguayo, Richardson, David, and colleagues, who demonstrated that spinal central axons are capable of long distance axonal

growth into peripheral nerve grafts (Richardson et al., 1980; David and Aguayo, 1981; Richardson et al., 1984). Although a detailed discussion of the mechanisms underlying extrinsic inhibition are outside the confines of this introduction, I provide an overview of several of the major ones: cavitation/substrate deficiencies, CNS myelin associated growth inhibitors, and the scar/associated extracellular matrix molecules.

1.2.2.1 Cavitation/substrate deficiencies

Cavitation commonly occurs in cases of human SCI and is a general characteristic of rat and monkey contusion SCI (Basso et al., 1996; Norenberg et al., 2004; Beattie et al., 2015). Such cysts are filled with extracellular fluid, and are an unsuitable substrate for axonal growth (Norenberg et al., 2004). In mouse SCI, cavitation does not occur, because pericyte-derived stromal cells form connective tissue that seals the injured tissue (Göritz et al., 2011).

1.2.2.2 CNS myelin

In the 1980s, Martin Berry postulated that the presence or absence of CNS myelin might be sufficient to explain cases where regeneration fails or succeeds, respectively. He noted that cases of successful regeneration in the mammalian CNS, such as in the early fetal CNS, occurred when axons were non-myelinated (Silver, 2010). Thereafter, the laboratory of Martin Schwab conducted a series of seminal experiments demonstrating that sensory neuron neurite outgrowth is inhibited by central, but not peripheral, myelin (Schwab and Caroni, 1988), that myelin is comprised of specific axon growth inhibitory factions (Caroni and Schwab, 1988), and that antibody targeted towards blocking the function of one of these

inhibitory factions can promote CNS axon growth (Schnell and Schwab, 1990). By the early 2000s, several growth inhibitory molecules present in adult myelin were identified, including Nogo (Chen et al., 2000; GrandPré et al., 2000; Prinjha et al., 2000), MAG (McKerracher et al., 1994), and OMgp (Wang et al., 2002b). Since then, various receptors for these MAIs and intracellular signaling pathways underlying their influence on the axon have been identified (Fournier et al., 2001; Wang et al., 2002a; Yiu and He, 2003; Park et al., 2005; Yiu and He, 2006).

Although a significant amount of research has been devoted to myelin axonal growth inhibition, whether it is a primary mechanism underlying central axon regeneration failure remains unclear. For example, Zheng and colleagues have found no evidence of axonal regeneration following genetic knockout of Nogo (Zheng et al., 2003), NgR (Zheng et al., 2005), or even Nogo, MAG, and OMgp together (Lee et al., 2010). In contrast, the groups of Schwab and Strittmatter have generally reported modest regeneration from knockout of MAIs (Kim et al., 2003; Simonen et al., 2003; Kim et al., 2004; Cafferty et al., 2010). The disparity may relate to differences in transgenic mouse lines, injury models, or, as noted above, whether axons are “sprouted” or “regenerated”(Woolf, 2003; Silver, 2010). In this regard, it is interesting to note recent work that has highlighted targeting MAIs as a means of promoting uninjured neuronal rewiring and shown functional benefits following CNS injury (Wahl et al., 2014; Siegel et al., 2015; Fink and Cafferty, 2016b).

1.2.3.3 The astroglial scar and extracellular matrix

In addition to myelin and substrate deficiencies, another major mechanism of extrinsic axon growth inhibition is the development of a scar around the lesion site (Cregg et al., 2014). Although initially considered principally made of reactive astrocytes, the scar is in fact comprised of a multitude of interacting cell types, including NG2 glia, fibroblasts, ependymal cells, and inflammatory cells (Meletis et al., 2008; Barnabé-Heider et al., 2010; Göritz et al., 2011; Soderblom et al., 2013). SCI causes leukocyte extravasation and inflammatory cell accumulation in the lesion core (Popovich et al., 1997; Popovich et al., 2002). Thereafter, astrocytes migrate from the inflammatory epicenter to form a scar at the penumbra of the lesion. There is limited astrocyte proliferation following SCI and the total density of astrocytes in lesioned tissue is 2-4 fold that of uninjured tissue (Ertürk et al., 2012). Reactive astrogliosis is characterized by large swelling of astrocytes in addition to their substantial upregulation of the intermediate filament proteins vimentin, nestin, and GFAP (Bignami and Dahl, 1976; Barrett et al., 1981; Yang et al., 1994). The glial scar is an important endogenous response to SCI: it restricts secondary damage following injury by limiting the extent of inflammatory cell loss and axonal degeneration (Faulkner et al., 2004; Sabelström et al., 2013). However, the glial scar is also a considerable impediment to regeneration because many of the cell types that comprise the scar express extracellular matrix molecules that are inhibitory to axon growth (Davies et al., 1997; Davies et al., 1999; Busch and Silver, 2007), such as CSPGs (Bradbury et al., 2002; Jones et al., 2002; Jones et al., 2003a) and KSPGs (Jones and Tuszynski, 2002; Imagama et al., 2011; Hilton et al., 2012). One principal mechanism through which CSPGs inhibit axon growth is by binding the axonal receptor PTPσ (Lang et al., 2015). When axonal growth cones expressing PTPσ bind

CSPGs for an extended period of time, excessive ligand/receptor binding leads to the conversion of the growth cone into an overly adhered and dystrophic state that precludes regeneration (Lang et al., 2015).

1.2.4 Intrinsic mechanisms of axonal regeneration failure

1.2.4.1 Overview of intrinsic mechanisms

In contrast to extrinsic mechanisms, intrinsic mechanisms of axon regeneration failure relate to the diminished growth capacity of adult mammalian central neurons, particularly after axotomy (Tetzlaff et al., 1991; Liu et al., 2011). For example, primary sensory neurons are pseudounipolar in morphology, with a single axon that bifurcates into two processes, one of which projects peripherally and the other, centrally (Ranvier, 1889). After peripheral axotomy, regeneration can occur, while after central axotomy, there is regeneration failure, consistent with the differential regenerative capacity of the CNS and the PNS. However, if a primary sensory neuron's peripheral process is axotomized, the regenerative response invoked can promote central axonal regeneration following the central process' axotomy (Richardson and Issa, 1984; Neumann and Woolf, 1999), even if the peripheral axotomy occurs well after the central axotomy (Ylera et al., 2009). This demonstrates that the differential regenerative capacity of peripheral versus central processes of primary sensory neurons is at least partially intrinsic to the neuron and not wholly related to the different environments of the two processes. In this regard, peripheral neurons are capable of a coordinated gene expression program that underlies their successful regeneration following

peripheral nerve injury (Lindner et al., 2013; He and Jin, 2016). Intrinsic growth potential is related to the capacity of the neuron to form a growth cone at the distal tip of the axon (Bradke et al., 2012), to successfully signal injury to the cell body (Plunet et al., 2002; Rishal and Fainzilber, 2010), and to surmount a regenerative response involving coordinated expression of regeneration-associated genes (Liu et al., 2011; Tedeschi, 2012; He and Jin, 2016).

1.2.4.2 Intrinsic VS. extrinsic: an oversimplification?

It is worth noting that the divide between "extrinsic" and "intrinsic" mechanisms of axonal regeneration failure is an oversimplification. For example, extrinsic mechanisms of regeneration failure rely at least partially on the expression of receptors for specific environmental blockades to growth (Shen et al., 2009; Schwab, 2010; Dickendesher et al., 2012) which can be considered intrinsic in nature while neurons with an "intrinsically high growth capacity" require suitable substrates for axon regeneration to occur as noted above. One of the earliest strategies successfully targeting intrinsic axon growth following SCI was the administration of trophic factors (Tetzlaff et al., 1994), which can promote regeneration associated gene expression and rubrospinal axon growth into peripheral nerve grafts (Kobayashi et al., 1997b).

1.2.4.3 PTEN: an intrinsic determinant of axon regenerative potential

Recent work has begun to elucidate the intracellular signaling pathways that underlie the capacity of central neurons to mount a significant regenerative response following injury. In

a seminal series of experiments, the laboratory of Dr. Zhigang He tested the hypothesis that genes that evolutionarily control cell growth and/or size are major impediments to regeneration. Therefore, they assessed whether genetic deletion of such genes could promote regeneration in the optic nerve, a common model of CNS regeneration failure(Park et al., 2008). Of the genes tested, PTEN showed the most significant effect on optic nerve regeneration: PTEN deleted RGCs harbor a capacity to regenerate ~3 mm, and PTEN deletion approximately doubles survival of RGCs following axotomy(Park et al., 2008). Because an investigation of PTEN deletion in promoting rubrospinal regeneration following SCI was carried out in this thesis, I provide a more thorough characterization of its role in axon regeneration below. However, it is important to note that PTEN is far from the only gene involved in the intrinsic regenerative response and various other signal transduction cascades have been implicated, including CREB (Gao et al., 2004), JAK/STAT3 (Smith et al., 2009), CBP/p300/PCAF-p53 (Tedeschi et al., 2009; Gaub et al., 2010; Gaub et al., 2011), and members of the KLF family of transcription factors (Moore et al., 2009; Blackmore et al., 2012).

1.2.4.4 PTEN: basic intracellular function and overview

PTEN is a tumour suppressor gene and a dual protein and lipid phosphatase, although its lipid phosphatase function is stronger (Backman et al., 2002; Chow and Baker, 2006). Intracellularly, cytoplasmitc PTEN directly dephosphorylates phosphatidylinositol (3,4,5)-triphosphae (PI3K) into phostadilyinositol (4,5)-biphosphate. In doing so, PTEN antagonizes activity of the PI3K/Akt/mTOR growth pathway. Upon its genetic deletion, the cell has no other gene to compensate for the loss of PTEN (Yamada and Araki, 2001). In addition to this

cytoplasmic function, PTEN also harbours a variety of nuclear roles, including chromosome stability, DNA repair, cell cycle arrest, and cellular stability (Planchon et al., 2008). PTEN is also one intracellular mediator of growth-cone collapse (Chadborn et al., 2006).

1.2.4.5 PTEN's role in axon growth in both the CNS and PNS

Since the seminal discovery that PTEN deletion promotes optic nerve regeneration (Park et al., 2008), there have been additional reports supporting the hypothesis that it is a general regulator of axonal growth in both the CNS and PNS. PTEN deletion or inhibition promotes corticospinal (Liu et al., 2010; Zukor et al., 2013; Lewandowski and Steward, 2014; Danilov and Steward, 2015) and rubrospinal (Geoffroy et al., 2016) axon regeneration. PTEN deletion also promotes compensatory sprouting of uninjured corticospinal neurons (Liu et al., 2010; Lee et al., 2014). Following peripheral nerve injury, inhibition of PTEN accelerates peripheral axon regeneration (Christie et al., 2010) and regeneration of diabetic peripheral axons (Singh et al., 2014b). Finally, PTEN deletion also promotes axon regeneration in both drosophilia (Song et al., 2012) and c elegans (Byrne et al., 2014b). Thus, PTEN inhibits axon regeneration in multiple organisms, branches of the mammalian nervous system, and pathways within the adult mammalian CNS.

1.2.4.6 How does PTEN inhibit axon regeneration?

How PTEN deletion promotes axonal regeneration remains poorly understood but recent work has implicated activity in the PI3K/Akt/mTOR pathway as being of central importance (Park et al., 2010). In the original paper on the role of PTEN in optic nerve axonal

regeneration, it was found that systematic treatment with the mTOR inhibitor rapamycin following optic nerve injury in PTEN deleted mice almost completely abolished the regenerative response (Park et al., 2008). Thus mTOR activity is of central importance in PTEN deletion mediated axon regeneration. More recent work has focused on the downstream effectors of mTORC1, S6K1 and 4E-BP, that have differential effects on regeneration (Yang et al., 2014a). More specifically, S6K1 activation is sufficient to promote axon regeneration but 4E-BP inhibition is not. Interestingly, while 4E-BP inhibition is not sufficient to drive optic nerve regeneration, it is necessary for PTEN-deletion mediated axon regeneration, demonstrating that both S6K1 and 4E-BP activity are likely mediators of the effect of PTEN deletion on regeneration. Still, mTOR is not the only downstream effector of PTEN deletion mediated axonal regeneration. PTEN may be directly involved in axon regeneration inhibition given its role in Sema3a-mediated growth cone collapse(Chadborn et al., 2006). In addition, GSK3 activity is inhibited by the kinase's phosphorylation by Akt (Cross et al., 1995). Given its role in regulating axonal outgrowth (Seira and Del Río, 2014), GSK may be an additional effector through which PTEN deletion promotes axonal regeneration.

1.2.4.7 Age and PTEN

Although PTEN is an important factor in axon regeneration, it is important to note that the majority of studies in mice occur with its deletion or inhibition at a very young age. In the studies on PTEN's influence on optic nerve and corticospinal regeneration, the enzyme's deletion occurred with AAV-Cre injection into floxed PTEN mice between postnatal day 1 up to 4 weeks of age (Park et al., 2008; Liu et al., 2010). The lifespan of the C57/Bl6 mouse

is ~24 months (Storer, 1966) with sexual productivity dropping rapidly at the age of 7-8 months. Thus, whether PTEN deletion remains effective in promoting regeneration at older adult ages remains unknown. More generally, given the extremely limited regenerative capacity of adult central mammalian neurons even at young adult ages, whether aging from young to mid-adulthood influences axon regeneration outcomes is also unknown. In the context of SCI research, this is an important point, as the average age at the time of injury has increased significantly in the last two decades, from ~29 in the 1970s to ~42 since 2010 in the United States (National Spinal Cord Injury Statistical Center). This is mainly due to an increase in SCI from falls in an increasingly active elderly population, leading to a bimodal age profile (Singh et al., 2014). Determining the influence of aging on axon regeneration will be important for the development of effective regenerative therapies for spinal cord repair.

1.3 The motor system

1.3.1 General overview of the motor system

An understanding of how SCI results in sustained paralysis requires some background knowledge of how the CNS orchestrates movement. Ultimately, all muscle contractions are controlled by motor neurons and each skeletal muscle fiber is innervated by a singular motor neuron, such that the motor neuron and the skeletal muscle fibers it innervates comprise the motor unit (Sherrington, 1910). In turn, the firing patterns of motor neurons are orchestrated by a complex system of circuits that can generally be divided into three components. First, there are intraspinal networks of neurons with projections confined to the spinal cord that are

essential for the production of patterned motor activity (Jankowska, 2001; Kiehn, 2011). Second, supraspinal centers largely regionalized to the cortex and brain stem descend pathways that are intricately involved in the activation and regulation of intraspinal networks or of motor neurons directly (Alstermark et al., 1981; Lemon, 2008). Third, sensory systems provide constant feedback on the execution of motor behaviour (Rossignol et al., 2006; Windhorst, 2007). These three components acting together are able to orchestrate the enormous repertoire of motor behaviours that the adult human is capable of, from ballet dancing to piano playing to weight lifting and everything in-between. A major focus of this thesis is this second component: descending motor pathways. In particular, I focused on two descending motor pathways principally involved in forelimb (hand and arm) motor control: the corticospinal and rubrospinal pathways (**Fig. 1.1**).

Figure 1.1 Rubrospinal and corticospinal anatomy in the adult mouse. The rubrospinal tract descends via the dorsolateral funiculus. The corticospinal tract descends principally via the dorsal column (~96%) with minor components projecting via the dorsolateral funiculus (~3%) and the ventral column (~1%).

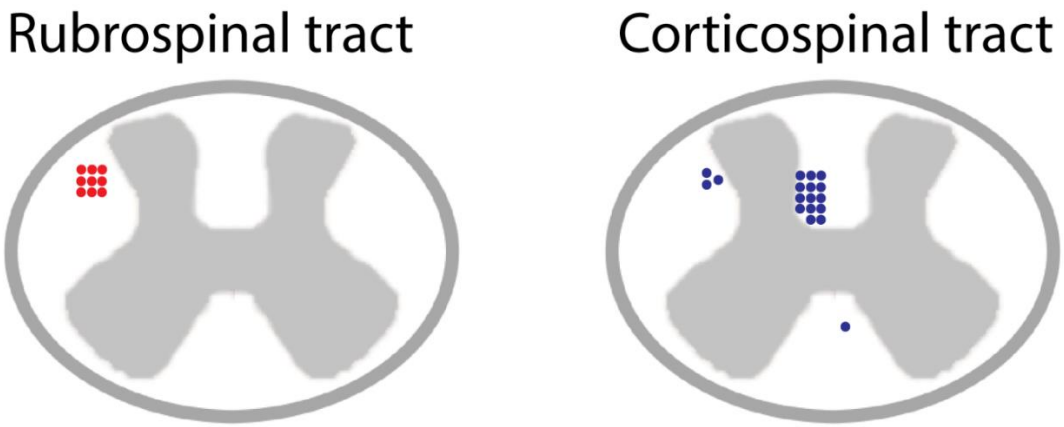

1.3.2 The corticospinal pathway

1.3.2.1 Corticospinal anatomy in primates

The term corticospinal is anatomical: it refers to any neuron that has a cell body residing in cortex that projects to the spinal cord. The corticospinal tract is the major or dominant descending pathway in primates (including humans), where it originates from a variety of motor cortical divisions (primary motor cortex, dorsal and ventral premotor cortices, supplementary motor area, and the cingulate motor areas) while ~40% arise from somatosensory areas of the parietal lobe (Dum and Strick, 1991; Galea and Darian-Smith, 1994; Rizzolatti et al., 1998; Lemon and Griffiths, 2005; Lemon, 2008). In the primate, most (~85-90%) corticospinal fibers cross the midline in the medulla and descend in the dorsolateral funiculus while ~10-15% descend ipsilaterally and in the dorsolateral or ventromedial funiculus (Liu and Chambers, 1964). In the spinal cord, corticospinal projections terminate throughout gray matter, with somatosensory cortex-derived corticospinal projections terminating mainly in the more dorsal spinal gray matter (Rexed laminae I-V) and the projections from M1 targeting most areas of the intermediate zone (Ralston and Ralston, 1985). In primates, corticospinal axons also target Rexed laminae IX, where they form monosynaptic connections with motor neurons that are considered to be particularly important in dexterous finger movements (Lemon and Griffiths, 2005; Courtine et al., 2007; Baker et al., 2015).

1.3.2.2 Corticospinal function in primates and anatomy/function in rodents

Given the many cortical areas from which corticospinal neurons originate, the corticospinal tract likely has a diversity of functions. The role of the corticospinal tract in motor behaviour has been gleaned using the pyramidotomy model of injury. At the level of the medulla, corticospinal fibers project in the pyramids, which are ventrally located white matter structures. As such, corticospinal input to the spinal cord can be abolished by transecting the pyramids (pyramidotomy) (Lawrence and Kuypers, 1968; Whishaw et al., 1993; Starkey et al., 2005; Lemon et al., 2012). It is important to note, however, that such lesions might also disrupt cortico-reticulospinal axons (Alstermark and Pettersson, 2015). Given the recently described role of a reticulospinal pathway from the medullary reticular formation ventral part in forelimb motor control (Esposito et al., 2014), it is possible that deficits in motor control resulting from pyramidotomies occur because of their disruption of reticulospinal connectivity.

Phylogenetically, the corticospinal tract is recently evolved (compared to the brain stem motor pathways) and its development coincides with the evolution of relatively independent finger movements (Heffner and Masterton, 1975; Heffner and Masterton, 1983). The classic work of Lawrence and Kuypers established the theory that corticospinal axons are particularly important for hand movements: lesions of the corticospinal system via bilateral pyramidotomy in the adult macaque resulted in permanent loss of independent movements of the digits (Lawrence and Kuypers, 1968). The corticospinal tract also likely makes an

important contribution to interlimb and intralimb coordination during basic locomotion, and to skilled movements of the foot, in the primate (Courtine et al., 2005). The functions of corticospinal neurons originating in somatosensory cortex and terminating in the dorsal horn of the spinal cord remain relatively poorly understood but are thought to include modulation of sensory input (Fetz, 1968; Lemon, 2008).

In the adult mouse, the anatomy and function of the corticospinal tract differs from the primate substantially. Approximately 99% decussate at the junction of the medulla and the rostral most area of the spinal cord, where ~96% then project via the dorsal column and ~3% via the dorsolateral funiculus. The remaining ~1% of corticospinal fibers project ipsilaterally via the ventral funiculus. The extent of corticospinal fibers projecting in the dorsolateral funiculus and ventral funiculus can vary somewhat from mouse strain to mouse strain and even from mouse to mouse. Corticospinal anatomy is similar in the adult rat but the ipsilateral ventral corticospinal tract is more prominent (Weidner et al., 2001). Corticospinal axons terminate in the dorsal horn and intermediate zone of the spinal cord in the adult mouse, with very few to no axons found within the vicinity of motor neurons in Rexed laminae IX in the uninjured spinal cord (Fink et al., 2015). Unilateral pyramidotomy to obstruct the corticospinal pathway results in deficits in forelimb function in a variety of behavioural tests (Starkey et al., 2005; Siegel et al., 2015), suggesting that corticospinal injury in the mouse can model aspects of the tract's function in humans. Similarly, in the adult rat, pyramidotomy impairs skilled reaching (Whishaw et al., 1993). The corticospinal tract has a limited influence on rodent locomotion (Starkey et al., 2005), but does function in

the placing response of the hindlimb in response to light touch of the dorsal skin of the foot (De Ryck et al., 1992).

1.3.3 The rubrospinal pathway

Like the word "corticospinal", "rubrospinal" is an anatomical term: it refers to any neuron with a cell body residing in the red nucleus that projects to the spinal cord. The red nucleus is a distinct cluster of neurons found in the midbrain. More than 98% of rubrospinal fibers decussate in the tegmentum and descend in the contralateral dorsolateral funiculus while the remaining 2% project in the ipsilateral dorsolateral funiculus (Brown, 1974a; Liang et al., 2012). Rubrospinal fibers terminate in the dorsolateral region of the intermediate zone, with some projecting to lateral motor nuclei innervating arm and hand muscles in rodents (Küchler et al., 2002). The anatomy of the rubrospinal tract makes it an advantageous model to study CNS axon regeneration. Because rubrospinal fibers project in the dorsolateral funiculus, the tract can be reliably transected by a dorsolateral funiculus injury while avoiding problematic axonal sparing (Steward et al., 2003; Ramer et al., 2004; Tuszynski and Steward, 2012; Hilton et al., 2013b; Geoffroy et al., 2016). Since rubrospinal fibers originate from a dense neuronal cluster in the midbrain, the red nucleus has been utilized as a model of the cell body response to axotomy (i.e. changes in cell body size and gene expression) with the advantage that changes that occur following axotomy can be related to the internal control of the other red nucleus that originates the uninjured rubrospinal tract (Tetzlaff et al., 1991; Tetzlaff et al., 1994; Kobayashi et al., 1997b; Fernandes et al., 1999; McPhail et al., 2004; Wannier-Morino et al., 2008; Geoffroy et al., 2016).

The function of the rubrospinal tract may vary considerably from rodent to non-human primate to human. Importantly, the rubrospinal tract may be weak or absent in human (Nathan and Smith, 1955; Onodera and Hicks, 2010). Instead, most efferent fibers from the red nucleus in human project to the olivary body (Nathan and Smith, 1982). Some researchers have argued, therefore, that its study in preclinical SCI regeneration experiments in rodents is less clinically relevant than the corticospinal system (Tuszynski and Steward, 2012). The function of the rubrospinal tract in motor control is inferred from studies where the pathway is injured in the spinal cord (through dorsolateral funiculus injuries) or from lesioning or ablating the red nucleus. In each of these cases, injury is not specific to rubrospinal neurons: dorsolateral funiculus injury will injure spinal cord neurons and glia local to the injury site and axons that might descend or ascend in this area of the spinal cord while red nucleus injury will disrupt rubral neurons that project to other areas of the brain such as the olivary body. Dorsolateral funiculus injuries and red nucleus injuries both result in sustained deficits in forelimb motor function in the adult rat (Whishaw et al., 1998; Bretzner et al., 2008). Morris and Whishaw attempted to define a specific role for the rubrospinal tract in motor control by performing fractionated injuries of the dorsolateral funiculus that primarily disrupted rubrospinal fibers without disrupting additional pathways and found that the rubrospinal tract is likely more involved in arpeggio movements during skilled reaching (Morris et al., 2011). Red nucleus lesions also result in subtle deficits in overground locomotion in the adult rat (Muir and Whishaw, 2000). Whether dorsolateral funiculus injuries that completely axotomize the rubrospinal tract in adult mice impair forelimb motor function is unknown and was a major goal of the work of Chapter 2.

1.3.4 Plasticity in descending motor pathways following SCI

Despite the limited regenerative capacity of the adult mammalian CNS, spontaneous recovery of motor function can occur after both human SCI and in rodent models of injury. It is believed that spared or uninjured descending motor pathways harbour a capacity to "reorganize" in order to partially mediate this recovery (Raineteau and Schwab, 2001; Fink and Cafferty, 2016a). Understanding the mechanisms underlying this is important primarily for two reasons. First, the vast majority of SCIs are anatomically incomplete (Kakulas, 1999), although despite this, the majority of individuals with SCI are motor complete functionally (Sekhon and Fehlings, 2001; Jackson et al., 2004). Understanding how the CNS attempts to rewire circuits to mediate recovery may provide new targets for therapies. Second, strategies to promote axon regeneration are sometimes accompanied by a deficit in motor function (Takeoka et al., 2011; Wang et al., 2015). Overexpression of the transcription factor Sox11 in corticospinal neurons promotes their regeneration following SCI but also interferes with spontaneous recovery (Wang et al., 2015). Thus, regenerative therapies to be applied in the human situation will need to be done so in the context of understanding how spontaneous recovery occurs, such that these therapies do not interfere with it or promote it.

1.3.4.1 Recovery of stepping

The recovery of stepping in rodent SCI models has also provided glimpses into the plasticity of descending motor pathways. In rodent cervical and thoracic lateral hemisections (Courtine et al., 2008; Filli et al., 2011), staggered lateral hemisections of the left and right side at T7

and T12 (Courtine et al., 2008; Murray et al., 2010), and moderate thoracic contusion injuries (Basso et al., 1996; Schucht et al., 2002), recovery of stepping typically occur over the weeks after injury. Instead of necessitating spared supraspinal pathways that descend past the injury site, the recovery of stepping can be mediated by relay connections between supraspinal neurons and propriospinal neurons (Courtine et al., 2008). Indeed, reticulospinal and corticospinal neurons both harbour a capacity to form relay connections with propriospinal neurons in incomplete models of SCI such that long-distance regeneration of these pathways back to their targets may not be necessary to promote substantial motor recovery (Bareyre et al., 2004; Vavrek et al., 2006; Filli et al., 2014). The reorganization of descending pathways and propriospinal neurons to facilitate the recovery of stepping relies on muscle spindle afferent feedback: in Egr3 knockout mice that lack muscle spindle feedback, recovery of stepping and the reorganization of most descending pathways does not occur (Takeoka et al., 2014). The recovery of stepping also relies on changes in motor neuron excitability following injury. Motor neurons recover a capacity to produce sustained muscle contractions by expressing constitutively active isoforms of the serotonin receptor; a neurotransmitter that maintains motor neuron excitability (Murray et al., 2010). Thus, changes in motor neurons, intraspinal networks, and descending motor pathways, converge to generate an activity-dependent (Caudle et al., 2011) form of motor system plasticity that leads to the recovery of stepping following incomplete SCI.

1.3.4.2 Corticospinal plasticity in forelimb functional recovery

Despite its incapacity for regeneration, uninjured corticospinal neurons are capable of some sprouting following SCI that has been associated with recovery of forelimb function. In a

seminal study, Weidner and colleagues hypothesized that the minor ventral component of the corticospinal tract in adult rat that comprises ~1% of all corticospinal fibers could mediate forelimb motor functional recovery following injury to the dorsal component comprising ~96% of corticospinal fibers (Weidner et al., 2001). They performed focal injuries to the dorsal, ventral, or both, areas of the spinal cord at cervical level C1 in order to assess this. When injury occurred to only the dorsal or ventral components, spontaneous recovery of pellet reaching ability occurred. However, when both were injured, recovery did not occur. Following dorsal injury, traced ventrally projecting corticospinal neurons were found to increase contacts with ChAT-immunolabeled motor neurons, and this increase correlated with the recovery. This implies that a very small number of corticospinal neurons, perhaps less than 1% of the total, are able to partially mediate recovery. After lateral hemisection injury in the adult primate, uninjured corticospinal fibers are able to reconstitute ~60% of the pre-lesion axonal density based on their extensive decussation at each spinal level and this sprouting is associated with improvement in hand function, locomotion, and coordinated muscle recruitment (Rosenzweig et al., 2009; Rosenzweig et al., 2010). Despite this, a causal demonstration that uninjured corticospinal neurons mediate recovery has yet to occur.

1.3.4.3 Rubrospinal VS corticospinal plasticity

Although the CST is the primary descending pathway underlying voluntary movement in primates, evolutionarily, the RST is thought to be a functional predecessor to the CST and capable of functionally compensating for corticospinal fiber loss. To address this hypothesis, Kanagal and Muir performed bilateral pyramidotomies and dorsolateral funiculus crush injuries in adult rats either simultaneously or spaced out by 6 weeks (Kanagal and Muir,

2009). When spaced by a 6 week period, the combined injury lead to a greater loss of performance on a pellet reaching task then when the injuries were instigated simultaneously, suggesting that the pathways in the dorsolateral funiculus (including the rubrospinal tract) compensate for corticospinal loss. More recently, Siegel and colleagues demonstrated the formation of a *de novo* circuit between the red nucleus and the nucleus raphe magnus following bilateral pyramidotomy that is at least one pathway underlying spontaneous recovery of skilled locomotion (Siegel et al., 2015). Therefore, rubral neurons likely substantiate recovery of skilled forelimb function following corticospinal loss.

1.3.5 Discerning the role of specific neural circuits in motor behaviour before and after injury

As denoted, a causal demonstration that specific neural circuits have a role in motor function is a challenge. Traditionally the role of specific areas of the brain or pathways in motor function has been discerned by physically or chemically injuring these elements and assaying motor function on a behavioural task before and after the injury (Whishaw et al., 1998; Muir and Whishaw, 2000). Although this approach has provided substantial evidence that specific pathways mediate specific motor functions, there are significant caveats. Physical or chemical injury is never completely specific to particular neuronal subsets or a pathway. For example, the injury model that is developed in Chapter 2 (dorsolateral funiculus crush) was developed specifically to axotomize the rubrospinal tract but other pathways travel within this region of the spinal cord that might contribute to motor behavioural function, including the dorsolateral corticospinal tract (Steward et al., 2004) and reticulsopinal axons emanating from the medullary reticular formation ventral part that harbour a role in skilled forelimb

motor function (Esposito et al., 2014). Lesions also disrupt blood flow and result in glial responses to injury that might have off-target effects.

1.4 Optogenetics

1.4.1 Overview

Optogenetics refers to the use of light to control live cells that have been genetically modified to express light sensitive ion channels. To date, the most common light sensitive ion channel used is Channelrhodopsin-2 (ChR2) which is a green algae-derived, light activated cation channel (Nagel et al., 2005). When expressed in mammalian neurons, activation of ChR2 can lead to depolarization of sufficient magnitude that action potential firing occurs (Boyden et al., 2005). Thus, ChR2 expression permits millisecond timescale control of neurons (Deisseroth, 2011; Yizhar et al., 2011). With respect to expression in mammalian cells, light sensitive ion channels are typically targeted in one of two ways. First, viral vectors encoding ChR2 can be targeted to specific regions of interest within the adult mammalian CNS. Cre-inducible expression variants have also been developed that permit the targeting of specific neuronal-subtypes within a given area based on differences in anatomy. In this approach, in order for a neuron to successfully express the gene, it requires infection with two viruses. By varying the locations at which the viruses are administered, expression of the gene can be confined to neurons with specific anatomical projection. Second, cell-type specific promoters can be used to express ChR2 specifically in cells in which such promoters are active.

1.4.2 Benefits of optogenetics over traditional methods to map the motor cortex

In the context of mapping the motor cortex and assessing functional connectivity between it and the limbs, there are several advantages to using optogenetics over electrode-based stimulation methods. First, electrode-based brain stimulation methods are incapable of selectively targeting neuronal subtypes. More specifically, direct electrical stimulation activates all cellular components/cell types within the area of stimulation, including both antridomic and orthodromic activation of neurons (Lim et al., 2013). In contrast, optogenetic stimulation provides the opportunity to selectively activate specific cell types through genetic or viral targeting strategies. In the Thy1-ChR2 mice used in Chapter 4, there is robust expression of ChR2 in layer V of cortex but little to no expression in the other cortical layers (Arenkiel et al., 2007). Thus, laser stimulation leads to specific activation of layer V neurons, which is the output layer that includes corticospinal neurons. Second, ICMS requires impalement of the cortex with an electrode and the damage to the brain incurred whereas optogenetic mapping can be conducted non-invasively through the intact skull (Silasi et al., 2013a; Hilton et al., 2016; Silasi et al., 2016), making it better suited for longitudinal studies (Ayling et al., 2009b; Harrison et al., 2013; Hilton et al., 2016). Third, optogenetic mapping is much faster than electrical approaches to motor cortical mapping such that studies very early after injury (Anenberg et al., 2014b; Hilton et al., 2016) can be conducted and alterations in anaesthetic plane are less of an issue. Finally, optogenetic mapping allows stimulation of the motor cortex in a grid of equally spaced sites, allowing more uniform sampling (Ayling et al., 2009b).

1.4.3 Insights into motor cortex biology in health and disease from optogenetic mapping

Despite its relative youth as a technique, optogenetic mapping has already provided key insights into the basic biology of the motor cortex (Harrison et al., 2012) and how it responds to both stroke (Harrison et al., 2013; Xie et al., 2013; Anenberg et al., 2014b) and spinal cord injury (Hilton et al., 2016; Hollis II et al., 2016). Harrison and colleagues described a functional subdivision of mouse forelimb motor cortex based on the direction of movement evoked and showed that this topography likely related to segregated output projections (Harrison et al., 2012). Anenberg and colleagues demonstrated that despite a maintenance of motor cortical excitability within an hour of photothrombotic stroke, that motor output to the forelimb as measured via electromyogrphy was significantly impaired (Anenberg et al., 2014b). Harrison and colleagues also found a disorganization of motor cortex using longitudinal mapping following photothrombotic mini-stroke: decreased motor cortical output at the center of the infarcted area is offset by peri-infarct excitability (Harrison et al., 2013).

1.4.4 Optogenetic mapping before and after spinal cord injury

In addition to the work described in Chapter 4, the only other published work to date that has used optogenetic motor mapping following spinal cord injury is the work by Hollis and colleagues (Hollis II et al., 2016). Using the same transgenic mouse line (Thy1-ChR2), they assessed forelimb flexion and extension maps after a C5 dorsal column lesion. They found that training on a pellet reaching task resulted in the development of a forelimb flexor map into an area of cortex that was devoted to hindlimb movement prior to injury. In addition,

eliminating the Wnt receptor Ryk genetically or through the infusion of a function-blocking antibody enhanced recovery on the pellet reaching task.

1.5 Chemogenetics

1.5.1 Overview

In addition to optogenetics, the work in Chapter 4 employed a relatively new technique that falls under the umbrella of the term “chemogenetics”, which is a method in which proteins are engineered to interact with previously unrecognized small molecule chemical actuators(Sternson and Roth, 2014; Roth, 2016). Various classes of chemogeneticallly engineered proteins have been developed but the most widely used to date are Designer Receptors Exclusively Activated by Designer Drugs (DREADDs)(Armbruster et al., 2007). DREADDs are bioengineered G-protein coupled receptors. Similarly to optogenetics, DREADDs can be used to selectively manipulate the activity level of neurons. Unlike optogenetics, DREADDs do not use light to accomplish this. Instead, neurons that express DREADDs respond to ligands that generally do not activate other receptors within the body. A major advantage of DREADDs relative to optogenetics is that focal light stimulus is not required. Instead, the designer drug can be administered non-invasively via either intraperitoneal injection or through drinking water.

1.5.2 hM4Di and CNO

The specific DREADD employed in this work is hM4Di. This DREADD is one of three developed so far to inhibit neuronal activity(Roth, 2016). Activation of hM4Di following receptor/ligand binding appears to inhibit neuronal activity via two different mechanisms. First, hM4Di activation leads to activation of G-protein inwardly rectifying potassium channels, thus hyperpolarizing the neuron (Armbruster et al., 2007; Vardy et al., 2015). Second, hM4Di activation inhibits the presynaptic release of neurotransmitters (Stachniak et al., 2014). The receptor acts through these mechanisms to silence neurons from seconds to hours post ligand-binding (Roth, 2016). CNO is the bioengineered "designer drug" ligand for hM4Di that has no known endogenous (wildtype) receptor with the adult mammalian central nervous system. CNO is a pharmacologically inert metabolite of the antipsychotic drug clozapine. In addition to its pharmacological inertness, it is also behaviourally inert in mice and rats when administered in the range of doses recommended (0.1-3 mg/kg). It has excellent drug-like properties with rapid CNS penetration and residence in vivo of at least 60 minutes following intraperitoneal administration (Bender et al., 1994). Given this, following systemic administration in rodents, CNO-mediated hM4Di activation typically leads to neuronal silencing from seconds to 1-2 hours but not longer. In this way, we can assay behaviour following the administration of CNO to activate Hm4Di and silence specific neuronal populations and make comparisons within the same animal following vehicle administration such that each animal acts as its own control. DREADD receptor technology harbours the capacity to permit the silencing or activation of specific neuronal populations in a transient fashion and thus allow the discernment of their role in motor behaviour in vivo.

1.6 Research hypotheses and aims

1.6.1 Hypothesis 1

C3/C4 dorsolateral funiculus crush injury results in deficits in adult mouse forelimb function up to 4 weeks post-injury and these deficits are more severe than after C5/C6 injury.

1.6.2 Hypothesis 2

PTEN deletion in rubrospinal neurons promotes their axon regeneration following spinal cord injury but aging significantly diminishes this regeneration.

1.6.3 Hypothesis 3

The motor cortex is able to re-establish output to the forelimb and hindlimb following C3/C4 ablation of the dorsal corticospinal tract.

1.6.4 Hypothesis 4

Spared, dorsolaterally projecting corticospinal neurons are necessary for spontaneous recovery following C3/C4 dorsal column spinal cord injury.

Aim 1: Develop an adult mouse spinal cord injury model that results in complete unilateral axotomy of the rubrospinal tract and behavioural deficits in forelimb function up to 4 weeks post-injury.

Aim 2: Apply the injury model developed in Aim 1 to investigate whether PTEN deletion promotes rubrospinal axon regeneration and whether the age at which PTEN is deleted has a significant influence on the regenerative response invoked.

Aim 3: Establish the extent to which the motor cortex can re-establish output to the limbs following ablation of the dorsal CST that descends ~96% of corticospinal fibers.

Aim 4: Determine whether spared corticospinal neurons can mediate spontaneous recovery following a spinal cord injury resulting in substantial corticospinal and sensory loss.

Chapter 2. Dorsolateral funiculus lesioning of the mouse cervical spinal cord at C4 but not at C6 results in sustained forelimb motor deficits.

2.1 Introduction

Regenerative failure of adult mammalian central nervous system (CNS) neurons is a significant contributor to sustained functional deficit following spinal cord injury (SCI). This failure is multi-factorial, and caused in part by the limited intrinsic capacity for growth of CNS neurons(Liu et al., 2011), the presence of environmental growth inhibitory molecules(Yiu and He, 2006), and substrate deficiencies within the damaged cord(Geller and Fawcett, 2002). Animal models of SCI have proven vital to our understanding of CNS regeneration and SCI pathological mechanisms at large. To date, most SCI models have been established in rats due to some similarity to humans in spinal cord pathology after injury, their inexpensiveness, and compatibility with surgical intervention(Kwon et al., 2002a). However, with the extensive development of transgenic mouse models and their use to define the molecular basis of CNS axonal degeneration and regeneration, there is a growing need to develop adult mouse paradigms in which functional locomotor regeneration can be assessed.

The rubrospinal tract (RST) is a major brainstem to spinal cord projection in the rat and mouse and frequently used to assess regenerative therapies. Arising principally out of the magnocellular division of the red nucleus, the RST projects through the dorsal part of the lateral column of the spinal cord(Massion, 1967; Murray and Gurule, 1979; Wild et al., 1979;

Strominger et al., 1987; Liang et al., 2012). Because >98% of RST axons are crossed, the tract can be reliably transected by lateral funicular lesions, making this an attractive regeneration model that invokes minimal disability to the animal while avoiding problematic axonal sparing(Tetzlaff et al., 1991; Kobayashi et al., 1997b). Cervical spinal cord lesions that damage the lateral funiculus, including the RST, cause significant deficits in skilled reaching in the rat(Anderson et al., 2007; Stackhouse et al., 2008) but an assessment of DLF lesions on behavioral deficits in mice is lacking. CNS regeneration models that invoke sustained deficits in skilled forelimb function are particularly useful, given the high percentage of human SCIs that occur in the cervical region of the cord and the need to develop therapies that promote motor function of the upper extremity(Anderson, 2004).

Here we performed a cervical dorsolateral funiculus crush to sever the RST in adult mice and assess functional impairments in five behavioural paradigms: the cylinder rearing test of forelimb preference and usage; the grooming test, which assesses forelimb range of motion during spontaneous grooming behaviour(Bertelli and Mira, 1993; Gensel et al., 2006), Catwalk gait analysis, which assesses gait and motor parameters during continuous locomotion along a walkway(Hamers et al., 2006), staircase pellet reaching, which assesses forelimb skilled reaching(Montoya et al., 1991; Baird et al., 2001), and horizontal ladder walking(Cummings et al., 2007; Hilton et al., 2013a). We sought to determine the extent to which DLF lesions result in long-term deficits when implemented at cervical levels C4 or C6, and thus the appropriateness of the injury at these levels in permitting the assessment of the extent to which RST regeneration correlates with motor recovery. Animals sustained a DLF crush lesion at C4 or C6, and behavior was evaluated over a four-week recovery period.

C4 DLF crush caused sustained deficits in ipsilateral forelimb skilled movement, reaching, and preference, whereas C6 DLF crush led to only transient deficits. This C4 DLF crush model should facilitate the assessment of molecular targets to promote axonal regeneration in promoting upper extremity recovery following SCI.

2.2 Materials and methods

2.2.1 DLF crush

A total of 28 adult female C57B*l*6 mice (Charles River Laboratories, Wilmington, MA) were used in this study. Animals were anesthetized with isofluorane. The skin in the neck region was shaved and disinfected, and animals were given a subcutaneous injection of Lactated-Ringer's (Hospira Inc., Lake Forest, IL) and Buprenorphine (0.03 mg/kg). Once a surgical plane of anaesthesia was reached, a hemilaminectomy was performed to expose the left half of either the fourth cervical spinal cord segment (C4; N=20; including an N=5 of sham operated mice which received no crush injury) or the sixth cervical spinal cord segment (C6; N=8) and the dura mater overlying the grey matter was pierced with a 26 gauge needle. Fine tipped Dumont #5 forceps were modified for this purpose by grinding their blades to a width of ~200 microns and placing a mark at 1 mm distance from the tip. One prong of these fine-tipped forceps was inserted into the dorsal horn gray matter to a depth of ~1 mm (using the mark), while the other prong remained outside the spinal cord, i.e. lateral to the DLF. The

forceps were closed and held for 15 seconds to crush the DLF, including the rubrospinal tract; the forceps was removed and inserted again in order to repeat this crush once. The muscles and skin were then closed with sutures, and the animals were permitted to recover in a heated incubator (35^{o}C) for 2-3 hours before returning to their home cage. Animal weights were recorded daily for a week post-surgery, and twice a week thereafter. Bladder function was also assessed for 7 days post-surgery, but every animal retained bladder function post-operatively and no expressions were necessary.

2.2.2 Behavioural assessments

Animals were kept on a 12-h:12-h light:dark cycle (lights off at 9:00 AM). On days 2, 7, 14, 21, and 28 post-operatively, mice were assessed in the pellet reaching and rearing tasks between the hours of 10:00 A.M. and 1:00 P.M. inclusive, and the Catwalk Analysis between 4:00 PM and 7:00 P.M. inclusive. On days 3, 8, 15, 22, and 29 post-operatively, mice were assessed in the grooming task between the hours of 10:00 A.M. and 12:00 PM inclusive, and the horizontal ladder task between 4:00 P.M. and 6:00 P.M. inclusive. All behavioural analyses were conducted by personnel blind to group inclusion.

2.2.3 Rearing test

The rearing test assesses forelimb preference during spontaneous vertical exploration and was previously developed for use in rats (Napieralski et al., 1998; Liu et al., 1999; Schallert et al., 2000; Soblosky et al., 2001; Gensel et al., 2006) but has been modified for use in mice(Baskin et al., 2003; Starkey et al., 2005; Wells et al., 2005). Like rats, mice, when

placed in a cylinder, spontaneously rear using either one or both forepaws for weight support against its wall. Forelimb preference for weight support against the wall is thought to be indicative of forelimb functionality. Mice were placed in a clear plexiglass cylinder (20 cm in height, 15 cm in diameter) for 15 minutes. Two mirrors were placed at an angle such that forepaws and rearing forelimb preferences could be viewed irrespective of mouse orientation. The testing session was videotaped, and a blinded experimenter scored initial and subsequent forepaw use for a total of 10 rearing sessions (characterized by the initial placement and any subsequent placements the animal does until they place a paw back down on the ground). Initial placements were scored as either "left" or "right" when the left or right forepaw was used for weight support for >0.25 seconds independently of the other forepaw, respectively. Otherwise, in cases where both forepaws were used within 0.25 seconds of each other for weight support, a score of both was given. After scoring a "both", every subsequent combination of two limb movements was described as a subsequent both unless both paws were removed from the cylinder and only one paw was re-placed, which would be described as a left or right forepaw subsequent placement. Prior to surgery, mice were placed in the cylinder for three sessions for habituation and to obtain pre-injury scores. Mice were then tested on days 2, 7, 14, 21, and 28 post-injury. Percent use of the ipsilateral limb, contralateral limb, and both limbs together for initial rears was calculated as a fraction of the total number of rears (=10) for each animal at each time point. Percent ipsilateral limb use was calculated based on the number of times the ipsilateral limb was used for both initial and subsequent rearing events over the course of the first 20 initial and subsequent events for each animal at each time point.

2.2.4 Grooming test

Forelimb grooming function was assessed using a scoring system adapted from Gensel and colleagues for use in rats(Gensel et al., 2006). Cool saline was applied to the mouse's head and back with gauze, and the animal was placed in a cylinder with mirrors at angles, as above, for 15 minutes. The gauze was only damp with saline and not completely saturated, such that the mouse's fur was only moderately wet to induce a grooming response. The testing session was videotaped with a high definition camera (Sony, HDR-Hc1). Mice were tested pre-operatively to obtain baseline scores, and on days 3, 8, 15, 22, and 29 post-surgery. At a later date, videos were watched frame-by-frame by an experimenter blinded to the treatment group of each mouse who scored the maximum grooming score achieved by each paw independently according to the following scoring system: 0, the animal was unable to contact any part of the face or head; 1, the animal's forepaw touched the underside of the chin and/or the mouth area; 2, the animal's forepaw contacted the area between the nose and the eyes, but not the eyes; 3, the animal's forepaw contacted the eyes and the area up to, but not including, the front of the ears; 4, the animal's forepaw contacted the front but not the back of the ears; 5, the animal's forepaw contacted the area of the head behind the ears.

2.2.5 Horizontal ladder

Error (slip, miss, or drag) frequency was assessed for each limb of each mouse using a horizontal ladder modified as previously described (Engesser-Cesar et al., 2005; Cummings et al., 2007; Hilton et al., 2013a). Briefly, mice were videotaped with a high-definition camera (Sony, HDR-Hc1) as they crossed a 5.2-cm-wide horizontal ladder with 31 rungs

each spaced 1.3 cm apart. Each mouse repeated the task 6 times, and 1 repetition was excluded from analysis for each mouse based on failure to complete the task appropriately (by turning around midway through the sequence, rearing against the wall of the apparatus, etc.). In cases where all 6 runs were completed adequately, the 6^{th} run was automatically excluded. Frame-by-frame video analysis provided scores for number of errors for each limb over each run, and summed for the total over the 5 runs for each animal at each time point to generate a limb-specific cumulative error score. Mice were tested pre-operatively to obtain pre-injury scores, and on days 3, 8, 15, 22, and 29 post-operatively.

2.2.6 Pellet reaching

The staircase test of pellet reaching assesses skilled forepaw reaching and was initially developed for rats(Montoya et al., 1989; Montoya et al., 1991) but a scaled down assessment is in use for mice(Baird et al., 2001; Starkey et al., 2005). Mice were placed in a holding box with access to a plinth with a graded staircase on each side (eight steps per side). Two 20 mg chocolate food pellets (NOYES Precision Pellets, Research Diets Inc., USA) were placed in each well of each staircase such that mice could retrieve them by reaching with their forepaw down either side of the plinth. In this manner, pellets in the left staircase were only reachable by the left forelimb, and the right staircase by the right forelimb. Mice were familiarized with food pellets for one week by placing ~100 into each home cage each day, and then pre-trained to complete the task itself by baiting each well with two pellets and placing each mouse within the apparatus for 15 minutes a day for one week. Mice were fasted for 18-20 hours prior to each pre-training session, and prior to each testing session throughout the experiment. During assessment of pre-operative scores and at each experimental time point,

pellets were marked with food colouring to allow for the assessment of how far each mouse could reach by placing pellets of different colours at different well heights. Each mouse was granted access to the apparatus individually for 30 minutes for each experimental testing session. The total number of pellets eaten from each side was calculated at the end of each testing session for each animal. Pellets eaten from the top two wells on each side were discounted from analysis since mice could retrieve these with the use of their tongues.

2.2.7 CatWalk gait analysis

The CatWalk apparatus and CatWalk XT 8.1 software (Noldus, The Netherlands) were used. Each animal was allowed to cross a transparent platform (5.2 cm wide and 60 cm long) with opaque and black walls in a darkened room. Animals were recorded from beneath with a high-definition camera (Sony, HDR-HC1) illuminated with a light source below the platform. The light internally reflects in the glass floor and illuminates the mouse's paws at the contact area, producing a footprint. Animals were trained to run across the runway consistently for 5 days prior to testing, with each training session consisting of 3 runs across the platform. Mice were then tested on days 2, 7, 14, 21, and 28 post-operatively. To ensure consistent performance of the task, mice were encouraged to run across the platform quickly. Additionally, mice were trained to run from a foreign cage back to their home cage, and inside their home cage chocolate pellets (NOYES Precision Pellets, Research Diets Inc., USA) were provided as a reward. At each experimental time point, three runs for each animal were recorded from below the glass by a digital video camera. Runs were then analyzed to measure stride length, swing duration, paw area, and paw intensity for each limb, in addition to base of support and speed in crossing the platform.

2.2.8 Anterograde tracing of rubrospinal axons

Two weeks before the end of the survival period and 30 days post-operatively, animals were anesthetized with isofluorane, the skin overlying the skull was shaved and disinfected, and animals were given a subcutaneous injection of Lactated-Ringer's (Hospira Inc., Lake Forest, IL) and Buprenorphine (0.03 mg/kg). Upon reaching a surgical plane of anaesthesia, a burr hole was drilled into the skull, and 1.0 µL of 10% biotinylated dextran amine (BDA; 10,000 kDa molecular mass, Molecular Probes, Eugene, OR) was stereotaxically injected into the vicinity of the right red nucleus at the following coordinates: 3.6 mm caudal to bregma, 0.7 mm lateral to the midline, and 3.6 mm depth with respect to the surface of the brain. The injection occurred at a rate of 100 nl/minute, and the syringe remained in place for 5 minutes after the injection to prevent efflux. Mice were permitted to recover in a heated incubator (35^{o}C) for 2-3 hours post-operatively before being returned to their homecages.

2.2.9 Immunohistochemistry

Two weeks after BDA injection, animals were killed with an overdose of chloral hydrate (100 mg/kg, i.p.) and perfused transcardially with PBS followed by phosphate buffered 4% paraformaldehyde (pH 7.4). The cervical spinal cords were dissected, post-fixed in 4% paraformaldehyde overnight, and cryoprotected in 12%, 18%, and 24% sucrose in 0.1 M phosphate buffer over 3 days before being snap frozen in isopentane over dry ice. Cervical segments from C2 to C8 were cut into 20-micron longitudinal sections in the horizontal plane on a cryostat and stored at -80°C. Frozen sections were thawed for an hour, rehydrated in 10

mM PBS for 10 minutes, and incubated with 10% normal donkey serum (in 0.1% Triton X-100) for 30 minutes to prevent non-specific binding. Chicken anti-GFAP (1:1000; Chemicon) was applied overnight at room temperature. Secondary antibody (1:200, Jackson) raised in donkey and conjugated to Dylight 405 was applied for 2 hours at room temperature. BDA was visualized by using Cy3-conjugated streptavidin (1:200, Jackson Laboratories) applied for 2 hours at room temperature. Sections were coverslipped in Fluoromount-G (Southern Biotech).

2.2.10 Image analysis and assessment of rubrospinal axon sparing

Digital images were captured with an Axioplan 2 microscope (Zeiss, Jena, Germany) equipped with Northern Eclipse software (Empix Imaging, Inc., Mississauga, ON, Canada) at 10X. GFAP+ staining was used to identify the center of the lesion, and images of the lesion center were taken in every section containing BDA+ labelling of the RST on every other slide, encompassing the entirety of the tract as well as it could be observed by the tracer. Images were then assessed for sparing by drawing a line through the middle of the lesion and noting the propensity of BDA+ axons to make it into or through the middle of the lesion site on every image captured. All histological analyses were conducted by personnel blinded to the experimental grouping.

2.2.11 Eriochrome cyanine R staining

Assessment of white and gray matter sparing was conducted by staining coronal sections through the injury site with Eriochrome Cyanine R (EC) to visualize myelinated white

matter. Sections were rehydrated through two toluene solutions followed by graded ethanol solutions: twice in 100%, once in 95%, once in 70%, and one in 50% ethanol. After rehydration in distilled water, slided were stained in EC Solution (0.16% EC, 0.4% Sulphuric Acid, and 0.4% ferric chloride) at room temperature for 10 minutes, and gently rinsed in distilled water. Sections were then differentiated in 0.5% ferric ammonium sulphate at room temperature for ~30 seconds, rinsed in distilled water, and then stained in 1% Neutral Red solution for 2 minutes before being dehydrated in graded ethanol solutions: once in 50%, once in 70%, once in 95%, and twice in 100%. Sections were then cleared in xylene two times and cover-slipped using Entallan mounting medium (EM Science, Gibbstown, NJ). Each section was digitally photographed (Zeiss AxioPlan2 imaging microscope; Zeiss, Inc., Thronwood, NY) and manually traced using imaging analysis software (Sigma Scan Pro 5, Systat Software Inc., San Jose, CA). White matter sparing was based on positive (blue) staining of myelin via EC while gray matter sparing was based on normal cytoarchitecture of gray matter relying on EC staining and Neutral Red counterstaining.

2.2.12 Statistical analysis

All statistical tests were carried out with Sigma Stat 3.0.1 (SPSS, Inc.). All data are presented as mean ± standard error of the mean (SEM). The grooming test, rearing test of forelimb asymmetry, horizontal ladder, and pellet reaching were analyzed using Mann-Whitney *U* Tests to compare groups at individual time points and the Wilcoxon test for paired samples to compare the same group at different time points. CatWalk Gait Analysis was analyzed using a two-way repeated measures (RM) analysis of variance (ANOVA) (groups VS. days) and follow-up Student's t-tests. Gray and white matter sparing histological

data were analyzed using one-way analysis of variance (ANOVA), and group differences were ascertained using Tukey's post hoc comparisons. The significance level for all tests was set at $p < 0.05$.

2.3 Results

2.3.1 Basic characterization of adult mouse cervical DLF crush spinal cord injury

We endeavoured to develop a unilateral RST injury model that would lead to sustained deficits in forelimb function and to ascertain the level of the cervical spinal cord at which such an injury would lead to functional deficits in forelimb motor function. To do so, DLF crush was employed (**Fig. 2.1A**). Following hemilaminectomy, the dura was pierced using a 26 gauge needle and one prong of the forceps was inserted ~1 mm into the gray matter of the spinal cord and the other lateral to the cord as shown. Modified #5 Dumont forceps that were thinned to a prong width of ~200 micrometres were used for this purpose (**Fig. 2.1B**).

Following either C4 or C6 DLF crush, mice displayed a closed forepaw on the injured side and uncoordinated overground locomotion. The mice are able to freely locomote around their cages and no observable deficit was observed in the forelimb on the contralateral side. No change in body weight was observed following C4 or C6 DLF crush at any time point post-operatively compared to pre-operatively or between C4 DLF crush, C6 DLF crush, and sham injured mice (**Fig. 2.1C**). Additionally, though typical animal monitoring within our

laboratory requires that we check at least daily for the first week post-operatively, no manual expression of the bladder was required.

2.3.2 Assessment of gray and white matter sparing in and around the lesion site

To visualize the rostral/caudal and dorsal/ventral extent of damage following DLF crush, coronal spinal cord sections of C4 DLF crushed (N=5) and control sham operated (N=5) mice were stained for Eriochrome Cyanine R /neutral red to visualize myelin six weeks post-operatively. Tissue damage in the white and gray matter following C4 DLF crush was predominantly confined to a 200 µm area surrounding the lesion epicenter (**Fig. 2.2**). Importantly, no damage to the dorsal columns (and thus the main contingent of corticospinal axons) was observed, nor was damage observed on the side of the spinal cord contralateral to the injury.

We quantified spared white and gray matter area at 100 µm intervals rostral and caudal to the lesion epicenter for a total distance of 800 µm on both the contralateral and ipsilateral side of the spinal cord with respect to the injury site (**Fig. 2.3**). At 100 µm rostral and caudal to the lesion epicenter and at the epicenter itself, there was a significant difference in the percentage of gray matter spared and white matter spared following C4 DLF crush compared to sham operated mice (Tukey's post hoc test; $p<0.05$). At the lesion epicenter, there was 43.98±3.18% and 35.26±4.77% sparing of white and gray matter, respectively.

2.3.3 Assessment of rubrospinal axotomy following DLF crush

To verify complete ablation of the RST, we injected BDA into the vicinity of the right red nucleus following the conclusion of behavioural assessments and two weeks prior to euthanizing a cohort of N=18 mice. The extent of RST sparing was determined using immunostaining for GFAP to identify the lesion site and BDA to visualize RST fibers (**Fig. 2.4**). We captured images on every section on which BDA+ RST fibers could be identified on every other slide, encompassing the entirety of the tract as well as it could be observed based on anterograde tracing. In 346 images taken, RST fibers could be identified within the lesion site itself, but no RST fibers with morphology of spared axons(Steward et al., 2003) were observed within white matter caudal to the lesion site in any of the animals.

2.3.4 Rearing test of forelimb asymmetry

During pre-operative baseline testing, our mice used their left forepaw alone for initial weight support against the wall in 37%(±7.89%) of the rears in the C4 injury group, and in 36.25%(±9.99%) of the rears in the C6 injury group. Somewhat surprisingly, the usage of their right forepaw for initial weight support was less frequent (25%±5.82% in the C4 group and 23.75%±8.% for C6 group). Both limbs together were used in 38.0%(±7.27%) and 40.00%(±10.00%) in the C4 and C6 group respectively. After DLF crush at C4, a sustained change in the pattern of forelimb use for initial weight support was observed (**Fig. 2.5A-C**). The percentage of initial placements made with the contralateral forepaw significantly increased (**Fig. 2.5B**) while the percentage of initial placements made with either the

ipsilateral forelimb or both forelimbs together significantly decreased at all time points post-injury compared to pre-operatively ($p<0.05$)(**Fig. 2.5A,C**). At 28 days post injury, mice with a C4 DLF crush lesion used their left/ipsilateral forelimb alone in 15%(±4.77%), their right/contralateral forelimb alone in 72%(±6.63%), and both forelimbs together in 14.0%(±3.40%) of the initial paw placements against the cylinder wall.

Following C6 DLF crush, the percentage of initial placements made with the contralateral forepaw and both forepaws together were significantly lower than post-operatively at all time points, except at 28 days post-injury. The percentage of initial placements with the ipsilateral forepaw was significantly decreased at 2 days post-injury compared to the pre-operative usage following C6 DLF crush, but not at any other time point (**Fig. 2.5A**). At 28 days post injury, mice with a C6 DLF crush lesion used their left/ipsilateral forelimb alone 25%(±9.64%), the right//contralateral forelimb alone 47.5%(±11.30%), and both forelimbs together 27.5%(±6.20%) to make initial placements. There was a trend towards a difference in initial contralateral forepaw use between C4 and C6 at 28 days post injury ($p=0.098$).

We also calculated percent ipsilateral limb use based on frequency of use during the first 20 initial and subsequent rearing events for each animal, and found a sustained decrease at each time point in comparison to baseline values in mice with a C4 DLF crush ($p<0.05$), but this difference in mice with a C6 DLF crush was only seen 2 days post injury. Thus, C4 DLF crush lesions lead to a decreased usage on the ipsilateral forelimb during rearing, while C6 DLF crush lesions lead to only a transient decline in usage of the ipsilateral forelimb.

2.3.5 Grooming test

We adapted a grooming assessment used in rats for use in mice (**Fig. 2.6**). The mouse is gently scrubbed with gauze coated in saline until their fur is displaced and recorded for 15 minutes in a cylinder with mirrors placed at angles to allow visualization of the mouse from every angle and assessment of grooming responses of the left and right forelimbs (**Fig. 2.6A**). Pre-operatively, mice displayed normal grooming patterns, repeatedly licking their forepaws and grooming from their mouth and nose up to the eye region and to the back of the head. Some mice only reached to the front of the head over the 15 minute testing period, obtaining a score of 4 in the absence of injury. A score of either 4 or 5 was also achieved by the contralateral limb of every mouse pre-operatively and at every time point post-injury, and there was no significant difference in grooming scores between the contralateral limb of C4 crushed and C6 crushed mice at any time point. Following DLF crush at C4, there was a permanent ipsilateral deficit for the duration of the experimental period ($p<0.05$) (**Fig. 2.5A)**. None of the animals injured at C4 could touch the front of the ears, such that they could not achieve a grooming score higher than 3. In contrast, the mice with C6 dorsolateral funiculus crush showed a deficit 2 days post injury ($p<0.05$) (**Fig. 2.6B**) yet by 7 days, there was no significant difference in grooming score compared to pre-operative scores. Importantly, at 7 and 28 days post injury, there was a significant difference in grooming score between C4 and C6 mice ($p<0.05$). There was no difference in grooming score in the contralateral forelimb in either group at any time point (**Fig. 2.6C**). There was no difference in grooming score following sham operation at 2 days and 7 days post-operatively compared to preoperatively.

2.3.6 Pellet reaching

Pre-operatively, mice were able to successfully reach, grasp, and eat 4-5 pellets with each of their forelimbs (**Fig. 2.7A,B**). After C4 DLF crush, there was a sustained deficit in the ability to successfully reach, grasp, and eat pellets with the ipsilateral forepaw at all time points post-injury ($p<0.05$). Pre-operatively, mice ate 5.1±0.43 pellets, whereas 28 days following C4 DLF crush, mice ate 2.0±0.20 pellets with the ipsilateral/left forelimb. In contrast, the apparent decline in the number of pellets eaten with the ipsilateral/left forelimb following C6 DLF crush did not reach significance (versus pre-operative values; $p=0.148$). At 28 days post-injury, fewer pellets were eaten by mice with a C4 DLF crush and those with a C6 DLF crush (2.0±0.20 pellets for C4 VS. 3.14±0.51 pellets for C6; $p<0.05$). The number of pellets eaten with the contralateral/right forelimb did not change at any time point post-injury and was similar in both groups. There was no difference in pellets eaten following sham operation at 2 days and 7 days post-operatively compared to pre-operatively.

2.3.7 Horizontal ladder

Pre-operatively, the mice were able to cross the ladder with few errors, though with significantly more errors made by the forelimbs than the hindlimbs across both groups ($p<0.05$). After C4 or C6 DLF crush, the cumulative error (CE) score (i.e. the number of errors committed by each limb over 5 trials runs) significantly increased for both the ipsilateral forelimb and hindlimb compared to pre-operative values, and a sustained increase was observed throughout the testing period in both ipsilateral limbs ($p<0.05$) (**Fig. 2.8A,B**). No differences were observed for CE score of the contralateral paws (**Fig. 2.8C,D**), nor were

differences observed in CE scores of sham operated mice at 2 or 7 days post-operatively compared to pre-operatively.

We also compared the ipsilateral versus contralateral CE scores to determine asymmetry between the limbs. After both C4 and C6 DLF crush, significant differences were observed between the CE scores on the left (ipsilateral) side versus the right (contralateral) (**Fig. 2.8C,D**) side for both forelimbs and hindlimbs ($p<0.05$, data not shown).

2.3.8 CatWalk gait analysis

Footprint analysis revealed a robust reduction of stride length during locomotion along a walkway following DLF crush at C4, but not at C6, compared to pre-operative stride lengths (**Fig. 2.9**). The length of strides taken by mice injured at C4 was significantly shorter than by mice with C6 DLF crush. These differences in the stride lengths between C4 and C6 lesioned mice were observed in all four limbs, the ipslateral/left forelimb at 2, 7, 21, and 28 days post injury (**Fig. 2.9A**), contralateral/right forelimb at 7, 14, 21, and 28 days post-injury (**Fig. 2.9C**), ipsilateral/left hindlimb at 2, 7, 21, and 28 days post injury (**Fig. 2.9B**), and contralateral/right hindlimb at 2, 7, 21, and 28 days post injury (**Fig. 2.9D**) ($p<0.05$ all, two-way RM ANOVA). Though mice with a C4 DLF crush and C6 DLF crush showed a significant difference compared to pre-operatively in base of support, paw contact area, and paw intensity at 2 days post-injury (all $p<0.05$, data not shown), these deficits were transient, with no significant differences observed seven days post-injury or later. There were no differences in swing speed at any time point (data not shown). In sham operated mice, there

was no difference in any parameter 2 and 7 days post-operatively compared to pre-operatively.

We also measured the speed at which the mice crossed the platform, since speed affects stride length. Although mice with a C4 DLF crush traveled slower at 2 days and 21 days post injury compared to their pre-operative speed and mice with a C6 DLF crush traveled slower at 14 days post injury compared to pre-operatively (both $p<0.05$), there was no significant difference in speed between mice with C4 DLF crush and those with C6 DLF crush at any time point (data not shown). Thus, the differences in stride length observed in mice with C4 DLF and those with C6 DLF cannot be explained by a difference in speed.

2.4 Discussion

In this study, we characterize a consistent and reliable dorsolateral funiculus (DLF) crush model in adult mice to axotomize the rubrospinal tract (RST) and compare the effects of this lesion when instigated at cervical level C4 or cervical level C6 in a number of tests that evaluate motor behaviour, particularly forelimb function. We sought to determine the cervical level at which DLF lesioning would result in sustained deficits up to four weeks post-injury. This timeline would permit the assessment of the extent to which RST regeneration correlates with motor function improvement. Ablation of the RST is a useful model for SCI research, particularly studies focused on degeneration and regeneration, because of its anatomical convenience. The mouse and rat RST cross the midline in the ventral tegmental decussation and travel in the ventrolateral hindbrain before descending in

the spinal cord within the DLF(Murray and Gurule, 1979; Liang et al., 2012). Because the vast majority of the tract is crossed, it can be reliably transected by DLF lesions, allowing assessment of regenerative outcome following SCI in the absence of sparing(Steward et al., 2003; Tuszynski and Steward, 2012). Additionally, because the RST arises from the red nucleus, a relatively dense neuronal cluster found within the midbrain, assessment of the cell body response to axotomy is achievable with comparisons to the relatively uninjured red nucleus of the contralateral tract(Tetzlaff et al., 1991; Liu et al., 1999; Geoffroy et al., 2016).

Our results in the pellet reaching and horizontal ladder tasks indicate that the DLF of the mouse is particularly important in skilled forelimb movement. Much of this deficit is likely due to disruption of the RST. Double staining analysis has previously indicated that rubrospinal axons make direct synaptic contact with motor neurons innervating distal muscles of the forelimb, which is consistent with the RST's role in skilled forelimb movement in the rat (Küchler et al., 2002). More recent evidence suggests that similar connections exist in the mouse (Liang et al., 2012). This importance of the RST in skilled reaching has further been documented in the rat using ibotenic acid lesions to the red nucleus which interfere with aiming, pronation, arpeggio, and supination of the limb(Whishaw and Gorny, 1996; Whishaw et al., 1998). In particular, LF lesioning indicates the RST's importance for arpeggio movement; that is, pronation of the paw and positioning of the digits with wrist movement when grasping for food (Morris et al., 2011). We found a significant reduction in the number of pellets eaten in the staircase pellet test with the ipsilesional forepaw after C4 dorsolateral crush. In the cat, Alstermark and colleagues have shown that ablation of the DLF at C5/C6 resulted in complete loss of food-taking ability(Alstermark et

al., 1981). Indeed, if the C5 DLF lesion was incomplete and as little as 20% of the RST was left intact, food taking ability recovery was faster and more complete. Interestingly, unilateral ablation of the corticospinal tract (CST) via pyramidotomy had no significant effect on the ability of mice to grasp and eat food pellets from the wells of a graded staircase(Starkey et al., 2005), suggesting that the circuitry encompassed within the DLF of the mouse is more important in this regard or at the very least able to compensate for the loss of the CST.

Our results also indicate that the DLF is important in spontaneous limb use. DLF ablation resulted in significant changes in patterns of weight bearing support during spontaneous vertical exploration and grooming. In the rat, C3/C4 DLF lesioning leads to a sustained decline in use of the ipsilateral limb in spontaneous vertical exploration, while transplantation of brain derived neurotrophic factor (BDNF) expressing fibroblasts aiming at the promotion of RST regeneration leads to a significant increase in ipsilateral forelimb use(Liu et al., 1999). Consistent with these results, Webb and Muir found that 88% of rubrospinal injured rats had decreased usage of the ipsilateral forelimb in the same task(Webb and Muir, 2003). In the mouse, it appears that the DLF and the corticospinal tract share a role in forepaw use in weight bearing support, as unilateral pyramidotomy results in a similar sustained impact on forelimb up to 28 days post-injury in the same task(Starkey et al., 2005). Additional pathways and cells involved in forelimb and hindlimb locomotion would be damaged by lateral funicular lesions, and the behavioural results observed here cannot be construed as arising from ablation of the RST alone. Dorsolateral corticospinal and lateral reticulospinal fibers contribute to motor function in the mouse and would be damaged in this model. Because our lesions included a significant extent of gray matter, the lesion area

included premotor interneurons, propriospinal neurons, and possibly motor neurons that form the segmental circuitry underlying forelimb movement(Sidman et al., 1971). In rats, retrograde tracing has shown that motor neurons supplying digital flexors are located in pools extending from C5 through T1(McKenna et al., 2000). Destruction of such segmental circuitry would be characterized by the symptoms of lower motor neuron injuries, including flaccid paralysis and loss of segmental reflexes. However, it is unlikely that motor neuron loss was a significant factor in the sustained deficits observed, as we were careful to avoid crushing the ventral horn and the rostrocaudal extend of our lesion was relatively small since the forceps were only ~200 microns in width; compared to the extent of the motor neuron pools over several segments.

DLF crush lesioning at either C4 or C6 had only transient effects on several parameters of overground locomotion determined via CatWalk Gait Analysis, including base of support, paw contact area, and paw intensity, while swing duration was not significantly different at any time point. Instead, the only difference observed was a decrease in stride length of both hindlimbs and forelimbs on both the ipsilateral and contralateral sides of the lesion following C4 DLF crush. These findings suggest that the role of DLF circuitry in overground locomotion is well compensated for following injury. Previous work in the rat has found only minor deficits in overground locomotion following red nucleus lesioning(Muir and Whishaw, 2000). Indeed, there is a high degree of correlation between stepping ability and spared white matter tissue in the region of the reticulospinal tract in the rat indicating that the ventrolateral funiculus is more important for general locomotion than the DLF(Schucht et al., 2002). Notably, unilateral pyramidotomy in the mouse also leads to a bilateral decrease in stride

length in both forelimbs and hindlimbs but has no effect on other parameters in CatWalk Gait Analysis(Starkey et al., 2005), suggesting a similar function of the CST and DLF in overground locomotion. Although overground locomotion was not overtly effected by DLF lesioning, our results in the horizontal ladder task are indicative of a role of this circuitry in hindlimb locomotion. More specifically, the increase in cumulative error score in the left hindpaw on this task following C4 DLF lesioning suggests that the RST may play a role in sensorimotor integration, which is required for successful placement of the hindpaw onto the ladder beam.

Assays that use animal behaviour to ascertain locomotor function have an inherent variability, and every effort should be made to minimize this variability whenever possible. We recommend at least 1 week of daily animal handling and environmental enrichment for successful implementation of this behavioural model, acknowledging that week-to-week variability in the outcome of any particular behavioural test can occur. It is for this reason that the assessment of animals across a battery of behavioural tests (instead of just one) is also recommended.

In conclusion, we have characterized a DLF crush model in adult mice which harbours several significant advantages in the assessment of potential treatment options and motor recovery following SCI. Because this model was developed in mice, it is of particular use in the assessment of molecular therapeutic targets reliant on transgenic mouse technologies. Since a DLF lesion results in complete ablation of the RST, it permits the assessment of

axonal regeneration and functional recovery without severe deficits in bladder or respiratory function, keeping animal care demands low. Finally, and in particular, because the cervical region of the spinal cord is the most common injury area in cases of human SCI(Jackson et al., 2004), this DLF crush injury leads to motor function loss in an area of especial importance to SCI patients.

Figure 2.1 Basic characterization of DLF crush lesion. (A) Cross sectional diagram of the intended lesion. Following hemilaminectomy, the dura overlying the left dorsal horn is punctured with a 26 gauge needle. One prong of modified Dumont #5 forceps is inserted to ~1 mm while the other prong is positioned lateral to the spinal cord. The DLF is crushed twice for 15 seconds to unilaterally ablate the RST. (B) Images of the modified forceps, which have fine tips ground down to ~200 μm, minimizing the rostral/caudal extent of the injury. (C) Body weight change of mice following C4/C6 DLF crush or sham operation. Error bars indicate SEM.

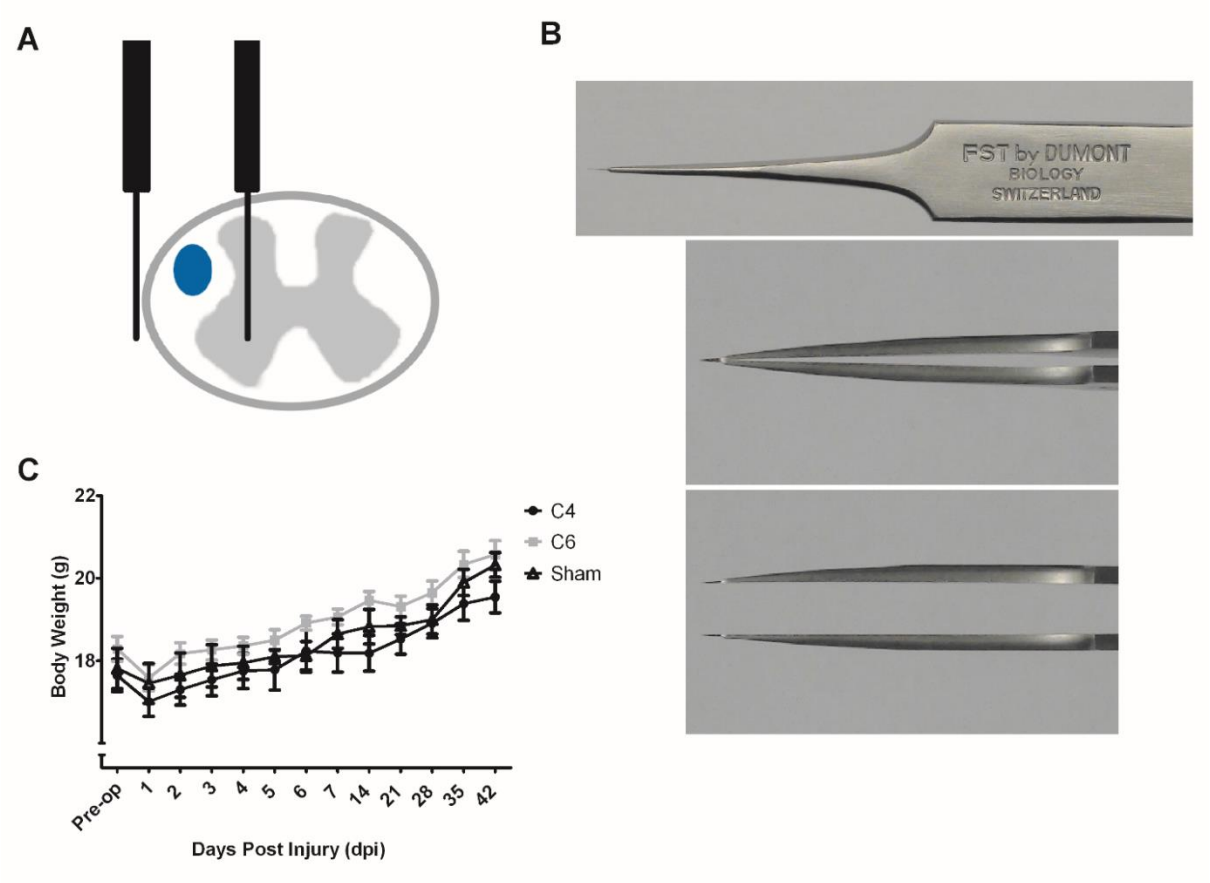
A
B
FST by DUMONT
BIOLOGY
SWITZERLAND
C
22
20
18
Body Weight (g)
C4
C6
Sham
Pre-op
1
2
3
4
5
6
7
14
21
28
35
42
Days Post Injury (dpi)

Figure 2.2 Eriochrome cyanine/neutral red-stained spinal cord following C4 DLF crush. From top left (rostral) to bottom right (caudal), photomicrographs of representative spinal cord cross sections are stained with myelin dye eriochrome cyanine at the epicentre and at 100 µm increments rostral-caudal to the epicentre to a total distance of 800 µm. At four weeks post-operatively, EC-stained sections demonstrate ipsilateral white matter and gray matter damage with extensive damage of the dorsolateral funiculus but complete sparing of the ipsilateral dorsal column which contains the main contingent of corticospinal axons. No damage is observed on the side contralateral to the injury.

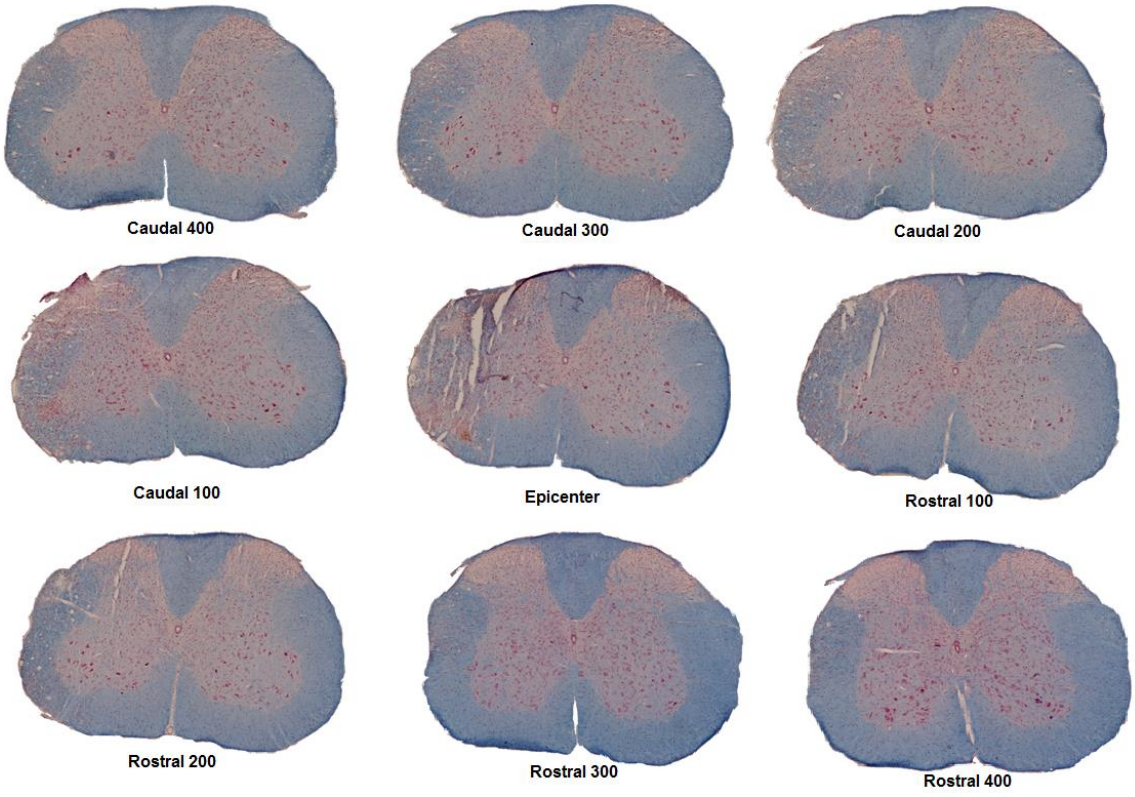
Caudal 400
Caudal 300
Caudal 200
Caudal 100
Epicenter
Rostral 100
Rostral 200
Rostral 300
Rostral 400

Figure 2.3 Tissue sparing quantification of spinal cord tissue following C4 DLF crush or sham operation. Measurement of the rostral-caudal extent of ipsilateral (A) white and (C) gray matter sparing of uninjured and injured spinal cord as well as contralateral (B) white and (D) gray matter For both white and gray matter sparing, C4 DLF crush led to a significant difference compared to sham operation at the lesion epicenter and at 100 µm rostral and caudal to the epicenter. *indicates $p<0.05$. Error bars indicate SEM.

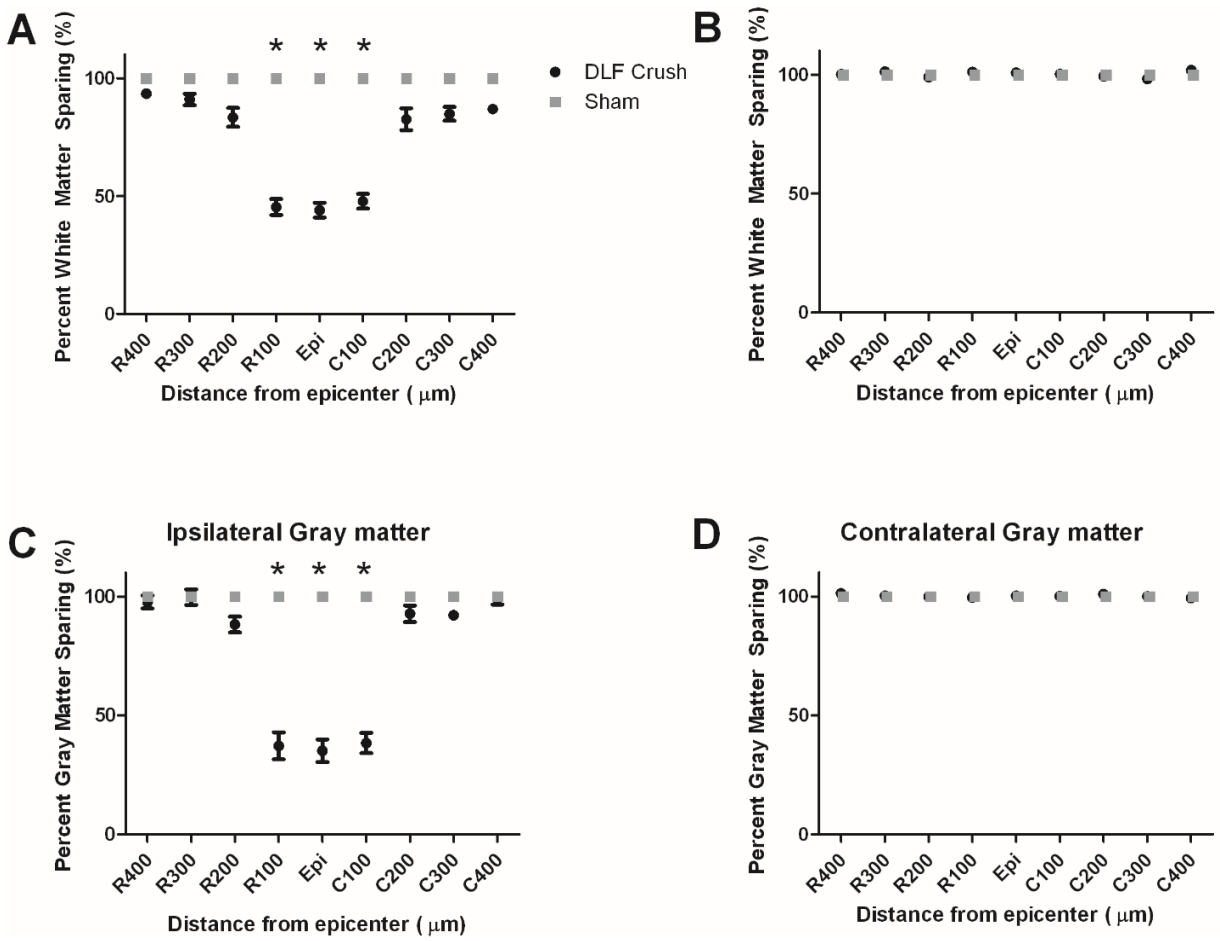
A
Percent White Matter Sparing (%)
100
50
0
*
*
*
DLF Crush
Sham
R400
R300
R200
R100
Epi
C100
C200
C300
C400
Distance from epicenter (μm)
B
Percent White Matter Sparing (%)
100
50
0
R400
R300
R200
R100
Epi
C100
C200
C300
C400
Distance from epicenter (μm)
C
Ipsilateral Gray matter
Percent Gray Matter Sparing (%)
100
50
0
*
*
*
R400
R300
R200
R100
Epi
C100
C200
C300
C400
Distance from epicenter (μm)
D
Contralateral Gray matter
Percent Gray Matter Sparing (%)
100
50
0
R400
R300
R200
R100
Epi
C100
C200
C300
C400
Distance from epicenter (μm)

Figure 2.4 Assessment of rubrospinal axotomy following DLF crush via immunostaining for BDA (red)/GFAP (blue) in longitudinal sections through the cervical spinal cord. Dorsal to ventral from top left to bottom right, images are spaced 80 µm apart, encompassing the main bundle of RST nerve fibers and their projections into gray matter in 420 µm total distance. 80 µm dorsal to the top left image or ventral to the bottom right image, only sparse labelling of BDA+ axons in lateral funicular white matter is observed. In 346 images taken of every other slide onto which sections were collected and every section on each slide labelling positive for BDA within the lateral funiculus (thus encompassing the entirety of the RST as well as it could be observed by BDA+ labelling), no BDA+ fibers were observed making it through the lesion site or in caudal white matter. White arrows denote the middle of the lesion site. Scale bars are 100 µm.

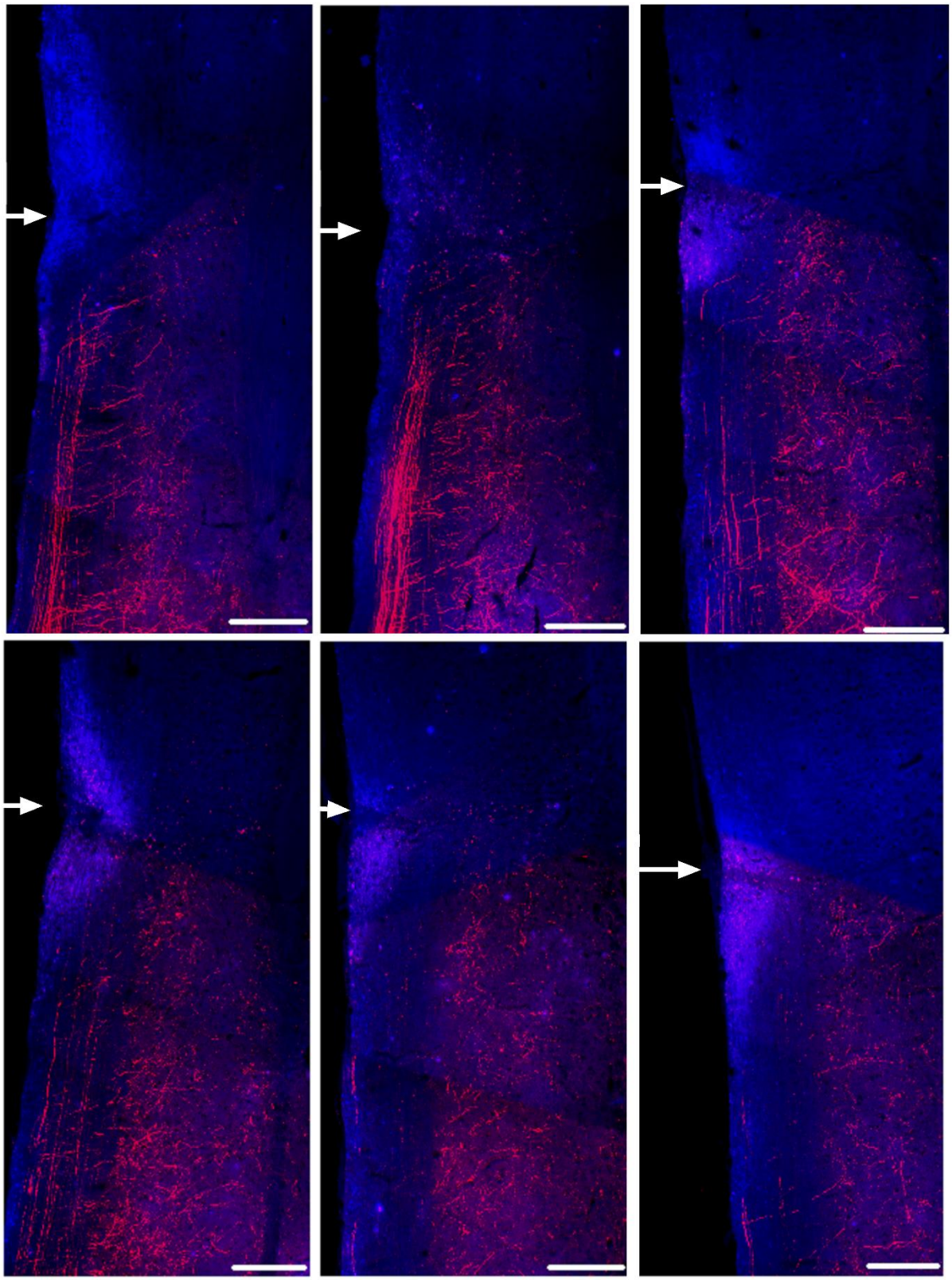

Figure 2.5 Effect of C4 and C6 DLF crush on the rearing test. (A,B,C) Following DLF crush at C4, mice used the ipsilateral forepaw and both forepaws together significantly less and the contralateral forepaw significantly more at all time points post-operatively compared to pre-operatively ($p<0.05$). Following DLF crush at C6, mice used the ipsilateral forepaw and both forepaws together significantly less and the contralateral forepaw significantly more 2 days post-operatively compared to pre-operatively ($p<0.05$). There was no significant difference in initial use of the ipsilateral forepaw, both forepaws together, or the contralateral forepaw, at any other time point post-operatively compared to pre-operatively. There was a trend towards a difference in contralateral forepaw use for initial rears between mice with a C4 DLF crush and those with a C6 DLF crush 28 days post injury ($p=0.098$). There was no significant difference in the use of the ipsilateral forepaw, contralateral forepaw, and both forepaws together 2 days and 7 days post-operatively compared to preoperatively in the sham injured group. (D) Following DLF crush at C4, mice used the ipsilateral forepaw for both initial and subsequent rears significantly less at all time points post-operatively compared to pre-operatively ($p<0.05$). Following DLF crush at C6, mice used the ipsilateral forepaw for both initial and subsequent rears significantly less at 2 days post-operatively compared to pre-operatively ($p<0.05$), but no significant difference was found at any other time point. Following sham operation, there was no difference in the use of the ipsilateral forepaw for both initial and subsequent rears at 2 days and 7 days post-operatively compared to pre-operatively. *indicates $p<0.05$. Error bars indicate SEM.

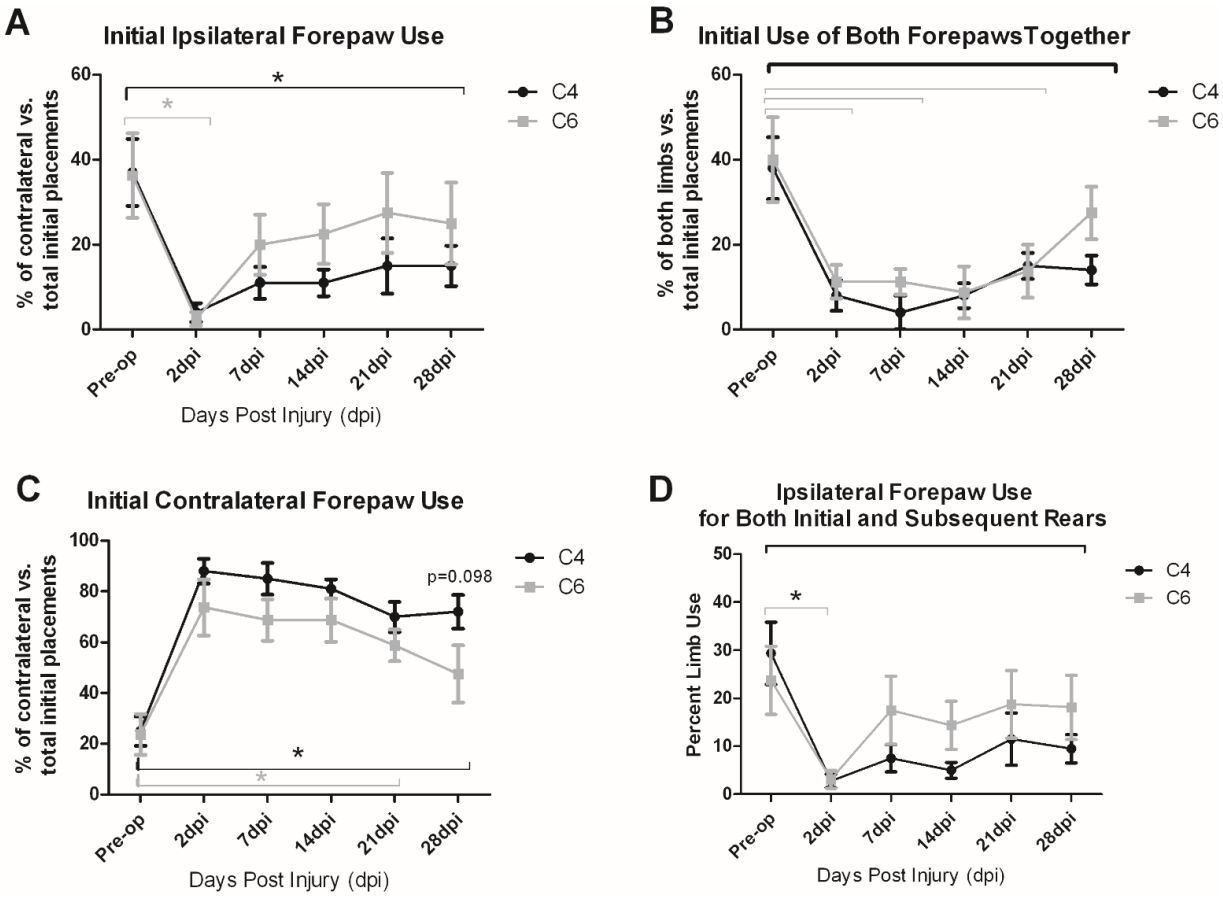
A
Initial Ipsilateral Forepaw Use
% of contralateral vs. total initial placements
60
40
20
0
*
*
C4
C6
Pre-op
2dpi
7dpi
14dpi
21dpi
28dpi
Days Post Injury (dpi)
B
Initial Use of Both ForepawsTogether
% of both limbs vs. total initial placements
60
40
20
0
C4
C6
Pre-op
2dpi
7dpi
14dpi
21dpi
28dpi
C
Initial Contralateral Forepaw Use
% of contralateral vs. total initial placements
100
80
60
40
20
0
p=0.098
*
*
C4
C6
Pre-op
2dpi
7dpi
14dpi
21dpi
28dpi
Days Post Injury (dpi)
D
Ipsilateral Forepaw Use
for Both Initial and Subsequent Rears
Percent Limb Use
50
40
30
20
10
0
*
C4
C6
Pre-op
2dpi
7dpi
14dpi
21dpi
28dpi
Days Post Injury (dpi)

Figure 2.6 Grooming. (A) Representative photo of the grooming set up. Mirrors are placed on angles behind the cylinder and a plastic sheet is placed over top to limit mouse escape. The mouse is videotaped for 15 minutes. (B) Grooming ability with the ipsilateral/left forelimb was significantly affected by C4 DLF crush at all time points post operatively ($p<0.05$). Pre-operatively, all mice could contract either the area of the head in to the front or back of the ears, achieving a score of 4 or 5. Post-operatively, mice with a C4 DLF crush could only contact the area around the eyes or below. C6 DLF crush had no significant affect on grooming ability at any time point post-operatively. At 7 and 28 days post-operatively, there was a significant difference in grooming ability between mice with a C4 DLF crush and those with a C6 DLF crush ($p<0.05$). Following sham operation, there was no significant difference in grooming ability at 2 and 7 days post-operatively compared to preoperatively. (C) Grooming ability with the contralateral/right forelimb. There was no significant difference between the groups or at any time point compared to pre-operatively. *indicates $p<0.05$. Error bars indicate SEM.

A

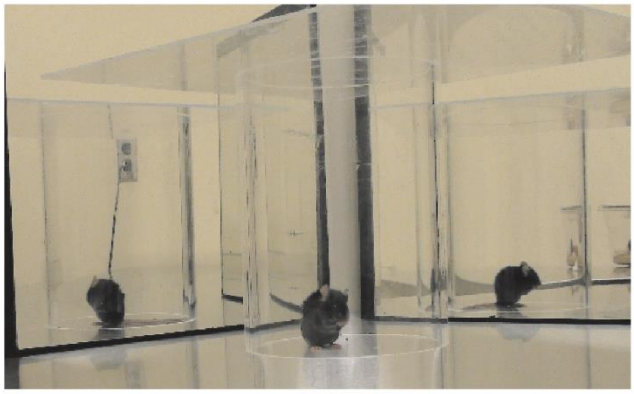

B Grooming Score Ipsilateral Forelimb

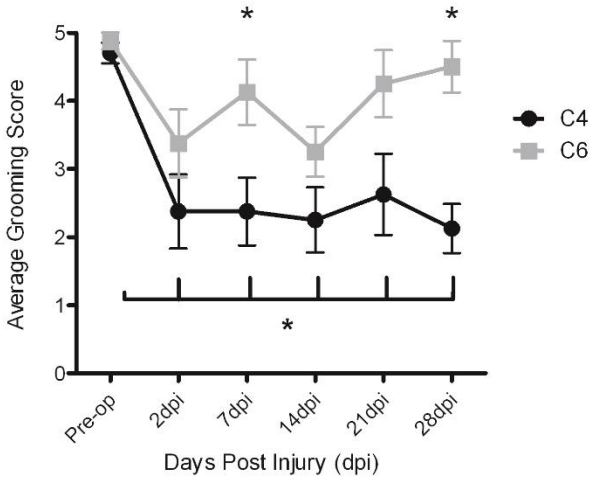

C Grooming Score Contralateral Forelimb

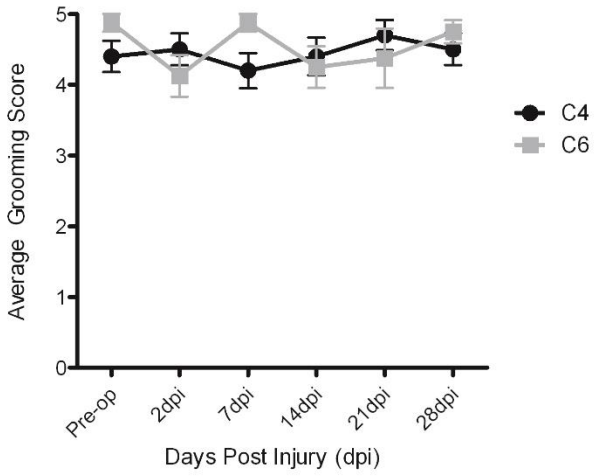

Figure 2.7 Staircase pellet reaching test (A,B) Quantification of the number of pellets eaten using the left/ipsilateral and right/contralateral forepaws, respectively. There was a sustained significant difference in the number of pellets eaten by mice with the left/ipsilateral forepaw compared to preoperatively following a C4 DLF crush ($p<0.05$). No significant differences were observed in the number of pellets eaten following C6 DLF crush. At 28 days post injury, there was a significant difference between the number of pellets eaten by mice with a C4 DLF crush and mice with a C6 DLF crush ($p<0.05$). No significant differences in the number of pellets eaten with the right/contralateral forepaw were observed. No significant difference in the number of pellets eaten with either the left/ipsilateral or right/contralateral forepaw was observed at 2 and 7 days post sham operation compared to pre-operatively. *indicates *p<0.05.* Error bars indicate SEM.

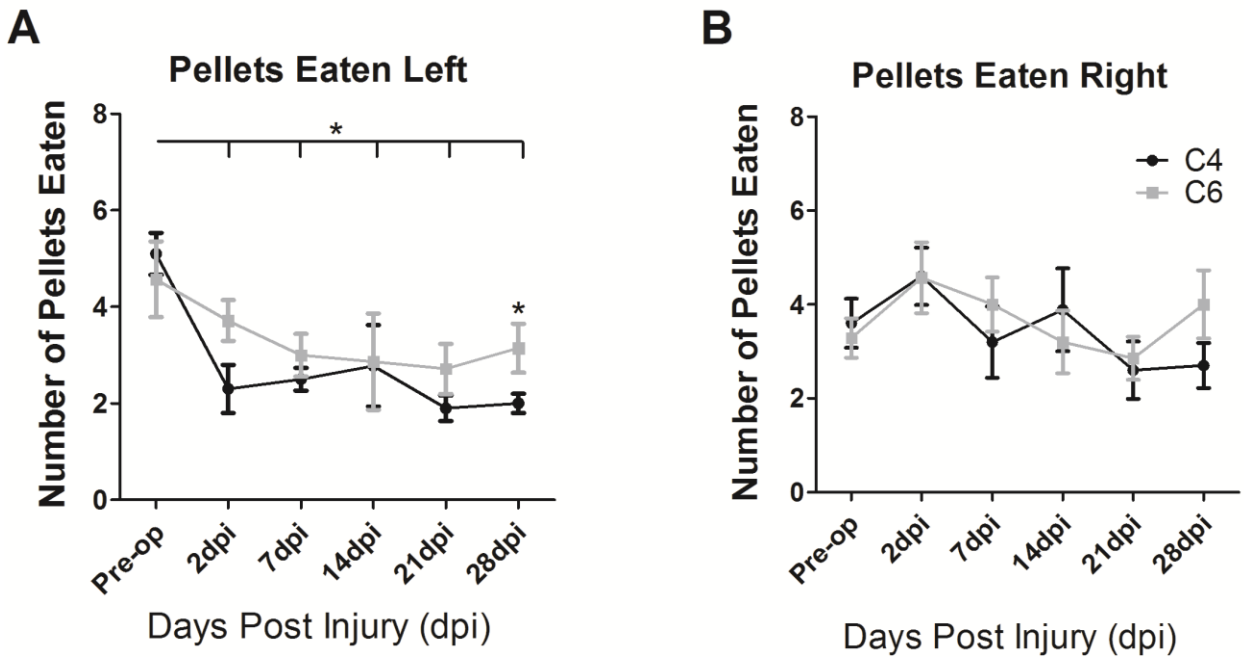

Figure 2.8 Horizontal ladder. (A,B) Cumulative error scores of the ipsilateral/left forelimb and ipsilateral/left hindlimb. After C4 DLF crush, there was a significant difference in CE score for both the ipsilesional forelimb and hindlimb at all time points post-operatively compared to pre-operatively ($p<0.05$). After C6 DLF crush, there was a significance difference in CE score for the ipsilesional forelimb at all time points except 28 days post-injury compared to pre-operatively ($p<0.05$). After C6 DLF crush, there was a significant difference in CE score for the ipsliesional hindlimb at all time points compared to preoperatively ($p<0.05$). No significant difference in CE score between those with a C4 DLF crush and those with a C6 DLF crush was found. No significant difference in CE score at 2 and 7 days post sham operation compared to pre-operation was found. (C,D) CE scores of the contralateral/right forelimb and contralateral/right hindlimb. There was no significant difference between the groups or at any time point compared to pre-operatively. *indicates $p<0.05$. Error bars indicate SEM.

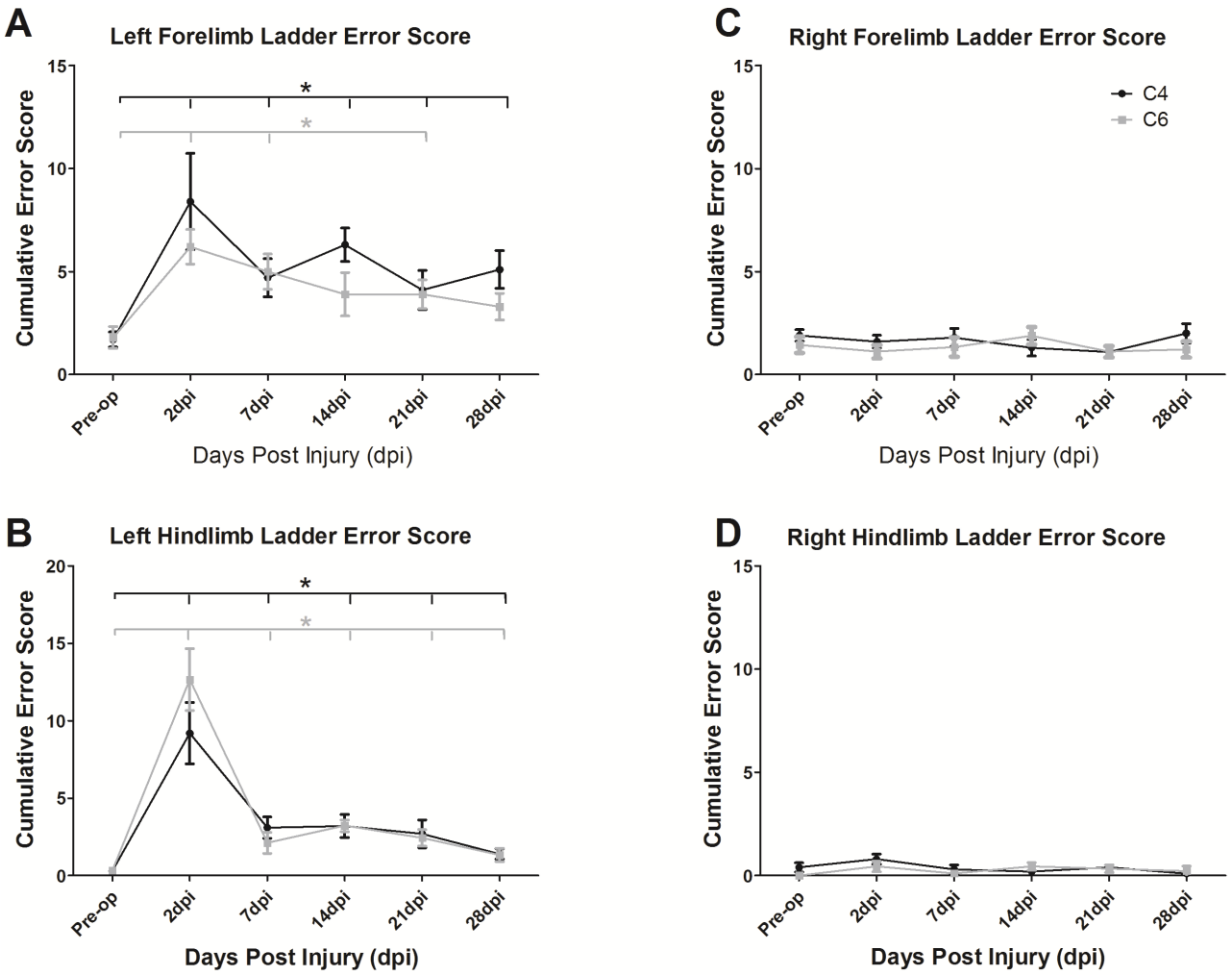
A
Left Forelimb Ladder Error Score
Cumulative Error Score
Days Post Injury (dpi)
C
Right Forelimb Ladder Error Score
C4
C6
B
Left Hindlimb Ladder Error Score
D
Right Hindlimb Ladder Error Score
Pre-op
2dpi
7dpi
14dpi
21dpi
28dpi

Figure 2.9 CatWalk automated gait analysis. (A,B,C,D) Quantification of stride length for the left and right forelimbs and hindlimbs. There was a significant decrease in stride length in mice following a DLF crush at C4 in both left and right forelimbs and hindlimbs ($p<0.05$). There was a significant difference in stride length between those with a C4 DLF crush and those with a C6 DLF crush in the ipsilateral/left forelimb at 2, 7, 21, and 28 days post-injury (A, $p<0.05$), in the contralateral/right forelimb at 7, 14, 21, and 28 days post-injury (C, $p<0.05$), in the ipsilateral/left hindlimb at 2, 7, 21, and 28 days post injury (B, $p<0.05$), and in the contralateral/right hindlimb at 2, 7, 21, and 28 days postinjury (D, $p<0.05$). There was no significant difference in any CatWalk parameter at 2 and 7 days following sham operation compared to pre-operatively. * indicates $p<0.05$. Error bars indicate SEM.

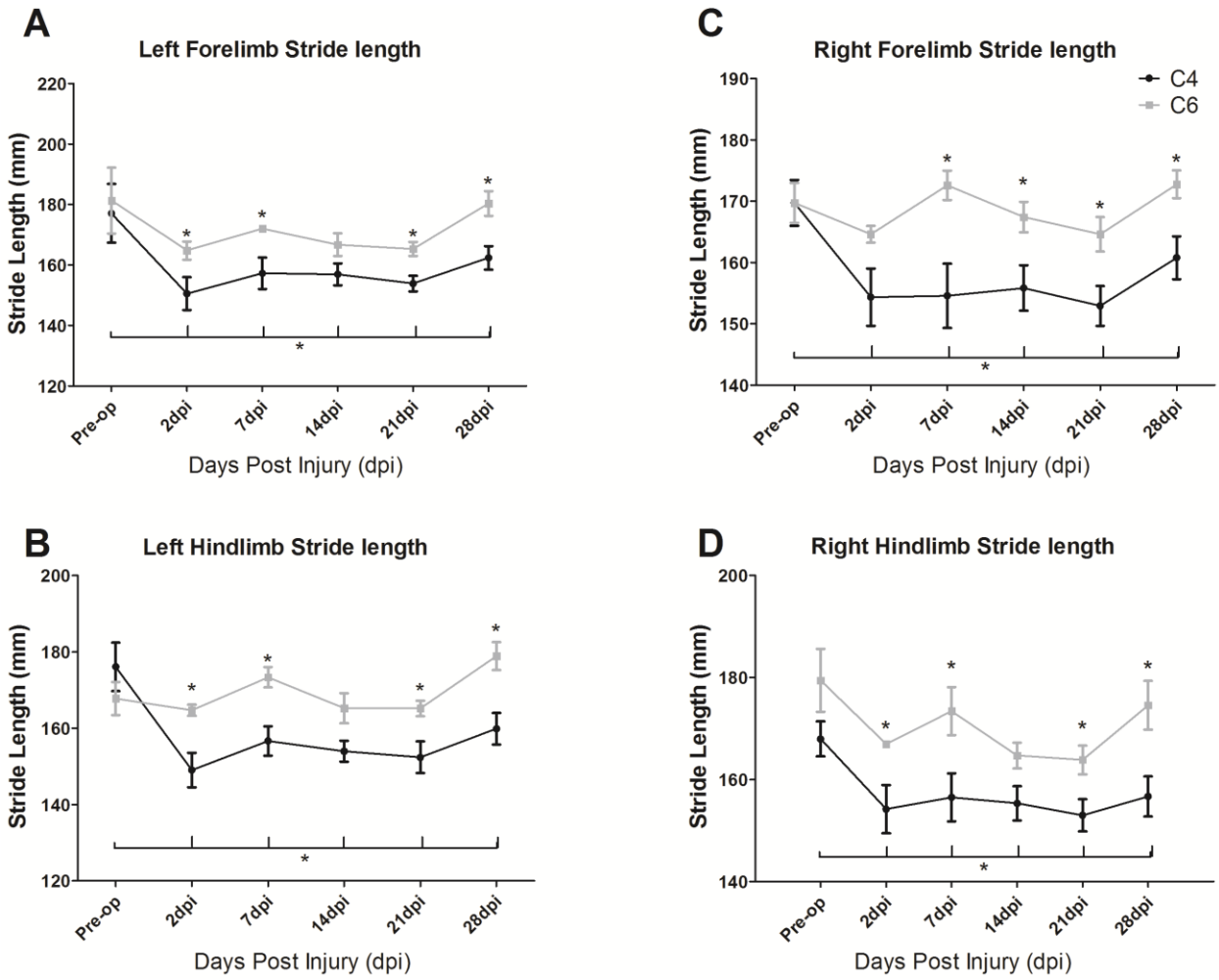
A
Left Forelimb Stride length
Stride Length (mm)
220
200
180
160
140
120
Pre-op
2dpi
7dpi
14dpi
21dpi
28dpi
Days Post Injury (dpi)
C
Right Forelimb Stride length
C4
C6
Stride Length (mm)
190
180
170
160
150
140
Days Post Injury (dpi)
B
Left Hindlimb Stride length
Stride Length (mm)
200
180
160
140
120
Days Post Injury (dpi)
D
Right Hindlimb Stride length
Stride Length (mm)
200
180
160
140
Days Post Injury (dpi)

Chapter 3. An age-related decline of PTEN deleted rubrospinal neurons for axon regeneration following spinal cord injury.

3.1 Introduction

SCI is increasingly inflicted in older populations (DeVivo and Chen, 2011; Singh et al., 2014a). The average age of incidence for spinal cord injury has risen substantially in recent years, from ~29 in the 1970s to ~42 since 2010 in the United States (National Spinal Cord Injury Statistical Center) due to an increasingly active older population. This changing demographic calls for a critical need to better understand how aging impacts recovery and repair after spinal cord injury. Despite the central importance of axon regeneration in spinal cord repair (Bradke and Marin, 2014; Silver et al., 2015), how aging impacts CNS axon regeneration is not well understood – largely because CNS axons even in young adult mammals naturally have a very limited ability to regenerate after injury. The recent discovery of neuron-intrinsic factors whose manipulation reproducibly promotes axon regeneration in the CNS (Lu et al., 2014) has made it possible to address this question.

To assess the impact of increased age on CNS axon regeneration, we asked whether genetic *Pten* deletion, a molecular manipulation that promotes significant CNS axon regeneration in young adult mammals (Park et al., 2008; Liu et al., 2010), remains effective in older animals (up to 7-8 months old). PTEN is a negative regulator of the mTOR (mammalian target of rapamycin) signaling pathway (Ma and Blenis, 2009). Neuronal mTOR activity undergoes

development-dependent decline and is further downregulated after axonal injury in the adult CNS (Park et al., 2008; Liu et al., 2010). Genetic *Pten* deletion in young animals prevents axotomy-induced reduction of mTOR activity and promotes the regeneration of both retinal ganglion and corticospinal tract (CST) axons after CNS injury (Park et al., 2008; Liu et al., 2010).

Here I examined the effect of age on axon regeneration in the mammalian CNS using the rubrospinal tract (RST) as the model system and the DLF crush injury model developed in Chapter 2. The data indicate that aging may dissociate neuron-intrinsic growth state and axon regeneration in *Pten* deleted mice, neuronal properties previously considered inseparable. Specifically, while *Pten* deletion in 7-8 month old mice continues to promote neuron-intrinsic growth state as assessed by mTOR activity, neuronal soma size and axonal growth proximal to a spinal cord injury, it loses effectiveness in promoting axon regeneration distal to the injury as compared with young (4 week old) mice. These results reveal an age-dependent decline in CNS axon regeneration and implicate changes in neuron-extrinsic influences in this age-dependent decline.

3.2 Materials & methods

3.2.1 Surgeries

All procedures were approved by the Animal Care Committee of the University of British

Columbia in accordance with the guidelines of the Canadian Council for Animal Care. The *Pten* conditional allele (*Pten*^{flox}, or *Pten*^{f}) was obtained from the Jackson Laboratory (B6.129S4-*Pten*^{tm1Hwu}*/J*; Stock # 006440) (Lesche et al., 2002). 4 week or 7-8 month old *Pten*$^{f/f}$ mice were injected with 0.5 µl of adeno-associated virus serotype 2 (AAV) encoding Cre and GFP or GFP only as control [Vector BioLabs; AAV2-Cre-GFP and AAV2-GFP, titer of 1 x 10^{12} GC/ml] into the right red nucleus (coordinates from bregma: 3.5 mm posterior, 0.7 mm lateral, 3.5 mm ventral to the surface of the brain). Four weeks following red nucleus AAV injection, mice underwent a dorsolateral funiculus (DLF) crush at the level of the fourth cervical vertebra (C4) to unilaterally sever the rubrospinal tract similarly to as previously described (Hilton et al., 2013a). Briefly, a midline incision was made over the cervical vertebrae and a C4 left hemilaminectomy was performed. The dura mater overlying the gray matter was pierced with a 26-gauge needle, and fine tipped Dumont #5 forceps with custom tips ~200 µm in width were inserted, with one prong inserted into the dorsal horn gray matter to a depth of ~ 1 mm and the other prong placed lateral to the dorsolateral funiculus. The forceps were closed and held for 15 seconds to sever the RST; the forceps were removed and inserted again in order to repeat this crush once. The muscles and skin were then closed with sutures and mice were permitted to recover in a heated incubator.

3.2.2 Immunostaining

Half of all longitudinal sections from each mouse were processed to visualize GFP+ RST axons by incubating sections overnight with antibodies specific to GFP (chicken α; Chemicon AB16901; 1:1000) and GFAP (DAKO Z0334; polyclonal Rabbit α; 1:1000). Brain and spinal cord sections were incubated overnight with antibodies specific to NeuN (guinea pig α;

Millipore ABN90P; 1:500), GFP (chicken α; Chemicon AB16901; 1:1000), Phospho-S6 (Rabbit α; Cell Signaling Ser235/236 2211S; 1:200), GFAP (Rat α; DAKO Z0334; 1:500), CS-56 (Mouse α; Sigma C8035; 1:100, Sox9 (Goat α; R&D, AF3075, 1:200), and Aldh1L1 (Rabbit α; Abcam, Ab87117, 1:1000) followed by appropriate Donkey α Guinea Pig Alexa Fluor 405 (706-156-148), Donkey α Chicken Alexa Fluor 488 (703-546-155), Donkey α Rabbit Alexa Fluor 594 (711-586-152), Donkey α Mouse546 (A10036) and Donkey α Rat 488 (A21208) for 2 hours.

3.2.3 Quantification of RST axon regeneration after DLF crush.

All quantifications were performed by observers blind to animal genotypes and age. Digital images were taken with an Axioplan 2 microscope (Zeiss, Jena, Germany) equipped with Northern Eclipse software at 10x (EMPIX Imaging, Inc., Mississauga, ON, Canada). Perpendicular lines were drawn on GFAP positive sections through the lesion epicenter and at 500 µm intervals to 1.5 mm rostral and 2.5 mm caudal total distance. GFP+ images were superimposed onto the lines and the sum of GFP+ axons crossing each line was recorded. The numbers of counted fibers was normalized by the value ascertained at 1.5 mm rostral to injury to obtain Axon Number Indices both rostral and caudal to injury. For the RST regeneration experiments, we quantified the following: N = 8 (4 week Ctrl), 8 (7-8 month Ctrl), 8 (4 week KO), 8 (7-8 month KO).

3.2.4 Quantification of soma area index and p-S6 intensity index.

Three sections spaced 120 µm apart through the caudal 400 µm of the magnocelullar red

nucleus for each mouse were used for measurement of cross-sectional area and p-S6 immunoreactivity. Images were taken with a Zeiss Axio Observer Z1 equipped with a Yokogawa X-1 Spinning Disk using Zen Blue software. The spline contour function in Zen Blue was used to manually measure NeuN+ rubrospinal neurons. NeuN+ neurons were outlined if their nucleus or nucleolus could be detected or if they possessed a characteristic stellate morphology. From these measurements, p-S6 immunoreactivity (Alexa Fluor 594 intensity), and cross sectional areas were obtained. At least 100 GFP+ NeuN+ and at least 400 NeuN+ neurons (200 per each red nucleus) were counted for each mouse. pS6-Intensity Indices were calculated for GFP+ NeuN+ neurons and GFP- NeuN+ neurons as a ratio in comparison to the uninjured side.

3.2.5 Quantification of GFAP/CS-56 immunoreactivity & astrocyte cell counts

A 300 µm wide (rostral/caudally) and 750 µm long (medial/lateral) rectangle was superimposed onto each longitudinal section at the lesion epicenter and on the contralateral uninjured side directly opposite to the lesion site. Immunoreactivity intensity for GFAP and CS-56 were calculated using Zen Blue with normalization to the contralateral uninjured side. Four sections encompassing the inner 640 µm of the lesion dorsal-to-ventral were averaged for each animal to calculate the Staining Ratio. A triple staining for GFAP, Aldh1L1 and Sox 9 was performed as this allows for unambiguous staining of astrocytes (Pompolo and Harley, 2001; Cahoy et al., 2008; Zhang et al., 2014); and personal communication, Michael Sofroniew). The total cell number co-expressing these three markers was quantified in a 500 µm radius around the injury site to obtain an astrocyte cell number / mm^2. Three sections per animal were averaged.

3.2.6 RST dieback analysis.

AAV-Cre-GFP or AAV-GFP for control were injected into the right red nucleus as above in *Pten*$^{f/f}$ mice that were 12-13 months of age. Six weeks later, mice underwent a left DLF crush SCI as above. One day later, 0.5 µL of BDA (10%, Invitrogen) was injected into the right red nucleus at the same coordinates as virus above to anterogradely trace the axotomized rubrospinal tract. At one week post-injury, mice were perfused as above and their cervical spinal cords from C2 to C8 cut into 20 µm longitudinal sections in the coronal (longitudinal) plane on a cryostat and stored at -80°C. Sections were thawed for one hour, and incubated with antibody towards GFAP polyclonal rabbit anti-GFAP (1:1000; DAKO Z0334) overnight after blocking with 10% normal donkey serum for half an hour. The next day, Donkey α Rabbit Alexa Fluor 405 and Streptavidin conjugated to Alexa Fluor 594 (both 1:200) were applied for 2 hours prior to coverslipping. In a blinded fashion, images were taken of the lesion site of three sections per mouse spaced 160 µm apart encompassing the major bundle of RST axons at the lesion site with a Zeiss Axio Observer Z1 equipped with a Yokogawa X-1 Spinning Disk using Zen Blue software. The injury epicenter was identified via GFAP staining, and the distance of axon tips in white matter to the lesion epicenter were measured to assess the effect of *Pten* deletion and aging on axonal dieback.

3.3 Results

3.3.1 Assessment of rubrospinal regeneration following PTEN KO

In control AAV-GFP injected control mice, the injured rubrospinal tract underwent characteristic dieback from the lesion site (**Fig. 3.1A-B''**). In contrast, when *Pten* deletion was initiated at 4 weeks of age, the main RST bundle extended into the lesion epicenter (**Fig. 3.2C-C'', E**), with Axon Number Index at the injury center significantly higher than controls (all normalized to 1.5 mm rostral to lesion) (**Fig. 3.1E**). Whereas in control mice there was no RST axon detected at or beyond 1.0 mm caudal to injury, in *Pten* deleted mice RST axons were found to extend up to 1.5 mm caudally to injury (**Fig. 3.1C-C'', F**). Injured RST axons took a route to grow laterally towards the injury site in the gray matter following *Pten* deletion (as seen on the horizontal sections in **Fig. 3.1C-C''**). These data demonstrate that, when initiated at a young age (4 weeks), *Pten* deletion can efficiently promote RST regeneration after injury.

3.3.2 Influence of aging on rubrospinal regeneration following PTEN KO

When *Pten* deletion was initiated at 7-8 months of age, a substantial decrease in RST regeneration caudal to the injury site was observed as compared with the 4-week group (**Fig. 3.1D-D'', F, H**). At 0.5 mm caudal to injury, Axon Number Index in the 7-8 month deletion group was not significantly different from (non *Pten*-deleted) control mice but was significantly lower than that of the 4-week group (**Fig. 3.1F**). This number dropped to zero

with no GFP positive axons observed at or beyond 1 mm caudal to injury (**Fig. 3.1H**). Nevertheless, *Pten* deletion resulted in a significantly higher Axon Number Index irrespective of age when compared with the control groups at 0.5 mm rostral to injury and at the injury epicenter (**Fig. 3.1E, G**). *Pten* deletion in old mice did not impact RST axonal dieback, assessed 7 days after injury, when compared with age-matched control wild-type mice (**Fig. 3.2D-F**). Together, these data indicate that *Pten* deletion in older mice remains effective in eliciting rostral RST axon growth towards and into the spinal cord injury site but has a substantially diminished effect on promoting RST regeneration beyond the injury site.

3.3.3 *Pten* deletion prevents axotomy-induced mTOR downregulation and cell atrophy in both rubrospinal regardless of age

Previous studies indicate that rubrospinal neurons undergo cell atrophy (as indicated by soma size shrinkage) following axonal injury (Kobayashi et al., 1997a; Carter et al., 2008) and that *Pten* deletion leads to enlarged soma size in retinal ganglion neurons (Park et al., 2008). Aging may impact the regeneration-promoting effect of targeting *Pten* in two different ways. First, *Pten* deletion in aging mice may not be as effective in rescuing axotomy-induced downregulation of mTOR activity and associated cell atrophy. Second, *Pten* deletion may still rescue axotomy-induced mTOR downregulation and cell atrophy in aging mice but other factors intrinsic or extrinsic to neurons contribute to regeneration failure. To distinguish these two possibilities, we analyzed the effect of different ages on the ability of *Pten* deletion to rescue axotomy-induced mTOR downregulation and cell atrophy.

The level of p-S6 (phospho-S6 ribosomal protein), an indicator of mTOR activity, is relatively high in the red nuclei compared to the rest of the midbrain in uninjured adult mice (**Fig. 3.3A-C**), consistent with the purportedly higher innate growth ability of RST neurons. In control AAV-GFP injected mice, p-S6 levels were significantly reduced in axotomized rubrospinal neurons as compared with uninjured contralateral neurons (**Fig. 3.3B, G**). This reduction occurred to a similar level in both the 4 week group and the 7-8 month group, regardless of GFP labeling (**Fig. 3.3D-E**). However, in AAV-Cre-GFP injected, *Pten*-deleted mice, GFP positive rubrospinal neurons did not undergo p-S6 downregulation regardless of age (**Fig. 3.3C, G**). In contrast, GFP negative rubrospinal neurons in the same red nuclei, which presumably had not undergone *Pten* deletion and were thus wild-type (WT), exhibited a similar level of p-S6 downregulation as in injured, AAV-GFP injected controls (**Fig. 3.3G**).

In control AAV-GFP injected mice, massive atrophy of rubrospinal neurons was observed regardless of GFP labeling (**Fig. 3.3B, H**), as indicated by a reduction in the average cell surface area of NeuN positive cells in the red nucleus as compared to that of contralateral uninjured neurons ($p < 0.05$, **Fig. 3.3H**). This occurred regardless of age as there was not a significant difference between the 4 week AAV-GFP injected group and the 7-8 month AAV-GFP injected group (**Fig. 3.3H**). In contrast, *Pten* deletion completely prevented rubrospinal cell body atrophy regardless of age (**Fig. 3.4**). Together, these data indicate that despite the greatly diminished regeneration, *Pten* deletion remains effective in preventing axotomy-induced downregulation of mTOR activity and associated cell atrophy in rubrospinal neurons at increased ages.

3.3.4 Increased expression of astroglial GFAP at the injury site in older animals

Because *Pten* deletion promoted mTOR signaling and axon growth rostral to injury irrespective of age in the rubrospinal system, we hypothesized that differences in environmental influences at and around the lesion site could be responsible for the age-dependent decline in axon regeneration beyond the injury site. To provide initial support for this hypothesis, we compared the expression of several well known markers associated with glia-derived growth inhibition in young and older mice by immunohistochemistry 6-8 weeks after injury such as the astroglial marker GFAP and chondroitin sulfate proteoglycans (CS-56).

3.3 Discussion

The changing demographics of people who sustain an SCI or other CNS injuries related to axonal pathology underscore the importance of understanding the effect of age on axon regeneration. In this study, we assessed the role of aging in regeneration following *Pten* deletion in rubrospinal neurons. The data indicate that *Pten* deletion prevents axotomy-induced mTOR downregulation and cell atrophy, and promotes axonal growth proximal to the injury site independent of age, indicating that *Pten* deletion remains effective in elevating neuron-intrinsic axon growth ability in older adults. However, axon regeneration distal to the injury site is greatly diminished at increasing ages in *Pten*-deleted mice, and astrogliosis in response to SCI is enhanced in aged animals relative to young animals, suggesting that other factors, in particular those associated with the injury site, are more prevalent in older mice.

These data suggest that regenerative therapies of mid-aged to aging individuals will have to take an increasingly hostile lesion environment into consideration.

Our finding that adult rubrospinal neurons express a relatively high level of p-S6 is consistent with the notion that these neurons possess a higher intrinsic axon growth capacity than CST neurons. Previous work by us and others indicates that treatment of the red nucleus with brain derived neurotrophic factor (BDNF) promotes rubrospinal axonal regeneration and rescues atrophy(Kobayashi et al., 1997a; Kwon et al., 2002b). In the present study, we showed for the first time that *Pten* deletion also promotes axonal regeneration from rubrospinal neurons. Downstream signaling from BDNF and its receptor TrkB involves the phoaphatidylinositol-4,5-biphosphate 3-kinase (PI3K)/Akt/mTOR pathway, of which PTEN is a primary antagonist(Numakawa et al., 2010). Thus, the effect of *Pten* deletion may at least in part reflect its role in regulating BDNF/TrkB signaling, which remains to be tested experimentally. The fact that both the CST, which is particularly refractory to regeneration, and the RST, which has some ability to grow after injury, can be driven to regenerate by *Pten* deletion strengthens the case for the PTEN/mTOR pathway as a central regulator of axon regeneration in multiple descending motor pathways. Consequently, a general PTEN inhibition strategy might be beneficial by promoting substantial axon growth in multiple descending systems concurrently.

Since most CNS neurons do not regenerate to any significant extent even in young adults, it has not been practically possible to systematically study the impact of different ages on the

regenerative ability of CNS neurons. *Pten* deletion promotes significant CST and RST regeneration, which allowed us, for the first time, to examine the effect of age on axon regeneration after injury in the adult mammalian CNS. Although CST and RST differ significantly in their innate regenerative abilities, the models employed here to study their regeneration differ significantly (thoracic dorsal hemisection vs. cervical dorsolateral funiculus crush respectively), and the two axonal tracts were studied in two different laboratories, strikingly similar results were found, indicating that our observations regarding the age effect on axon regeneration may be generally applicable to other CNS neurons.

The most important conclusion from this study is that at increased age, the regeneration-promoting effect of *Pten* deletion is greatly diminished. While *Pten* deletion in young mice (4 week old at the time of AAV injection) promotes rubrospinal axon regeneration >1 mm caudal to the injury, *Pten* deletion in mid aged mice (7-8 month old at the time of AAV injection) no longer elicits significant regeneration over control levels. In the CST, *Pten* deletion has increasingly diminished effect on regeneration from P1, 4-6 weeks, 10 weeks to 12months of age at the time of AAV injection, such that there was little if any regeneration in the oldest age group, and very limited regeneration even at the 10 week group. The small degree of regeneration in the 10 week group was surprising. However, this may be partially due to a relatively short survival time in our CST experiments (6 weeks). Indeed, because our comparisons were made with the same survival time between different groups, it is possible that aging simply slows the speed at which regeneration can occur. A longer survival time may allow for a higher degree of CST or RST regeneration in all age groups. A time point analysis of the extent of regeneration at each age will be important to determine if this is the

case.

Despite the greatly diminished regeneration distal to the injury site, three pieces of evidence indicate that *Pten* deletion in older adults remained effective in elevating neuron-intrinsic growth potential in rubrospinal neurons. First, axonal growth rostral to the injury site were enhanced in older PTEN-deleted mice just as in their younger counterparts. Second, *Pten* deletion prevented axotomy-induced downregulation of mTOR activity (as assessed by p-S6 immunoreactivity) regardless of age. Third, *Pten* deletion prevented axotomy-induced cell atrophy (as assessed by cell soma area) regardless of age. Consistent with this, a recent study using *C. elegans* as the model system showed that loss of PTEN increased axon regeneration independent of age(Byrne et al., 2014a). Thus, PTEN inhibiting neuron-intrinsic growth potential in an age-independent manner may be evolutionarily conserved, except that in the aging mammalian CNS, additional factors may become prevalent in influencing the outcome of regeneration. The same *C. elegans* study further showed that insulin/IGF1 signaling specifically inhibited axon regeneration in aging worms but not young worms(Byrne et al., 2014a). Whether insulin/IGF1 signaling specifically inhibits central axon regeneration in aging adult mammals is an interesting avenue for further research.

Thus, it appears that while targeting PTEN continues to elevate neuron-intrinsic growth potential in older adults, additional growth restrictions become activated during a transition between young and middle adulthood. One possibility is that the effect of aging is neuron-intrinsic. Indeed, it has been shown that aging changes the cortical transcriptome after SCI in

aged mice in comparison to young mice(Jaerve et al., 2012). Although we assessed p-S6 immunoreactivity following axotomy and *Pten* deletion, finding no age related differences, it is conceivable that other downstream effectors of mTOR besides p-S6 (e.g. 4E-BP(Guertin and Sabatini, 2007; Yang et al., 2014b)) may be affected differently in aging versus young *Pten* deleted neurons. On the other hand, other downstream effectors of the PI3K/Akt pathway besides mTOR (e.g. GSK-3(Zhou and Snider, 2005; Adler et al., 2006; Dupraz et al., 2009)) may also be differently regulated with aging and result in a decrease of axon regeneration in the old animal.

Another possibility is that the extrinsic environment of the CNS changes with age to exert increased inhibition of axon regeneration, and/or that older neurons acquire a higher sensitivity to these extrinsic inhibitory cues. Our observations that *Pten* deletion rescued axotomy-induced mTOR downregulation and cell atrophy and promoted rostral axonal growth but failed to promote caudal axon regeneration support this hypothesis. Obvious candidates include the glial scar and its associated inhibitors such as chondroitin sulfate proteoglycans, myelin debris and associated inhibitors, but other factors may also play a role(O'Callaghan and Miller, 1991). We did not observe change in overall CSPGs or NogoA expression levels. However we cannot exclude that the exact CSPGs composition is altered after SCI in aged animals(Jones et al., 2003b; Andrews et al., 2012). Alternatively, the peak of expression of such inhibitory molecules could have occurred at earlier time points, as is the case for Nogo (our unpublished observation). Following stroke, aging has been shown to increase the expression of genes associated with stress and inflammation, and to increase expression of MAG and OMgp, components of myelin known to inhibit axon growth, as well

as Lingo-1, co-receptor of the NgR1 inhibitory complex(Li and Carmichael, 2006; Li et al., 2010). Moreover, it has been suggested that NgR1 receptor expression is increased in the spinal cold of older mice(McGee et al., 2005). It would be of interest to determine if similar, or even more pronounced changes occur after SCI in aged mice.

Interestingly, we found that SCI in mid-aged animals increased gliosis following injury relative to young adult animals. An increase in gliosis in the CNS has been previously documented(Barrett et al., 1984; O'Callaghan and Miller, 1991; Kullberg et al., 1998), but this is the first time to our knowledge that such an increase has been associated with SCI. In this regard, it is notable that following traumatic brain injury and stroke, glial reactivity and scar formation are accelerated in aged animals compared to young(Badan et al., 2003; Castillo-Ruiz et al., 2007; Sandhir et al., 2008). Neurite outgrowth from embryonic neurons is markedly less when cultured with aged (24 month) versus young neurons through a GFAP-dependent mechanism(Jones et al., 2003b) and GFAP null astrocytes provide a favorable substrate for neurite outgrowth(Miron et al., 2013). Still, caution is warranted, as our results do not provide conclusive evidence that heightened GFAP expression or gliosis specifically diminishes axon growth in aged PTEN deleted neurons.

In summary, we show that while rubrospinal axonal regeneration occurs following *Pten* deletion, the regenerative response evoked is heavily dependent on age, suggesting that additional mechanisms of axonal inhibition become more prevalent during the transition from young to mid-adulthood. Since many injuries occur at higher ages, elucidating the

mechanisms underlying this may be necessary for the development of robust therapeutic strategies to promote functional regeneration following CNS injury.

Figure 3.1 The effect of age on RST regeneration in *Pten* deleted mice after C4 dorsolateral funiculus crush spinal cord injury. (A-D") Representative images of spinal cord horizontal sections showing GFP-labeled RST axons around the injury site (arrow) from control (Ctrl) or *Pten* deleted mice (KO). 4 week and 7-8 month refer to the age at which *Pten* deletion was initiated by AAV-Cre-GFP injection into the right red nucleus of $Pten^{f/f}$ mice. Panels A', B', C', and D' are 160 μm ventral to A, B, C, and D respectively, while panels A'', B'', C'', and D'' are 320 μm ventral to A, B, C, and D respectively. AAV-GFP injection served as the control. Here we include a 7-8m KO animal with relatively higher GFP labeling (D) to exemplify the lack of caudal axon growth in aged *Pten* KO animals. Scale bar = 200 μm. (E) Quantification of RST axon labeling rostral to and at (0.0 mm) the injury site. Two-way ANOVA followed by Bonferroni's *post hoc* test, $*P < 0.05$, Black *, 4w and 7-8m KO vs. 4w and 7-8m WT. (F) Quantification of caudal RST axon regeneration. Two-way ANOVA followed by Bonferroni's *post hoc* test, $**P < 0.01$, Red **, 4w KO vs. 7-8 m KO, 4w WT, and 7-8m WT. (G) Axon Number Index observed at the middle of the injury site. This is the same information shown at 0.0 mm from injury site in (E). (H) Cumulative Axon Number Index observed at ≥1 mm caudal to the injury site. N = 8 (4w WT); 8 (7-8m WT); 8 (4w KO); 8 (7-8m KO).

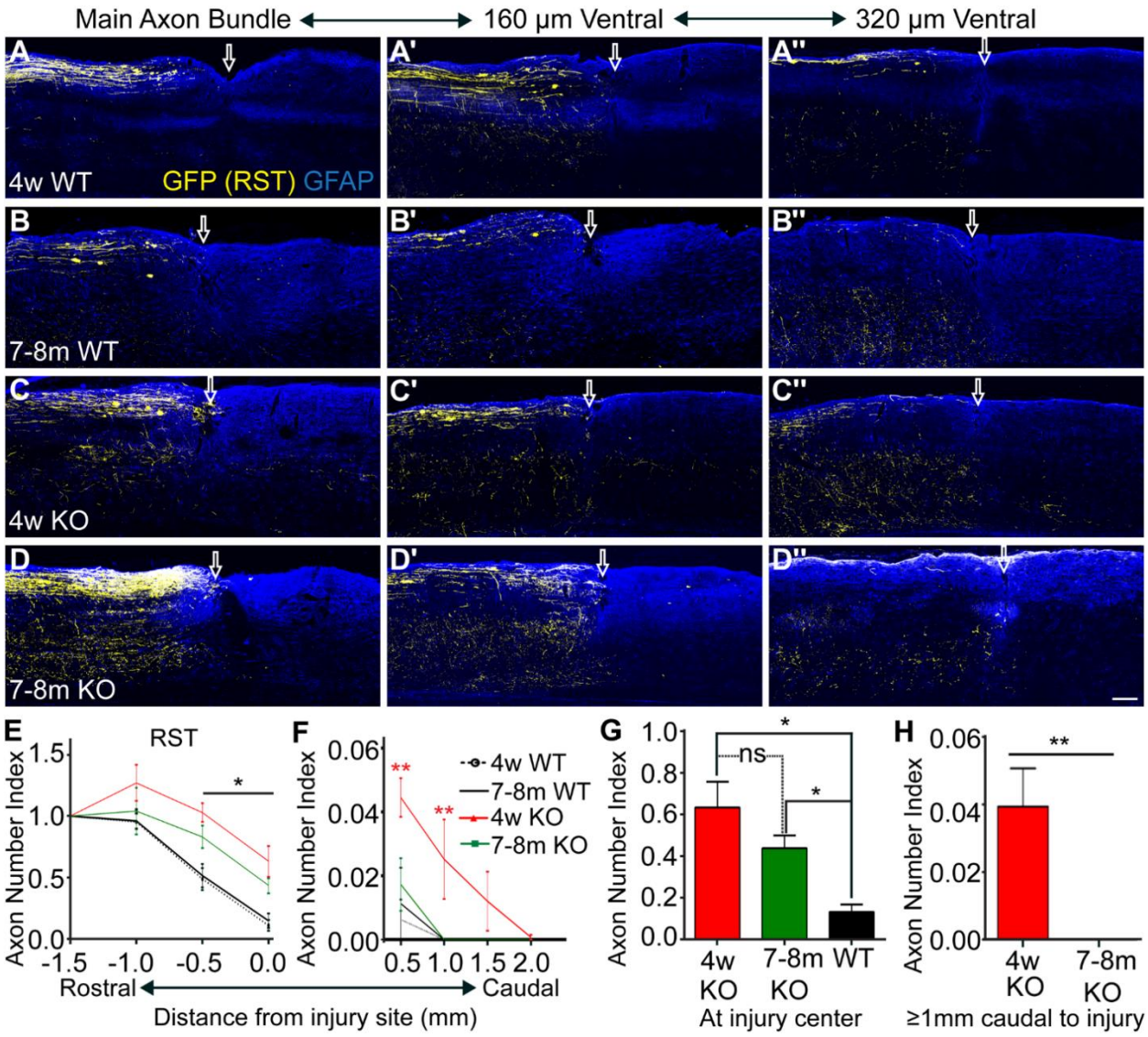
Main Axon Bundle
160 µm Ventral
320 µm Ventral
A
A'
A''
4w WT
GFP (RST) GFAP
B
B'
B''
7-8m WT
C
C'
C''
4w KO
D
D'
D''
7-8m KO
E
RST
Axon Number Index
Rostral
Caudal
Distance from injury site (mm)
F
4w WT
7-8m WT
4w KO
7-8m KO
G
ns
At injury center
H
≥1mm caudal to injury

Figure 3.2. Axonal dieback in 4-6 week old and 12-13month old mice. A-B) Representative images of spinal cord horizontal sections showing BDA labelled RST axons in 4-6 week old (A, C) or 12-13 month old (B, D) mice that are wild-type (A,B) or *Pten* KO (C,D) at 7 days post-injury. C) Average retraction from the injury site of RST axons in white matter in aging mice. Axonal dieback at 7 days post-injury is significantly higher in aged VS. young mice irrespective of *Pten* KO. N = 3 per group. Scale bar = 100 µm.

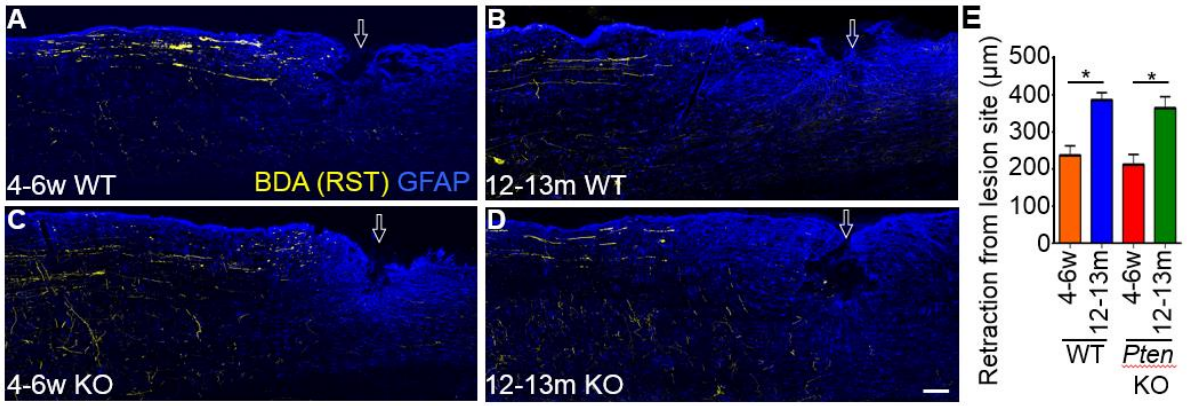

Figure 3.3 *Pten* deletion prevents axotomy-induced p-S6 downregulation and soma size reduction of rubrospinal neurons of both the young and old groups. Lower (A) and higher (B, C) magnification views of a representative transverse section through midbrain and magnocellular red nuclei stained with antibody to p-S6. Note the relatively high expression of p-S6 by magnocellular red nucleus. This 7-8 month old control mouse underwent C4 dorsolateral funiculus (DLF) lesioning of the RST and was euthanized 8 weeks later. Note the lower p-S6 levels on the injured side (C) as compared to the uninjured side (B). (D) Representative images of rubrospinal neurons stained for NeuN (aqua), GFP (green), and p-S6 (red) following AAV injection into the vicinity of the right red nucleus. (E) Quantification of p-S6 intensity of rubrospinal neurons on the injured and AAV-injected side (ipsilateral) normalized to the uninjured red nucleus (contralateral). (F) Quantification of average soma area of NeuN+ rubrospinal neurons after injury with and without *Pten* deletion. Sham, uninjured control. (G) Quantification of Soma Area Index expressed as the ratio of the average cross sectional area of NeuN+ neurons in axotomized red nucleus over that of contralateral uninjured red nucleus. Scale bar = 250 μm (A); 50 μm (B, C, D). One-way ANOVA followed by Bonferroni's *post hoc* test, $*P < 0.05$.

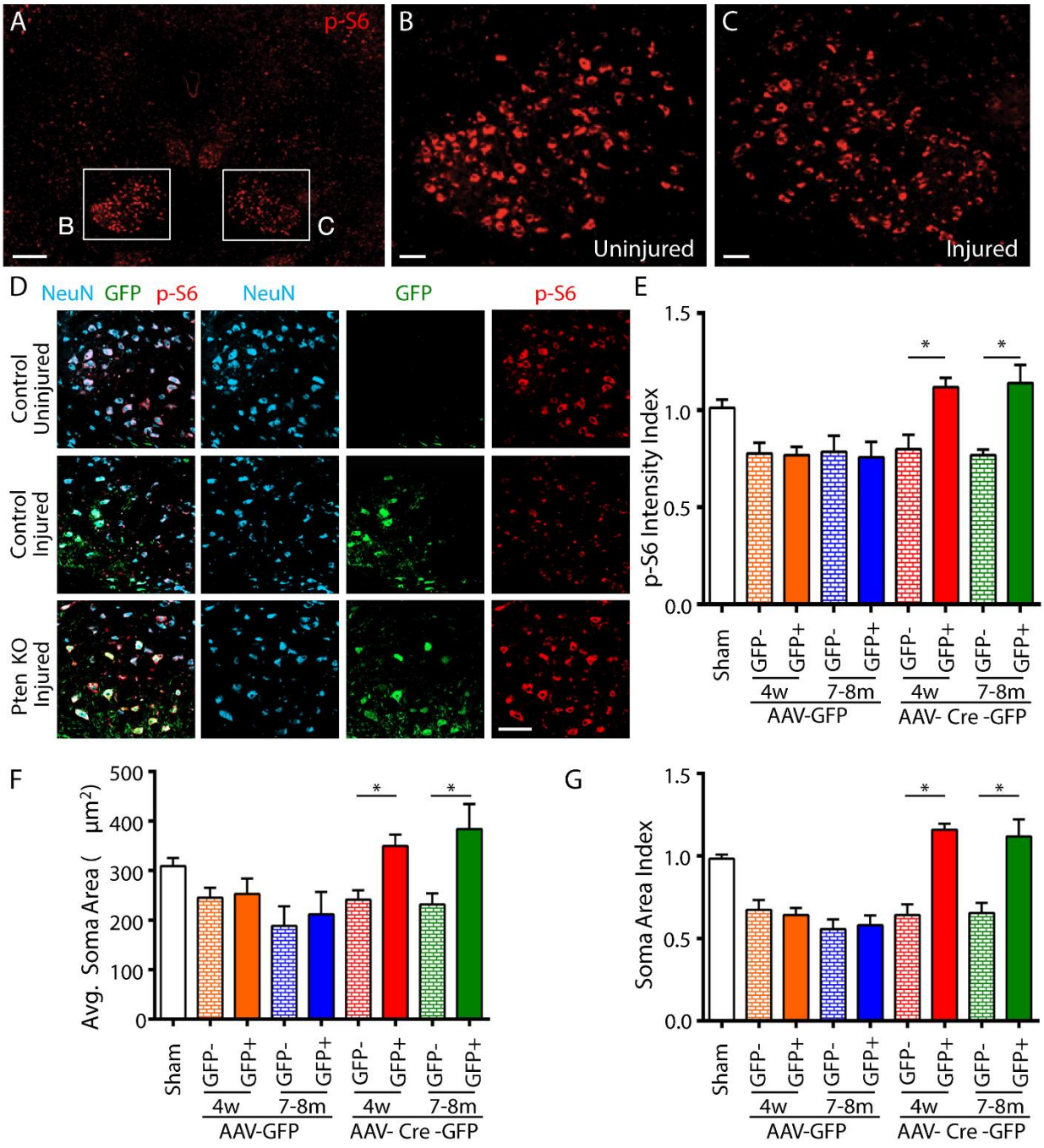
A
p-S6
B
C
B
Uninjured
C
Injured
D
NeuN GFP p-S6
NeuN
GFP
p-S6
Control Uninjured
Control Injured
Pten KO Injured
E
p-S6 Intensity Index
1.5
1.0
0.5
0.0
*
*
Sham
GFP-
GFP+
GFP-
GFP+
GFP-
GFP+
GFP-
GFP+
4w
7-8m
4w
7-8m
AAV-GFP
AAV- Cre -GFP
F
Avg. Soma Area (µm²)
500
400
300
200
100
0
*
*
Sham
GFP-
GFP+
GFP-
GFP+
GFP-
GFP+
GFP-
GFP+
4w
7-8m
4w
7-8m
AAV-GFP
AAV- Cre -GFP
G
Soma Area Index
1.5
1.0
0.5
0.0
*
*
Sham
GFP-
GFP+
GFP-
GFP+
GFP-
GFP+
GFP-
GFP+
4w
7-8m
4w
7-8m
AAV-GFP
AAV- Cre -GFP

Figure 3.4 Histogram of cross-sectional area plotting neurons in 100-μm^2 increments demonstrates a normalization of the distribution of cell sizes with *Pten* deletion. A) Histogram of cross-sectional area following AAV-GFP injection. B) Histogram of cross-sectional area following AAV-Cre-GFP injection. Note the predominance of small soma areas in GFP- neurons with AAV-Cre-GFP administration (B) and GFP+ or GFP- neurons with AAV-GFP administration (A).

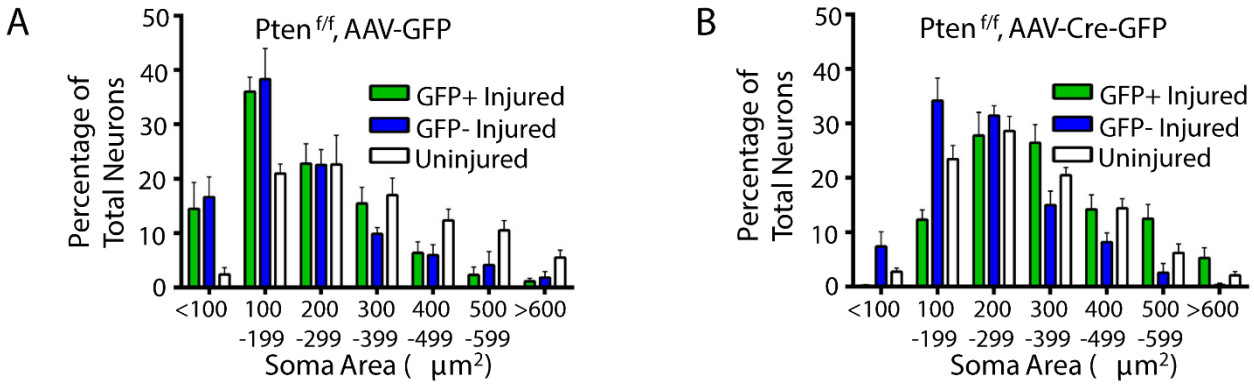

Figure 3.5 Aging is associated with increased expression of GFAP around the spinal cord injury site. A-B) Representative images and quantification (normalized to the contralateral side) of GFAP and CS-56 immunoreactivity 8 weeks after dorsolateral funiculus (DLF) crush injury in mice of different ages. Close up panels A1, A2, B1, and B2 show CS-56 immunoreactivity from A and B and close up panels A3, A4, B3, and B4 show GFAP immunoreactivity from A' and B'. C) GFAP and CS-56 quantification between young and aged mice following DLF Crush. There is significantly higher GFAP immunoreactivity in 7-8m aged mice VS. 4w aged mice (*$p<0.05$). There is no difference in CS-56 immunoreactivity between 7-8m aged VS. 4w aged mice.

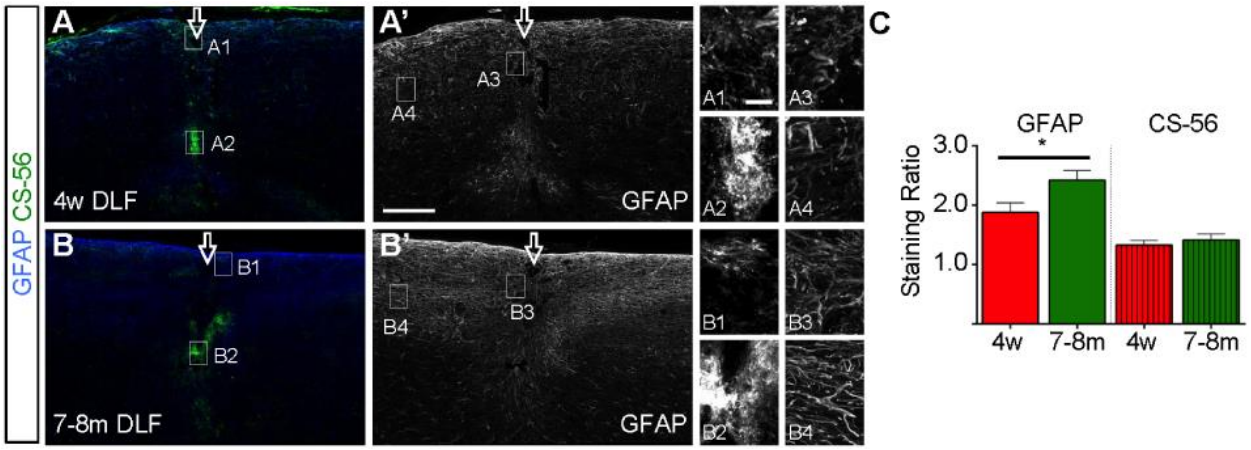

Figure 3.6 Astrocyte number following DLF crush does not increase with aging. A, B) Photomicrographs of GFAP, Aldh1L1 and SOX9 triple staining 8 weeks after dorsolateral funiculus lesion in mice with AAV injection at 4 weeks (A) and 7-8 months (B) of age. A', B') Close-up photomicrographs from A and B respectively. C) Quantification of astrocyte numbers. No significant difference in the number of astrocytes were observed between 4w and 7-8m aged mice at 8 weeks post injury. Scale bars are 200 µm in A and B and are 40 µm in A' and B'.

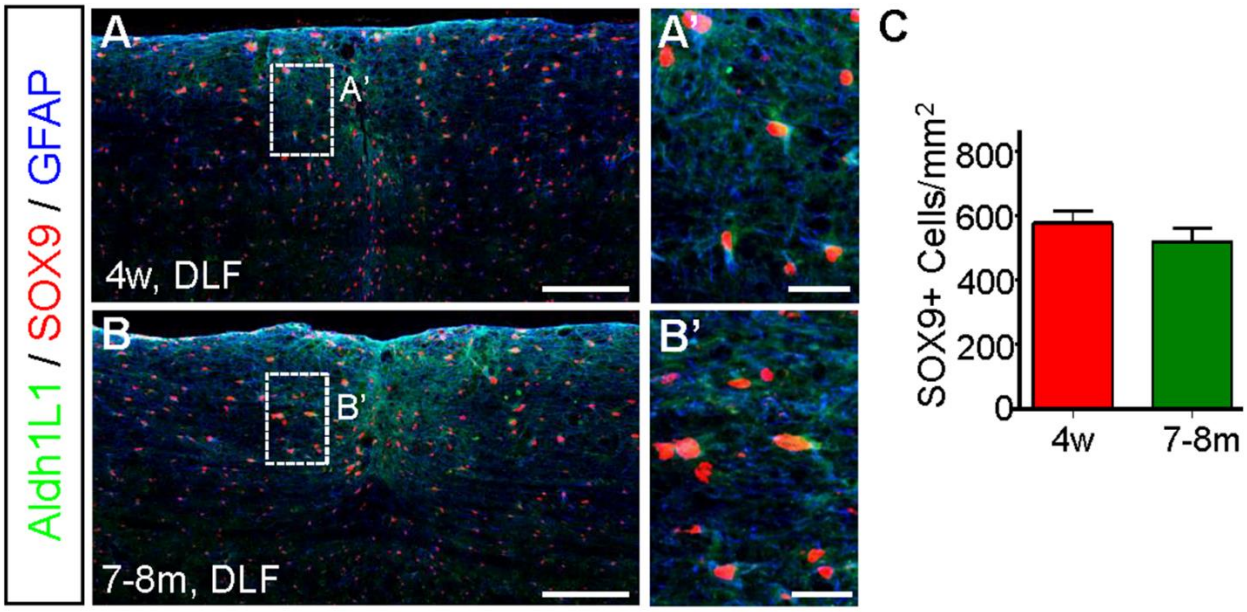

Chapter 4. Re-establishment of cortical motor output maps and spontaneous functional recovery via spared dorsolaterally projecting corticospinal neurons following dorsal column spinal cord injury in adult mice.

4.1 Introduction

Spinal cord injury (SCI) typically results in sustained motor, sensory, and autonomic dysfunction as a result of the limited capacity of the adult mammalian CNS to regenerate lost connections (Ramer et al., 2014). However, some spontaneous functional improvement commonly occurs, even after cervical, functionally sensorimotor complete injuries (Roth et al., 1991; Steeves et al., 2011), by one year post-injury. Such spontaneous recovery is well recapitulated by animal models of SCI, where a detectable degree of functional recovery is observed without intervention in both cervical and thoracic injury models (Basso et al., 1995; Gensel et al., 2006; Hilton et al., 2013a). The sensorimotor cortex is one substrate underlying spontaneous recovery following SCI and a wide range of other CNS disorders (Fouad et al., 2001; Raineteau and Schwab, 2001; Nudo, 2006; Nishimura and Isa, 2009). Corticospinal fibers exhibit anatomical plasticity which is correlated with spontaneous recovery based on some recovery observed when these fibers are spared in partial injury models (Weidner et al., 2001; Ghosh et al., 2009; Krajacic et al., 2010; Rosenzweig et al., 2010; Oudega and Perez, 2012). Corticospinal fibers also have the capacity to form relay circuits with propriospinal neurons following SCI in the absence of intervention(Bareyre et al., 2004; Vavrek et al., 2006; Ghosh et al., 2010). Still, the pathways through which the motor cortex mediates repair remain

only partially understood, and the extent to which corticospinal mediated recovery is a result of injured vs. uninjured pathways is unknown.

Here we performed a series of optogenetic, pharmacogenetic, behavioural, and anatomical experiments to assess the role of the motor cortex in mediating spontaneous recovery following a cervical level C3/C4 dorsal column SCI, which ablates the dorsal corticospinal tract (dCST) containing ~96% of corticospinal fibers. This lesion also severs dorsal column sensory afferents bilaterally cranial to most spinal neurons subserving forelimb function (Asante and Martin, 2013) and all spinal neurons subserving hindlimb function. Using optogenetic mapping, which provides a non-invasive, longitudinal, and quantitative approach to assessing cortical motor output (Ayling et al., 2009a), we find that the motor cortex is able to re-establish motor output to forelimb and hindlimb at the same latencies as pre-operatively by four weeks post-injury despite massive corticospinal and sensory loss. In C57/Bl6 background mice, there are ~12000 dorsal, ~400 dorsolateral, and ~100 ventral corticospinal axons at the cervical level, corresponding respectively to ~96%, ~3%, and ~1% of the total (Fink et al., 2015). Hypothesizing that uninjured corticospinal neurons substantiated the re-establishment of cortical motor output and spontaneous recovery, we took a pharmacogenetic approach to transiently inactivate spared dorsolaterally projecting corticospinal neurons by injecting an adeno-associated virus (AAV) expressing Cre-dependent hM4Di in sensorimotor cortex and an AAV expressing Cre in the dorsolateral funiculus well caudal to the injury in both injured and uninjured mice(Rogan and Roth, 2011). Following CNO administration in mice with C3/C4 dorsal column SCI, spontaneous recovery was abrogated and there was a greater change in skilled locomotion than in control uninjured mice using the same inactivation approach.

Given that only a fraction of the corticospinal neurons in the dorsolateral funiculus are effectively silenced, these data indicate that small numbers of spared dorsolaterally projecting corticospinal neurons mediate remarkable motor cortical plasticity and recovery following SCI. Targeting the plasticity of a few spared corticospinal neurons may thus be sufficient to drive substantial recovery following SCI and perhaps other CNS disorders or diseases.

4.2 Materials & methods

4.2.1 Spinal cord injury

All procedures were approved by the University of British Columbia Animal Care Committee in accordance with the guidelines of the Canadian Council on Animal Care. Female 3-4 month old mice expressing Channelrhodopsin-2 under the Thy-1 promoter [line 18, stock 007612, strain B6.Cg-Tg(Thy1-COP4/EYFP)18Gfng/J] on the C57/Bl6 background were used. For all surgeries and mapping procedures, body temperature was maintained at 37 ± 0.5 °C with an electric heating pad regulated by a rectal thermometer. Animals were anaesthetized with Isoflurane (4% for induction and 1.5% for maintenance). The skin overlying the neck was shaved, disinfected with Betadine and wiped off with 70% ethanol, and cut with a scalpel blade. The muscles of the dorsal neck were split along the midline, a laminectomy was performed to expose the third cervical spinal cord segment, and the dura mater overlying the centers of the dorsal horns was pierced on each side of the spinal cord with a 26-gauge needle.

Fine tipped Dumont #5 forceps with blades ground to a width of ~200 μm were inserted into the dorsal horns on each side of the dorsal column to a depth of ~1 mm. The forceps were closed and held for 20 s to crush the dorsal column completely, including the main contingent of corticospinal axons; the forceps were removed and inserted again in order to repeat this crush once. Sham operated mice received a laminectomy only (Hilton et al. 2013).

4.2.2 Horizontal ladder

Error frequency was assessed for the forelimbs and hindlimbs using a horizontal ladder modified as previously described (Cummings et al., 2007; Hilton et al., 2013a). Briefly, mice were videotaped with a high-definition camera (Sony, HDR-Hc1) as they crossed a 5.2 cm wide horizontal ladder with 31 rungs spaced 1.3 cm apart. Each mouse repeated the task five times. Frame-by-frame video analysis by a blinded observer was used to generate scores for the number of errors (rung misses, rung slips, or rung drags) and number of steps for the forelimbs and hindlimbs over each run and percent error values were calculated from each (percent error = number of errors/number of steps x 100). Mice were trained to perform the task by crossing the ladder 3 times each 2 and 3 days prior to injury. One day prior to injury, mice were tested preoperatively to obtain pre-injury scores, 4 hours post-operatively for acute, and on 3, 7, 14, 21, 28, 42, and 56 postoperatively.

4.2.3 Chronic cranial window

Under isofluorane anaesthesia (4% for induction and 1.5% for maintenance mixed with 1% oxygen), Metabond (Edgewood, NY, USA; Product: C&B Metabond) was applied generously

on top of the skull and a 5 X 5 mm cover glass was placed on top of the right hemisphere over intact skull and pressed flat into the adhesive. If necessary, more adhesive was applied around the cover glass for reinforcement. Mice were permitted to recover under a heat lamp and pre-injury mapping commenced one week following the chronic cranial window preparation.

4.2.4 Optogenetic motor mapping

The methodology for optogenetic motor mapping has been described in detail (Ayling et al., 2009a). Briefly, we used a scanning stage (ASAI MS-2000) controlled by custom Igor Pro software (Wavemetrics) to direct a fixed 473 nm laser beam (Crystalaser, 10 msec pulses, 0.5-2 mW total or 63-252 mW/mm^2) to a grid of cortical sites, typically 12 X 14, with 300 μm spacing. This process was repeated 2-3 times to obtain a mean value for each pixel of the map. Stimulation was delivered in a semi-random order with the requirement that sites stimulated in sequence be >750 μm away from each other. Optogenetic motor mapping occurred with identical stimulus intensity for all sites within a map and for each mouse at all time-points before and after SCI. Movements were detected using laser range motion sensors (Keyence LK-081) with sub-mm sensitivity targeted to the left forelimb and hindlimb, which were fitted with bracelets made of rubber tubing (Etsy; Brooklyn NY) glued to 12 mm diameter round cover slips painted white which provided large, flat targets for the motion sensors. The limbs were suspended slightly above the ground so that they could move freely along the axes of measurement of the motion sensors. Responses were considered to be genuine only if their amplitude exceeded three times the standard deviation of the 500 msec prestimulus period

within 100 msec following stimulus onset. A single injection of ketamine/xylazine (100/10 mg/kg) was administered at the beginning of each mapping session (duration 20-30 min). With this dose of anaesthetics mapping of the entire cortex could be performed in 20-30 minutes, not requiring a supplementary dose which might have introduced the possibility of anaesthetic artefacts. We mapped each mouse 1 week prior to injury to establish baseline maps, acutely, and at 3, 7, 14, 21, and 28 days post-operatively.

4.2.5 Dorsolateral corticospinal DREADD Experiment

Viral mediated expression of a G protein-coupled receptor (Gi/o-coupled human muscarinic M4 designer receptor exclusively activated by a designer drug, hM4Di) activated by the otherwise pharmacologically inert ligand clozapine-N-oxide (CNO) was used to pharmacogenetically and transiently (1-2 hours(Rogan and Roth, 2011)) silence dorsolateral corticospinal fibers that projected 3-4 segments caudal to the injury. Cre-dependent AAV1-*hSyn-dio-hM4D(Gi)-mCherry* (UNC Vector Core, University of North Carolina at Chapel Hill) was injected into the sensorimotor cortices of mice (1.5 µl total, 0.5 µl per injection site at 3 injection sites: rostral/caudal coordinates from bregma in mm: 0.6 mm, 0.1 mm, -0.4 mm; all 1.5 mm right of the midline and 0.7 mm depth from the surface of the brain) in n = 12 mice at 4 weeks post-injury and n = 12 mice 4 weeks post-sham operation. In n = 6 injured and n = 6 sham mice, cortical AAV injection was followed by spinal injection with AAV1-Cre (Vector Biolabs; Malvern, Pennsylvania) into the left dorsolateral funiculus (0.6 µl total, 0.3 µl per injection site into 2 injection sites; into dorsolateral gray matter at 0.5 mm depth at C6/C7 and C7/C8 following hemilaminectomies at these sites. Control animals received cortical AAV injections only. At 56 days post-injury, mice were recorded for 5 runs on the horizontal ladder

task starting 10 minutes following i.p. injection of CNO (1 mg/kg; Enzo Life Sciences; Farmingdale, NY). This was repeated at 58 days post-injury, while on days 55 and 57 post-injury, mice were recorded on the horizontal ladder task following vehicle i.p. administration. The number of errors and placements by the forelimbs were recorded in a blinded fashion by a naïve rater scoring the videos, and the results from days 56 and 58 post-injury were averaged for each animal to generate a CNO error score while the result from days 55 and 57 were the vehicle error score.

4.2.6 Sensorimotor cortical immunohistochemistry

Following the DREADD experiment as above, at 59 or 60 days post-injury, half of the injured and half of the sham operated mice were administered CNO (1 mg/kg) while the other half received vehicle. Mice were then ran repeatedly on the horizontal ladder for 15 minutes in an effort to induce *c-fos* gene expression. One hour after the conclusion of the horizontal ladder, mice were killed with an overdose of chloral hydrate (100 mg/kg, i.p.) and perfused transcardially with phosphate-buffered saline (PBS) followed by phosphate-buffered freshly hydrolysed 4% paraformaldehyde (pH 7.5). Motor cortices and cervical spinal cords were dissected, post-fixed in 4% paraformaldehyde overnight, and cryoprotected in 12%, 18%, and 24% sucrose in 0.1 M phosphate buffer over 3 days before being snap frozen in isopentane over dry ice. Motor cortices (from ~2 mm caudal to bregma to ~2 mm rostral to bregma) were cut into 20 µm cross sections on a cryostat and stored at -80°C. Frozen sections were thawed for 1 hour, rehydrated in 10 mM PBS for 10 min, and incubated with 10% normal donkey serum (in 0.1% Triton X-100) for 30 min. Goat anti-c-Fos (1:500; Santa Cruz Biotechnology and rabbit anti-dsRed (1:200; Clontech) were applied overnight at room temperature.

Secondary antibody (1:200, Jackson) raised in donkey and conjugated to AlexaFluor 405 and 594 were applied for 2 hours at room temperature in addition to fluorescent Nissl 640/660 (1:500; Neurotrace Invitrogen). Sections were cover-slipped in Fluoromount-G (Southern Biotech). In a blinded fashion, images were taken of sensorimotor cortex sections (~2 mm caudal to bregma to ~2 mm rostral to bregma; consistent with area that, when optically stimulated, led to limb movement) on which mCherry+ neurons could be identified with a Zeiss Axio Observer Z1 equipped with a Yokogawa X-1 Spinning Disk using Zen Blue software at 20x magnification. Counts of mCherry+ neuron numbers and c-fos+ mCherry+ neuron numbers were then made based on these images. The layer identification of mCherry+ neurons was made based on Nissl staining. Imaging and counts were made blind to injury status and CNO/vehicle administration.

4.2.7 mCherry spinal cord analysis

Sections of cervical spinal cord were incubated with rabbit anti-dsRed (1:200; Clontech) overnight at room temperature followed by secondary antibody raised in donkey and conjugated to AlexaFluor 594 (1:200; Jackson) for 2 hours at room temperature. Sections were coverslipped in Fluoromount-G (Southern Biotech). In a blinded fashion, images of 3 sections for each animal of the dorsal columns, left dorsolateral funiculus, and ventral funiculus were taken with a Zeiss Axio Observer Z1 equipped with a Yokogawa X-1 Spinning Disk using Zen Blue software at 40x magnification. Counts of mCherry+ fiber numbers in the dorsal and dorsolateral funiculi were then made based on these images and averaged. Imaging and counts were made blinded to injury.

4.2.8 dCST Injury Analysis

Frozen cervical spinal cord sections were thawed for 1 hour, rehydrated in 10 mM PBS for 10 min, and incubated with 10% normal donkey serum (in 0.1% Triton X-100) for 30 min. Rabbit anti-PKCγ (1:200; Millipore), and goat anti-green fluorescent protein (GFP) (1:1000; DAKO) were applied overnight at room temperature. Secondary antibody (1:200, Jackson) raised in donkey and conjugated to AlexaFluor 488 and 594 were applied for 2 hours at room temperature. Sections were cover-slipped in Fluoromount-G (Southern Biotech). To verify injury to the corticospinal tract, digital images of transverse sections of C1 and C8 spinal segments in addition to transverse sections of the lesion site were captured with an Axioplan 2 microscope (Zeiss, Jena, Germany) equipped with Northern Eclipse software (Empix Imaging, Inc., Mississuga, ON, Canada) at 10x. Eriochrome Cyanine R staining was used to assess lesion epicenter area, while PKCγ and YFP immunoreactivity were used to assess the completeness of dCST lesions.

4.2.9 Statistics

All data are presented as mean ± S.E.M. Statistical significance was set at $p<0.05$. Homogeneity of variance was tested for using Bartlett's test. Normality was tested for using the Shapiro Wilk test. Horizontal Ladder data and optogenetic motor mapping data were analyzed using two-way repeated measures ANOVAs (groups vs. time). DREADD experimental data were analyzed using both a two-way ANOVA (groups vs. time) as well as with a one-way ANOVA comparing CNO vs. vehicle scores across groups. mCherry fiber

counts were analyzed using either the Mann Whitney U-Test or a One-Sample t-test. mCherry and *c-fos* neuron counts/percentages were analyzed using Mann Whitney U-Tests. Multiple comparisons corrections and statistical significance were determined using the Holm-Sidak method. Statistical tests were performed using GraphPad Prism version 6.0.

4.3 Results

4.3.1 Longitudinal optogenetic and behavioural analysis of motor system deficits and recovery following spinal cord injury.

We performed a series of optogenetic, pharmacogenetic, behavioural, and anatomical experiments in line-18 transgenic mice which express ChR-2 robustly in layer 5 pyramidal neurons driven by the Thy-1 promoter (Arenkiel et al. 2007; Ayling et al. 2009). In Thy1-ChR2 mice, we found high expression of ChR-2 within the dorsal corticospinal tract (dCST) via immunostaining of sections of cervical spinal cord (**Fig. 4.1A**) and performed anterograde tracing of sensorimotor cortex with BDA to assess corticospinal anatomy. This revealed that the vast majority of corticospinal axons descended via the dCST (**Fig. 4.1B**) with a minor component descending via the dorsolateral funiculus (dlCST) (**Fig. 4.1C**). Very little to no BDA was found within the ventral funiculus (**Fig. 4.1D**), although a new study with near complete labelling of the CST has found that there are ~100 ventral corticospinal axons in C57/Bl6 mice in addition to ~12000 dorsal and ~400 dorsolateral (Fink et al., 2015), corresponding to ~96% dCST, ~3% dlCST, and ~1% vCST.

The motor cortex projects to the spinal cord via the dCST, dlCST, and vCST, but also provides major excitatory input to brainstem motor nuclei which also descend spinal pathways involved in limb control, including the red nucleus (RN; which projects the rubrospinal tract) and the reticular formation (RF; which projects the reticulospinal tract) (**Fig. 4.1E**). After C3/C4 dorsal column SCI, the dCST is interrupted, but corticofugal pathways to these brain stem nuclei in addition to the dlCST and vCST are spared and might mediate recovery. We assessed sensorimotor behavioural dysfunction using a horizontal ladder task and quantified motor cortical output to the limbs from acute to chronic stages of injury using optogenetic motor mapping (Ayling et al., 2009a; Harrison et al., 2012; Harrison et al., 2013; Anenberg et al., 2014) which provides repeated, fast, and relatively selective optical interrogation of motor corticofugal circuitry. To map as noninvasively as possible, we employed a chronic cranial window preparation through the intact skull which provided optical access to the right cortical hemisphere (**Fig. 4.1G**)(Silasi et al., 2013b). Cranial windows were 5 x 5 mm in size, extending ~1 mm across the midline and ~2.5 mm rostral and ~2.5 mm caudal from bregma. Mice were allowed at least one week to recover from cranial window surgery before motor mapping commenced. To generate cortical motor maps, laser motion sensors directed at targets worn by the left wrist and ankle of the mouse recorded movements evoked by optogenetic stimulation of a 12 x 14 grid of cortical points over the right hemisphere (**Fig. 4.1G**), with maps generated as the mean of responses from 2-3 repetitions with the minimum laser amplitude (0.5-2 mW) necessary to evoke movement for each animal prior to injury. In order to exclude artifactual movement, responses were only considered to be genuine if their amplitude exceeded three

times the standard deviation of the 500 msec pre-stimulus period within 100 msec following stimulus onset.

4.3.2 C3/C4 dorsal column SCI results in sustained deficits and partial recovery on the horizontal ladder task.

We first employed an SCI model to bilaterally ablate the dorsal corticospinal tract (dCST) and dorsal column sensory afferents and assessed the effect of this injury on behavioural sensorimotor function using a horizontal ladder task (Hilton et al., 2013; Wang et al., 2015). To sever the dCST and sensory afferents, custom made forceps with tips ground to ~200 μm (Hilton et al., 2013a) were used to lesion the dorsal column at the cervical C3/C4 level ventral to the level of at least the central canal, which disrupted the dorsal columns and dorsal CST axons and partially compromised the gray matter of the dorsal horns and intermediate zone (**Fig. 4.2A-C**). Animals whose lesions did not sever the entire dCST by absence of either YFP or PKCy staining caudal to injury were excluded from analysis (n = 1). Sham operated animals received a laminectomy at C3/C4 only. On the horizontal ladder task, while C3/C4 dorsal column injury resulted in a deficit in forelimb skilled locomotion to 56 days post-injury, there was spontaneous yet incomplete recovery on days 42 and 56 post-injury (**Fig. 4.2D-E**). At 7 days post-injury, mice with C3/C4 dorsal column SCI made forelimb errors during 24.4±2.6% of placement attempts made vs. 3.78±0.65% prior to injury. However, at 56 days post-injury, the same mice made forelimb errors during 11.3±1.02% of placement attempts, representing a 48.7±5.17% recovery from the 7 day post-injury time point ($p<0.01$). Still, even at 56 days post-injury, the error percentage for the forelimbs was higher than preoperatively, indicating that the recovery was only partial ($p<0.05$). Hindlimb horizontal ladder function completely

and spontaneously recovered by 14-21 days post-injury relative to sham operation (**Fig. 4.2 F-G**). Thus, C3/C4 dorsal column SCI results in sustained deficits and partial spontaneous recovery in forelimb skilled locomotion by 56 days post-injury.

4.3.3 Effect of acute SCI on cortical motor output.

Because optogenetic motor mapping can generate representations in as few as 5 minutes, it is at least an order of magnitude faster than electrical stimulation based approaches and thus capable of assessing how the motor cortex responds immediately following injury (Anenberg et al., 2014a). To assess how the motor cortex responds following acute SCI, we initiated mapping 10-30 minutes following injury. To aid map analysis, motor maps were upsampled to pixel sizes of 100 x 100 μm and aligned based on the position of bregma. Acutely, although optogenetic stimulation consistently evoked forelimb and hindlimb movement, FL and HL were greatly diminished in area and output (**Fig. 4.3**). FL was reduced from an area of 7.69 ±0.89 mm^2 preoperatively to an area of 2.34 ±0.17 mm^2 acutely ($p<0.001$). Forelimb motor output was also reduced to 24.29±12.25% that of baseline ($p<0.01$). Notably, FL was displaced following acute SCI, with a caudal shift in center position from 0.30±0.14 mm rostral to bregma preoperatively to 0.35±0.07mm caudal to bregma acutely, occupying a similar territory as HL ($p<0.01$). HL was also reduced in area from 5.14±0.49 mm^2 to 1.95±0.24mm^2 ($p<0.001$) and output was reduced to 39.57±22.81% that of baseline ($p<0.05$). In sham operated mice, no changes in map properties were observed (all $p>0.24$).

4.3.4 Longitudinal re-establishment of motor cortical output by four weeks post-injury.

Next we investigated the capacity of forelimb and hindlimb motor cortex to re-establish output following C3/C4 dorsal column injury by mapping the same mice at 3, 7, 14, 21, and 28 days post-operatively. We observed spontaneous re-establishment of both FL and HL motor maps longitudinally (**Fig. 4.4**). Although FL remained displaced caudally at 3 days post-injury relative to preoperatively ($p<0.05$), by 7 days post-injury it had re-established the same position as preoperatively, and remained in this position up to 28 days post-injury. On a similar timeline, FL motor output was re-established by 7 days post-injury, while map area and latency to forelimb movement were re-established by 21 days post-injury. HL also re-established output spontaneously following injury, with motor map area and output diminished at 3 days post-injury but re-established by 7 days post-injury and latency to hindlimb movement re-established by 14 days post-injury. Thus, even in the absence of the vast majority of descending corticospinal transmission and substantial sensory loss, the adult mouse cortex has the capacity to re-establish forelimb and hindlimb motor output (with properties such as latency similar to pre-injury) by 4 weeks post-injury.

4.3.5 Specific DREADD Receptor expression in dorsolaterally projecting corticospinal neurons.

Our optogenetic motor mapping experiments demonstrated that the motor cortex was able, over the course of 3-4 weeks, to longitudinally re-establish output to forelimb and hindlimb following C3/C4 dorsal column SCI at the same latency as preoperatively, suggesting that the corticospinal pathway underlies the partial recovery observed on the horizontal ladder.

Axotomized corticospinal neurons harbour a capacity for relay formation with propriospinal neurons which may have mediated the recovery observed (Bareyre et al., 2004; Vavrek et al., 2006; Nishimura and Isa, 2012). Alternatively, recovery may have occurred due to rewiring of the minor dorsolateral corticospinal pathway that was spared from our injury paradigm. To dissociate between these two possibilities, we use a Cre-dependent pharmacogenetic strategy to specifically and transiently inactivate spared dorsolaterally projecting corticospinal neurons (**Fig. 4.5**). Corticospinal neurons harbour a capacity for retrograde transduction by AAVs following spinal administration (Jara et al., 2012; Jara et al., 2014; Wahl et al., 2014). We took advantage of this characteristic by administering a Cre-dependent hM4Di expressing AAV to sensorimotor cortex and AAV expressing Cre several (3-4) segments caudal to injury or sham operation at 4 weeks post-injury (hM4Di Cre+). Thus, only dorsolaterally projecting corticospinal neurons would be dual transduced in injured mice, since the dCST would not be in proximity to the Cre virus at C6/C7 or C7/C8 following its ablation at C3/C4. In control mice, no Cre virus was administered (hM4Di Cre-). hM4Di is a Gi/o-coupled DREADD (Designer receptor exclusively activated by designer drug) receptor which is specifically activated by the pharmacologically inert ligand clozapine-*N*-oxide (CNO). Following CNO activation, hM4Di activates G-protein associated inwardly rectifying potassium channels, leading to membrane hyperpolarization and silencing of neurons for ~1-2 hours (Rogan and Roth, 2011). hM4Di was tagged with mCherry, allowing us to verify that expression was confined to dorsolaterally projecting corticospinal neurons in injured mice (**Fig. 4.5D**). No mCherry+ labelling was found within the ventral funiculus, excluding dual transduction of ventrally projecting corticospinal neurons (**Fig. 4.5F**). This was not a surprise, since the vCST is an ipsilaterally projecting pathway (Weidner et al.,

2001) and thus the left vCST descended from the left motor cortex, which was not injected with virus. In total, we counted 12.17±0.79 mCherry+ dorsolateral corticospinal fibers in injured mice and 11.67±0.67 dorsolateral corticospinal fibers in uninjured mice (**Fig. 4.5E**; p=0.55). However, in sham operated mice, our dual viral strategy also led to the appearance of 83.67±22.23 mCherry+ dorsal corticospinal fibers, in contrast to the absence of any dorsal CST fibers observed in SCI mice (**Fig. 4.5F**; $p<0.05$), as a result of transduction of the uninjured dCST in sham operated mice. Thus, there was a significantly higher total # of mCherry+ corticospinal fibers in sham operated mice vs. SCI mice ($p<0.01$) but in injured mice mCherry was confined to dorsolaterally projecting corticospinal neurons.

4.3.6 DREADD receptor activation in dorsolaterally projecting corticospinal neurons abrogates spontaneous recovery on the horizontal ladder.

We assessed the necessity of dorsolaterally projecting corticospinal neuronal function in the spontaneous recovery observed on the horizontal ladder task with hM4Di activation by CNO at 56 and 58 days post-injury with comparison to execution of the task at 55 and 57 days post-injury following vehicle administration (**Fig. 4.6**). Although a lower left forelimb error percentage was observed following vehicle administration at 55 and 57 days vs. 7 days post-injury, no difference was observed vs. 7 days post-injury following CNO administration at 56 and 58 days (**Fig. 4.6B**; $p<0.01$), indicating that the dorsolaterally projecting corticospinal neurons silenced were necessary for the spontaneous recovery observed. CNO administration led to a higher left forelimb error percentage in SCI and sham operated hM4Di Cre+ mice ($p<0.001$ for SCI and $p<0.05$ for sham; **Fig. 4.6C**) but the loss of performance in CNO vs vehicle treated mice was higher in the SCI vs. sham operated group. ($p<0.01$; **Fig. 4.6D**)

despite there being no difference in the number of mCherry+ dorsolateral corticospinal fibers between the groups and an overall higher number of mCherry+ corticospinal fibers in the sham operated mice as a result of partial transduction of the uninjured dCST. Thus, spared dorsolaterally projecting corticospinal neurons compensated for SCI in mediating partial behavioural recovery.

4.3.7 Assessment of mCherry and c-fos in sensorimotor cortex following DREADD receptor activation.

To validate our approach, we assessed mCherry labelling in sensorimotor cortices of both SCI and sham hM4Di Cre+ mice and counted the number of mCherry+ neurons to provide a more direct assessment of the number of hM4Di-mCherry+ neurons (**Fig. 4.7**). Consistent with specific corticospinal transduction, mCherry labelling was confined to layer V neurons (**Fig. 4.7A**). Counts of mCherry+ neurons revealed there were significantly more in sham operated mice vs. SCI mice ($p<0.01$). In total, we counted 30.83±2.91 mCherry+ neurons in injured mice and 211.3±55.49 mCherry+ neurons in uninjured mice ($p<0.01$). Thus, the behavioural effect observed, which included a greater loss of performance in SCI mice vs. sham operated mice (**Fig. 4.6C**) occurred despite there being substantially more mCherry+ corticospinal neurons in sham operated mice than in SCI mice (**Fig. 4.7B**).

To provide a more direct demonstration that hM4Di activation silences CST neurons, we also assessed immunoreactivity for the marker of neuronal activity *c-fos* within mCherry+ neurons as a molecular indicator of hM4Di activation in mice that had been administered

CNO or vehicle and subsequently ran on the horizontal ladder task repeatedly for 15 minutes with euthanasia 1 ~1/2 hours later (Siegel et al., 2015) (**Fig. 4.7A-A'**). In vehicle administered mice, 20.10±2.67% of mCherry+ neurons were *c-fos+*, while in CNO administered mice, significantly fewer (11.55±2.054%) of mCherry+ neurons were *c-fos+* ($p<0.05$; **Fig. 4.7C**). Thus, CNO administration significantly decreased the number of c-fos+ mCherry+ corticospinal neurons, providing direct evidence that hM4Di activation silences corticospinal neurons.

4.4 Discussion

We performed a series of optogenetic, pharmacogenetic, anatomical, and behavioural experiments to, for the first time, dissociate the role of spared dorsolaterally projecting corticospinal neurons in mediating spontaneous recovery following SCI. Using longitudinal mapping in Channelrhodopsin-2 expressing mice, we demonstrate that the motor cortex has the capacity to re-establish motor output to both forelimb and hindlimb following ablation of the dorsal CST and substantial sensory loss. We then took a pharmacogenetic approach to discriminate between the contribution of plasticity in spared vs. injured corticospinal neurons to recovery and show that transient silencing of uninjured dorsolaterally projecting corticospinal neurons is sufficient to result in the re-appearance of deficits in skilled locomotion observed early after injury. This effect was only observed following CNO administration, and only in SCI mice that were administered both Cre-dependent hM4Di and Cre expressing viruses, highlighting the specificity of these neurons in mediating this behavioural effect. The dorsolateral CST represents ~400 of 12500 cervical CST axons

(~3%) in adult mouse (Fink et al., 2015). Thus, few spared corticospinal neurons can substantiate remarkable cortical plasticity in the injured adult mammalian CNS, which has important implications for treatment, rehabilitation, and recovery.

Early after injury, we found a substantial reduction in forelimb and hindlimb motor cortical output and map area following a C3/C4 dorsal column injury that ablated the dCST. While optogenetic stimulation consistently evoked both forelimb and hindlimb movement despite our transection of the dCST, motor output to the forelimb and hindlimb was reduced to ~25% and ~40% that of baseline respectively acutely after injury. At this acute time point, the motor cortical output that does occur is likely substantiated by spared corticospinal neurons in addition to motor cortical circuits to brain stem targets, such as cortico-reticulospinal and cortico-rubrospinal pathways. This may be reflected by the increase in latency that occurs. Alternatively, the latency change might also reflect a challenge to fast signal propagation that occurs as a result of the injury itself. One strength of optogenetic mapping relative to traditional mapping techniques is the capacity to assess quantitatively motor cortical output in the same animals repeatedly from acute to chronic stages of injury. Doing this, we found longitudinal re-establishment of cortical motor output maps by 4 weeks post-injury which demonstrates that the adult mammalian motor cortex is able to re-establish limb output following interruption of >95% of the direct corticospinal transmission. This provides substantive evidence that, although the dorsal CST is the major cortical output pathway to the forelimb and hindlimb in uninjured adult mice, the motor cortex spontaneously re-routes signals through other corticofugal pathways to re-establish cortical/limb connectivity following the dorsal CST's ablation (**Fig. 4.8**). We have highlighted the dorsolateral CST,

which represents ~3% of corticospinal fibers in cervical spinal cord, as one pathway underlying this. However, multiple other corticofugal pathways might also exhibit plasticity in this regard and underlie spontaneous recovery. The extent to which these pathways can be targeted for therapy will be an important avenue for further research. For example, the demonstration of a de novo rubral/raphe circuit following bilateral pyramidotomy was recently made(Siegel et al., 2015) and cortico-rubrospinal plasticity may be involved. One significant limitation of our motor mapping paradigm is the inability to dissociate movements along particular joints of the fore-limb and hind-limb axes. It will be important in the future to assess whether motor cortical output re-establishment is limited to specific joints and motor tasks.

Our pharmacogenetic approach provides strong evidence that a small number of spared dorsolaterally projecting corticospinal neurons are necessary for spontaneous recovery on the horizontal ladder task following C3/C4 dorsal column SCI (**Fig. 4.8 IV-V**). Because we injected AAV expressing Cre-dependent hM4Di into the sensorimotor cortex, only cortical neurons would be transduced by this virus. Because we injected AAV expressing Cre 3-4 mm caudal to an SCI that resulted in complete ablation of the dCST and thus the vast majority of corticospinal axons, only the small percentage of spared dorsolaterally projecting corticospinal neurons would be local to this virus administration. The administration of CNO led to a re-appearance of the deficits observed early after injury in SCI mice administered both Cre-dependent hM4Di expressing and Cre expressing viruses but not in mice administered only the Cre-dependent virus. In addition, the difference observed following CNO administration vs. vehicle administration in SCI hM4Di Cre+ mice was greater than in

uninjured hM4Di Cre+ mice despite an equal level of mCherry+ dorsolateral corticospinal axons at C2, a higher level of total corticospinal mCherry+ fibers as a result of partial transduction of the dorsal CST in uninjured mice, and a higher total number of mCherry+ neurons in uninjured mice. Still, although we were able to quantify the number of mCherry+ neurons in cortex, we cannot rule out the possibility that some corticospinal neurons may have been dual transduced by the required two viruses and silenced by the drug but not expressing the threshold level of mCherry necessary for our detection in cortex. Thus, we cannot be certain of the minimum number of corticospinal neurons silenced necessary to exert the difference observed.

Numerous studies have demonstrated corticospinal axonal plasticity associated with recovery following CNS injury (Nudo, 2006; Nishimura and Isa, 2009) but, to the best of our knowledge, a causal demonstration of uninjured corticospinal neurons mediating spontaneous recovery has not been made. For example, in a seminal study, the sparing of ventral corticospinal axons was correlated with spontaneous recovery of skilled forelimb function in the adult rat (Weidner et al., 2001). We did not observe mCherry+ fibers within the ventral funiculus, however, suggesting that our approach was specific to dorsolaterally projecting corticospinal neurons in injured mice. Given that the vCST projects ipsilaterally(Weidner et al., 2001), we did not expect it to be targeted/silenced using our approach with Cre targeted to the contralateral side. More recently, substantial spontaneous plasticity of corticospinal axons associated with forelimb recovery was demonstrated in the adult primate (Rosenzweig et al., 2010; Friedli et al., 2015) Given the capacity of individuals with Brown-Séquard syndrome to exhibit a capacity to spontaneously recover volitionally guided locomotion

(Roth et al., 1991) and the extent of corticospinal plasticity in non-human primates (Rosenzweig et al., 2010), it is likely that corticospinal plasticity occurs extensively in humans following incomplete SCI (Friedli et al., 2015). Our results demonstrate that spared dorsolateral corticospinal neurons are pivotal for spontaneous recovery of skilled locomotion in adult mice despite the limited reconstitution of corticospinal density following injury (Weidner et al., 2001; Brus-Ramer et al., 2007; Maier et al., 2008). Dorsolateral corticospinal fibers can increase their contact with lumbar motor neuron pools following midthoracic dorsal column injury (Bareyre et al., 2005) and are found in the vicinity of motor neuron pools following cervical dorsal column injury(Steward et al., 2004). We found the silencing of dorsolateral corticospinal neurons projecting caudal to the injury site was sufficient to result in the re-appearance of deficits on the horizontal ladder task early after injury. However, whether dorsolaterally projecting corticospinal neurons contribute to spontaneous recovery in more skilled tasks such as pellet reaching remains to be determined.

Importantly, although our pharmacogenetic approach targeted dorsolaterally projecting corticospinal neurons following injury, our data do not demonstrate that compensation occurs specifically at the synapses of the dorsolateral corticospinal fibers at the spinal levels C6/C7 or C7/C8. Pharmacogenetic silencing via DREADD receptor activation will have silenced the entire neuron, so we cannot rule out the possibility (indeed, the probability) that these neurons project and synapse elsewhere between the sensorimotor cortex and the spinal cord (via collaterals) and that silencing these other connections between these neurons contribute to the deficits observed following CNO administration. Corticospinal neurons harbour a capacity for de novo connections with propriospinal neurons following injury (Bareyre et al.,

2004; Vavrek et al., 2006) and corticofugal neurons project extensively throughout the brain stem to other motor nuclei, including the red nucleus and reticular formation, which harbour rubrospinal and reticulospinal tracts respectively (Brown, 1974b; Esposito et al., 2014).

Our pharmacogenetic approach to silencing a descending spared pathway following SCI is broadly applicable to the study of plasticity and regeneration following CNS injury. Such strategies have been used to decipher forelimb circuit function in the uninjured CNS (Esposito et al., 2014) and recovery following stroke (Wahl et al., 2014) and pyramidotomy (Siegel et al., 2015). We took advantage of the development of Cre-dependent versions of hM4Di to inactivate a specific descending pathway. Since some AAVs are capable of retrograde transduction of neurons, even after SCI(Klaw et al., 2013), this approach may yield valuable insight into the roles of other pathways in mediating spontaneous, regeneration-based or rehabilitation-based recovery following SCI.

In conclusion, we demonstrate for the first time that small numbers of spared dorsolaterally projecting corticospinal neurons can substantiate remarkable motor cortical plasticity and partial recovery following cervical SCI resulting in substantial corticospinal and sensory loss. Targeting spared corticospinal neurons represents a key substrate to promote repair following SCI and perhaps other CNS diseases/disorders.

Figure 4.1 Optogenetic and pharmacogenetic dissection of motor cortical plasticity underlying recovery following spinal cord injury. A) Cross section through cervical spinal cord in a Thy1-ChR2 mouse immunostained for PKCγ (red), YFP (green), and BDA (pink) with euthanasia 2 weeks following BDA injections into sensorimotor cortex. B) Close-up of the dorsal column showing BDA+ corticospinal axons comprising the dCST. C) Close-up of the dorsolateral funiculus showing BDA+ corticospinal axons comprising the dorsolateral CST and their branches into gray matter. D) Close-up of the ventral column showing sparse BDA+ immunoreactivity. E) Schematic of descending motor corticofugal pathways involved in distal limb control. The motor cortex projects directly to the spinal cord via the dCST (~96%), dlCST (~3%), and vCST (~1%) but also provides major excitatory input to the red nucleus (RN) and reticular formation (RF) which descend the rubrospinal tract and reticulospinal tract respectively. After C3/C4 SCI, the dCST is bilaterally interrupted, but other motor corticofugal pathways remain intact. F) Horizontal ladder task of sensorimotor dysfunction and recovery following C3/C4 dorsal column SCI. Arrows denote errors of the forelimb and/or hindlimb. G) Longitudinal optogenetic motor mapping through intact skull before and after SCI. Anaesthetized, head-fixed mice are placed with their left forelimb and hindlimb suspended from the ground to allow free movement. Laser motion sensors direct at targets on the limbs record movements evoked by optogenetic cortical stimulation. Mapping is repeated in the same animal at multiple time points following SCI. (A chronic cranial window preparation allows optical access through completely intact skull. The window is directed over the right cortical hemisphere and centered around bregma (yellow square) rostro-caudally. A 12 x 14 array of cortical points with 300 μm spacing is stimulated in semi-random order by a fixed ~100 μm diameter 473 nm laser (10 msec pulse). Following 3

repetitions of stimulation, a map of average evoked forelimb and hindlimb movements are assembled and scaled based on amplitude. Inset brain atlas adapted from the Allen Brain atlas and indicates approximate location of motor mapping area within the red outline. Bright green area is an approximate area of primary motor cortex. Scale bars in A are 500 µm. Scale bars in B-D are 50 µm.

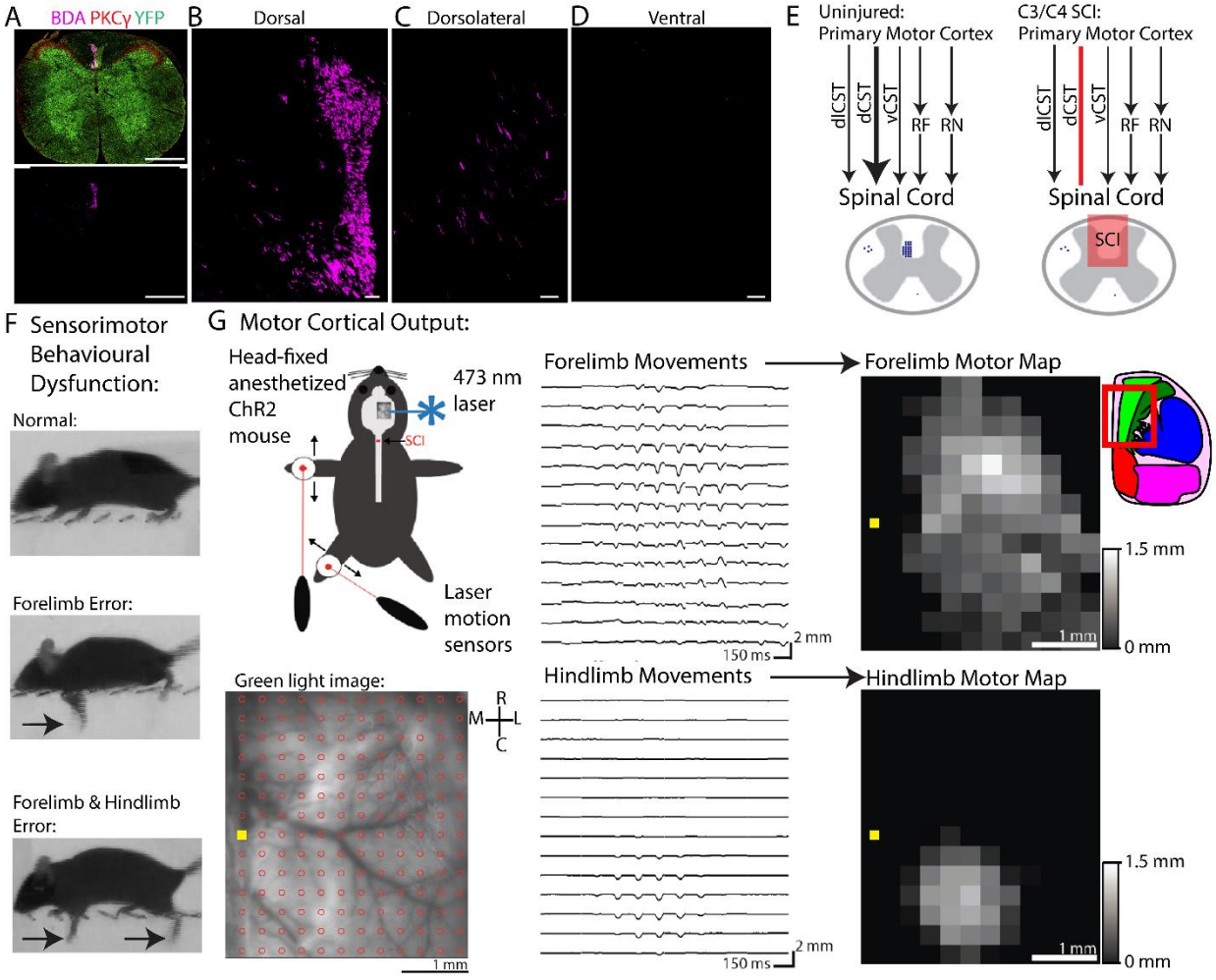

Figure 4.2 Partial spontaneous recovery and sustained deficits in skilled locomotion followed C3/C4 dorsal column SCI. A) Left: transverse (cross) sections of cervical spinal cord rostral to a dorsal column lesion immunostained for YFP and PKCγ showing the presence of the dorsal corticospinal tract. YFP labels neurons diffusely in both gray and white matter and extensively labels the dCST in Thy1-ChR2/YFP mice. Middle: transverse sections of cervical spinal cord at the lesion epicenter immunostained for PKCy and YFP. The lesion includes the dorsal column and the dCST bilaterally. Right: transverse sections of cervical spinal cord caudal to the spinal cord injury immunostained for PKCy and YFP. B, C) Close up on dorsal column for PKCy and YFP rostral (B) and caudal (C) to injury. Note the absence of the dCST caudal to injury. C) A-D Horizontal ladder error percentage (errors/steps*100) for the left forelimb (A), right forelimb (B), left hindlimb (C), and right hindlimb (D) analyzed using two-way ANOVA with a Holm-Sidak's multiple comparisons test. The left and right forelimbs have significantly higher error percentages up to 56 days post-injury vs. pre-injury (***$p<0.001$, **$p<0.01$, *$p<0.05$, vs. pre-operation). The left and right forelimbs have significantly lower error percentages at 42 and 56 days post-injury vs. 7 days post-injury (##$p<0.01$, #$p<0.05$ vs. 7 days post-injury). The left and right hindlimbs completely recover horizontal ladder placement by 7-14 days post-injury (***$p<0.001$, **$p<0.01$, *$p<0.05$, vs. pre-operation). N = 16 SCI and 8 sham operated mice. Error bars indicate SEM. Scale bar in A is 500 μm and in B is 50 μm.

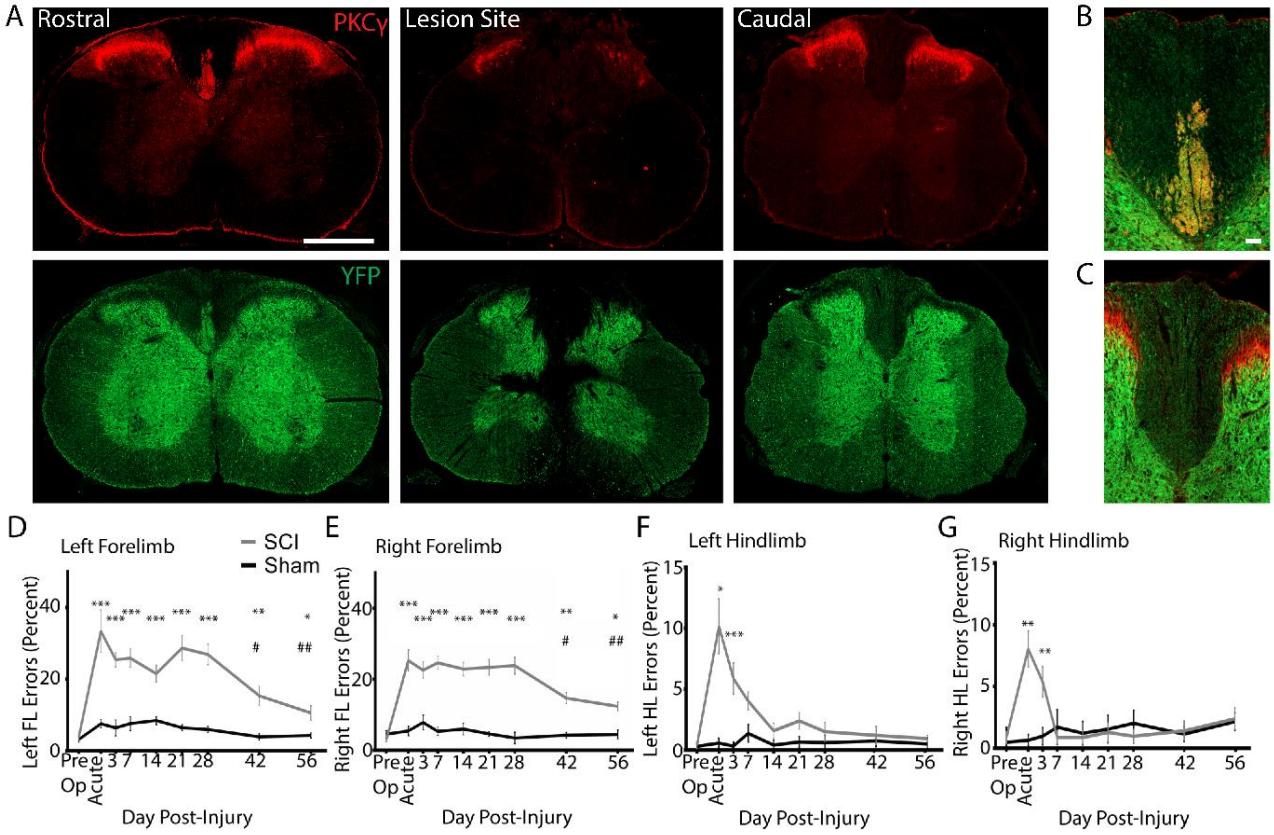
A
Rostral
PKCγ
Lesion Site
Caudal
YFP
B
C
D
Left Forelimb
SCI
Sham
Left FL Errors (Percent)
Day Post-Injury
E
Right Forelimb
Right FL Errors (Percent)
Day Post-Injury
F
Left Hindlimb
Left HL Errors (Percent)
Day Post-Injury
G
Right Hindlimb
Right HL Errors (Percent)
Day Post-Injury
Pre Op
Acute
3 7 14 21 28 42 56

Figure 4.3 Effect of acute SCI on motor maps. A) Average upsampled ChR2 stimulated motor maps (100 x 100 µm pixels) normalized to their respective mean and aligned based on the location of bregma (yellow square). Average forelimb (FL) and hindlimb (HL) motor maps (Ai) prior to injury and (Aii) immediately following C3/C4 dorsal column SCI (<1 hour post-injury; n=8). Inset brain atlas adapted from the Allen Brain Atlas and indicates approximate location of motor mapping area within the red outline. Bright green area is an approximate area of primary motor cortex. B) Position of centre of gravity of FL and HL maps with respect to bregma. FL is displaced caudally from 0.30±0.14 mm rostral to bregma preoperatively to 0.35±0.07mm caudal to bregma acutely. C) FL and HL motor amplitude are reduced following acute SCI. D) FL and HL map area, defined by the number of cortical sites capable of generating forelimb and hindlimb movement respectively, are reduced following acute SCI. E) Latencies of optogenetic stimulation to forelimb and hindlimb movement are increased following acute SCI. N = 8 injured mice. *p<0.05, **p<0.01, ***p<0.001; pre-injury vs. acute. Error bars indicate SEM.

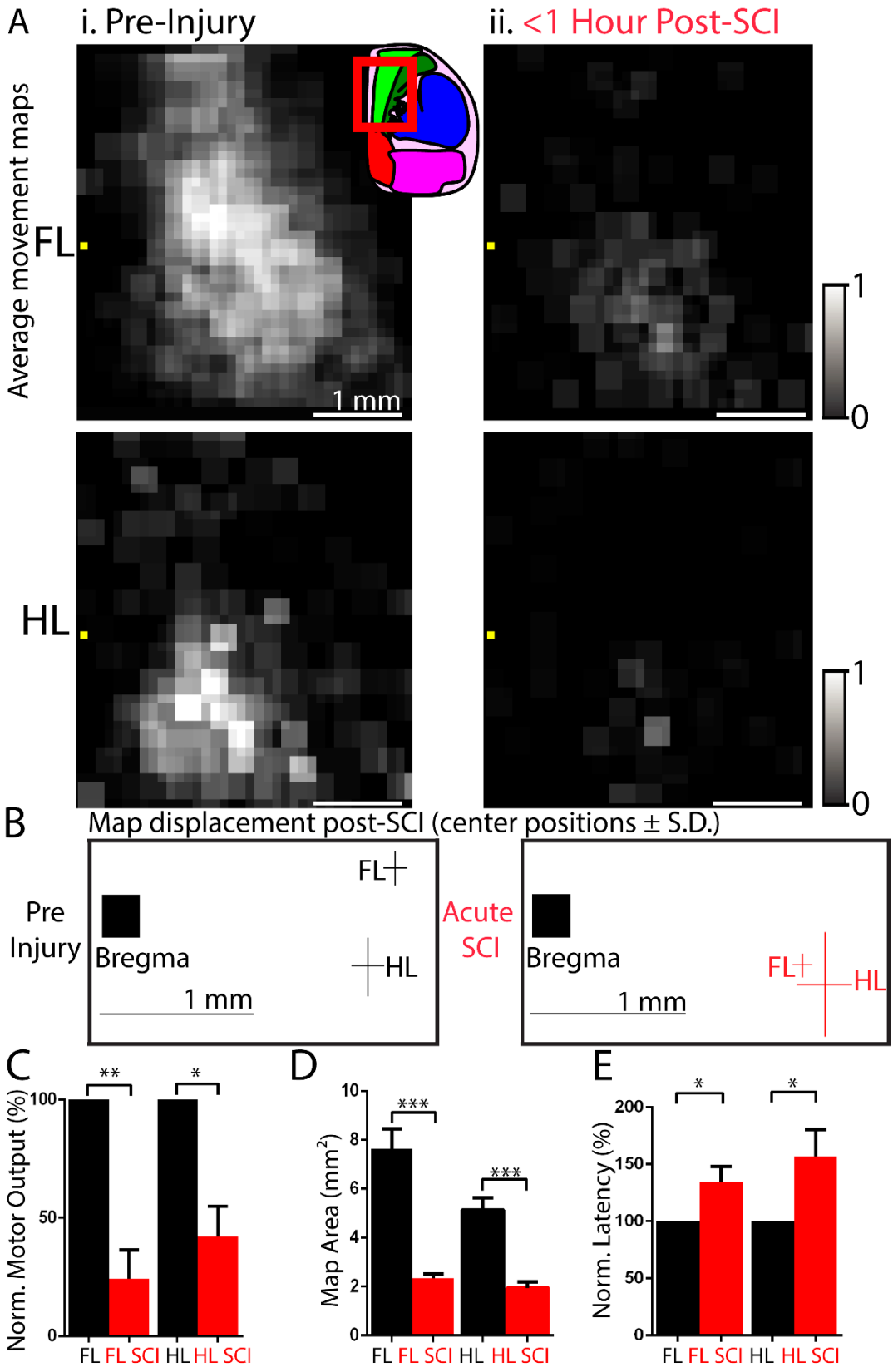
A
i. Pre-Injury
ii. <1 Hour Post-SCI
Average movement maps
FL
HL
1 mm
1
0
B
Map displacement post-SCI (center positions ± S.D.)
Pre Injury
Bregma
1 mm
FL
HL
Acute SCI
C
Norm. Motor Output (%)
FL FL SCI HL HL SCI
D
Map Area (mm²)
E
Norm. Latency (%)

Figure 4.4 Spontaneous motor map re-establishment following C3/C4 dorsal column SCI. A) Baseline averaged ChR2-stimulated motor maps of the forelimb (FL) and hindlimb (HL) at multiple time points before and after SCI. Bregma is denoted by the yellow square in each panel. B) Forelimb motor map area, defined by the number of cortical sites from which movement could be generated, is lower acutely, and 3, 7, and 14 days post-SCI. C) Forelimb motor output, defined as the average maximal displacement at the 9 pixels encompassing the center of gravity, is significantly lower acutely and at 3 and 7 days post-SCI. D) Latency to forelimb movement is longer acutely and at 3, 7, and 14 days post-SCI. E) The forelimb map shifts caudally following SCI acutely and at 3 days post-injury. F) Hindlimb motor map area is lower acutely and at 3 days post-SCI. G) Hindlimb motor output is lower acutely and at 3 and 7 days post-SCI. H) Latency to hindlimb movement is longer acutely and at 3 and 7 days post-SCI. I) The hindlimb map does not shift in center position following SCI. N = 8 injured and 8 sham mice. *$p<0.05$, **$p<0.01$, ***$p<0.001$ between groups. Error bars indicate SEM.

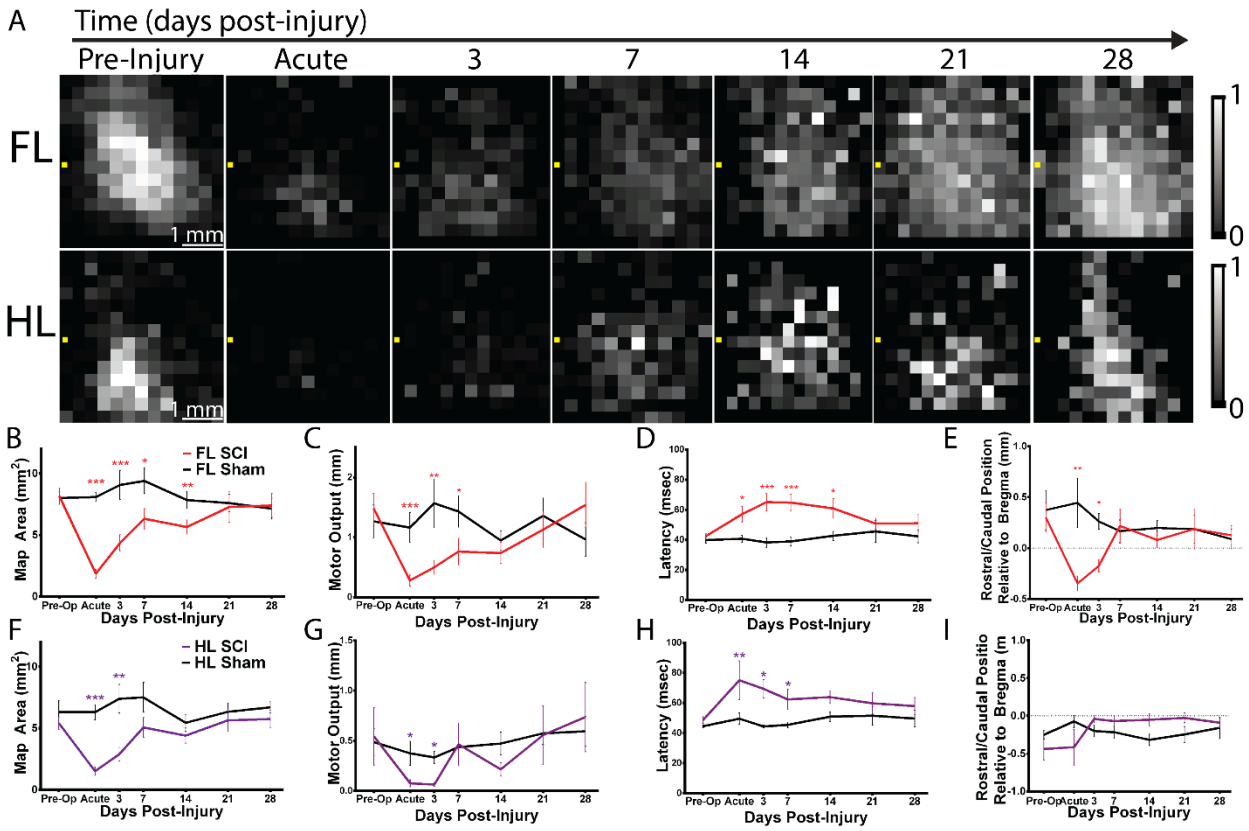
A
Time (days post-injury)
Pre-Injury
Acute
3
7
14
21
28
FL
HL
1 mm
1 mm
1
0
1
0
B
FL SCI
FL Sham
Map Area (mm²)
Days Post-Injury
C
Motor Output (mm)
Days Post-Injury
D
Latency (msec)
Days Post-Injury
E
Rostral/Caudal Position Relative to Bregma (mm)
Days Post-Injury
F
HL SCI
HL Sham
Map Area (mm²)
Days Post-Injury
G
Motor Output (mm)
Days Post-Injury
H
Latency (msec)
Days Post-Injury
I
Rostral/Caudal Positio Relative to Bregma (m
Days Post-Injury

Figure 4.5 Specific targeting of DREADD receptor hM4Di to spared dorsolaterally projecting corticospinal neurons. A-C) Schematic of targeting uninjured dorsolaterally projecting corticospinal neurons. A) Corticospinal neurons originating in layer V motor cortex project their axons via the dorsal column (dCST) and dorsolateral funiculus (dlCST). B) At four weeks post-injury, an AAV expressing Cre-dependent hM4Di (AAV1-hSyn-dio-hM4D(Gi)-mCherry) is administered to sensorimotor cortex and an AAV expressing Cre (AAV1-Cre) is administered to the dorsolateral funiculus at C7/C8, such that only spared dorsolaterally projecting corticospinal neurons are transduced by both viruses in injured animals. C) Following CNO administration, only corticospinal neurons expressing both viruses are silenced for 1-2 hours (red). dCST neurons axotomized by the dorsal column SCI are not silenced. D) Histological verification of mCherry+ dual transduced corticospinal axons at C2 spinal cord rostral to the injury. Following SCI, mCherry+ corticospinal axons can be observed in the dorsolateral funiculus (D') but not in the dorsal column (D''). Following sham operation, mCherry+ corticospinal axons can be observed in both the dorsolateral funiculus (D''') and in the dorsal column (D''''). E, F) Quantification of mCherry+ axon numbers in the dorsolateral funiculus and dorsal column in injured and sham operated mice. E) There is no difference in the number of mCherry+ axons found in the dorsolateral funiculus between SCI and sham operated mice. F) There are significantly more mCherry+ axons in the dorsal column in sham operated mice vs. SCI mice. *$p<0.05$. Scale bars in D are 20 μm. Error bars indicate SEM.

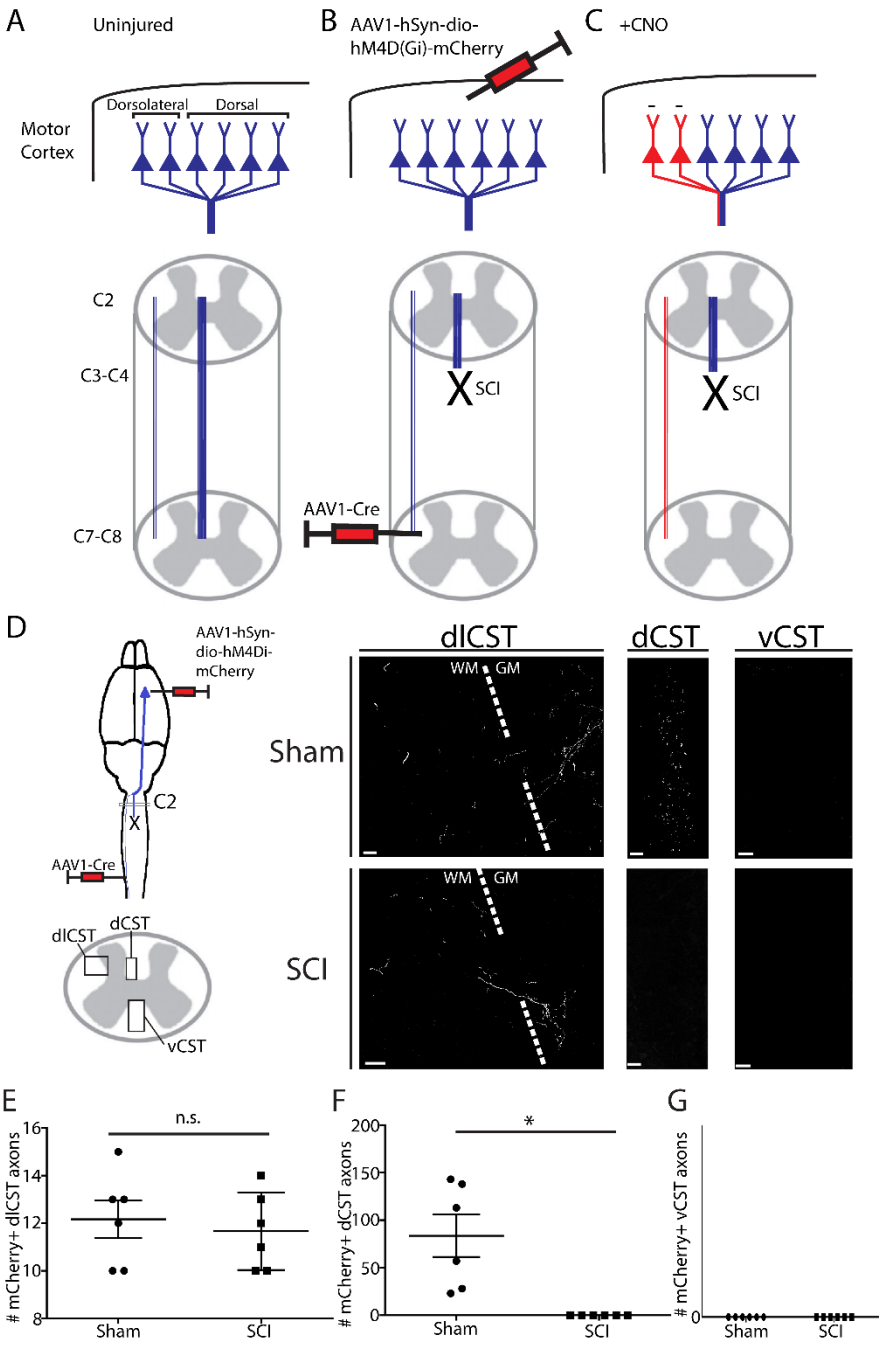
A
Uninjured
B
AAV1-hSyn-dio-hM4D(Gi)-mCherry
C
+CNO
Motor Cortex
Dorsolateral
Dorsal
C2
C3-C4
C7-C8
SCI
AAV1-Cre
D
AAV1-hSyn-dio-hM4Di-mCherry
C2
AAV1-Cre
dlCST
dCST
vCST
Sham
SCI
WM
GM
E
n.s.
mCherry+ dlCST axons
F
*
mCherry+ dCST axons
G
mCherry+ vCST axons

Figure 4.6 Activation of hM4Di in spared dorsolaterally projecting corticospinal neurons abrogates spontaneous recovery on the horizontal ladder task after C3/C4 dorsal column SCI. (A) Experimental schedule. AAV injections were made at 4 weeks post-injury and DREADD receptor behavioural experiments at 55-58 days post-injury by administering CNO on day 56 and 58. (B) Timeline of left forelimb error percentage in injured and sham operated mice with AAV1-hSyn-dio-hM4D(Gi)-mCherry + AAV1-iCre injections (hm4Di Cre+) or just AAV1-hSyn-dio-hM4D(Gi)-mCherry for control (hm4Di Cre-). HM4Di Cre- SCI mice have lower error percentage at 55-58 days post-injury vs. 7 days post-injury. HM4Di Cre+ SCI mice have lower error percentage at 55 and 57 days post-injury vs. 7 days post-injury but not at 56 and 58 days post-injury, the two days when CNO was administered. (C) Left forelimb error percentages following vehicle administration and CNO administration for each group (calculated as an average of scores on 55&57 days and 56&58 days respectively). HM4Di SCI Cre+ mice have a higher error percentage following CNO administration vs. vehicle administration and vs. sham hM4Di Cre+ mice following CNO administration. hM4DI sham operated mice have a higher error percentage following CNO administration vs. vehicle administration. (D) Left Forelimb delta error percent, calculated as the absolute difference between CNO error percent and vehicle error percent. hM4Di SCI Cre+ mice have a higher delta error percent than hM4Di Sham Cre+ mice. (E) Timeline of right forelimb error percentage in injured and sham operated mice as in (B). All four groups have a lower error percentage at 55-58 days post-injury vs. 7 days post-injury. (F) Right forelimb error percentages following vehicle administration and CNO administration for each group. hM4Di SCI Cre+ mice trend towards a higher error percentage following CNO

administration vs. vehicle administration (p=0.06). (G) Right Forelimb delta error percent. ***p<0.001, **p<0.01, *p<0.05. Error bars indicate SEM.

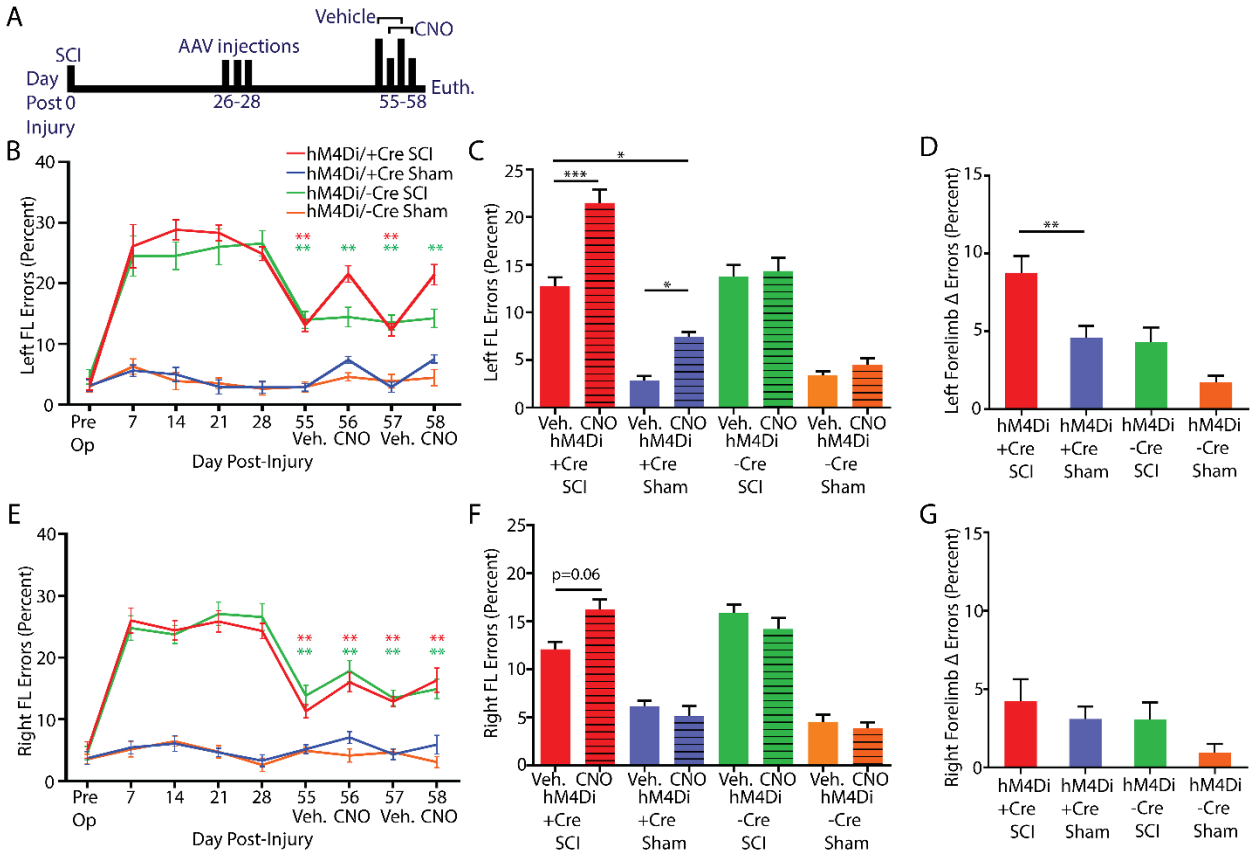

Figure 4.7 Sensorimotor cortical analysis of mCherry and c-fos expression. A) Photomicrographs of coronal sections of sensorimotor cortex with antibodies to mCherry (red) and c-fos (light blue) in addition to fluoro-Nissl staining (dark blue) to illuminate the cortical layers. MCherry is confined to layer V, consistent with specific transduction of corticospinal neurons. A') Close up images of mCherry positive neurons from A showing mCherry (red) and c-fos (light blue). Arrows denote c-fos negative mCherry positive corticospinal neurons, and arrowheads denote c-fos positive mCherry positive corticospinal neurons. B) Quantification of total mCherry positive neurons in sensorimotor cortex. There are significantly more mCherry positive neurons in sham-operated mice (with dual transduction of dlCST and dCST) than in C3/C4 dorsal column SCI mice (with transduction confined to dlCST). C) Quantification of percentage of *c-fos* positive nuclei in mCherry positive corticospinal neurons following administration of CNO to activate hM4Di or vehicle for control. $^{**}p<0.01$, $^{*}p<0.05$. Scale bars are 50 μm in A and 25 μm in A'. Error bars indicate SEM.

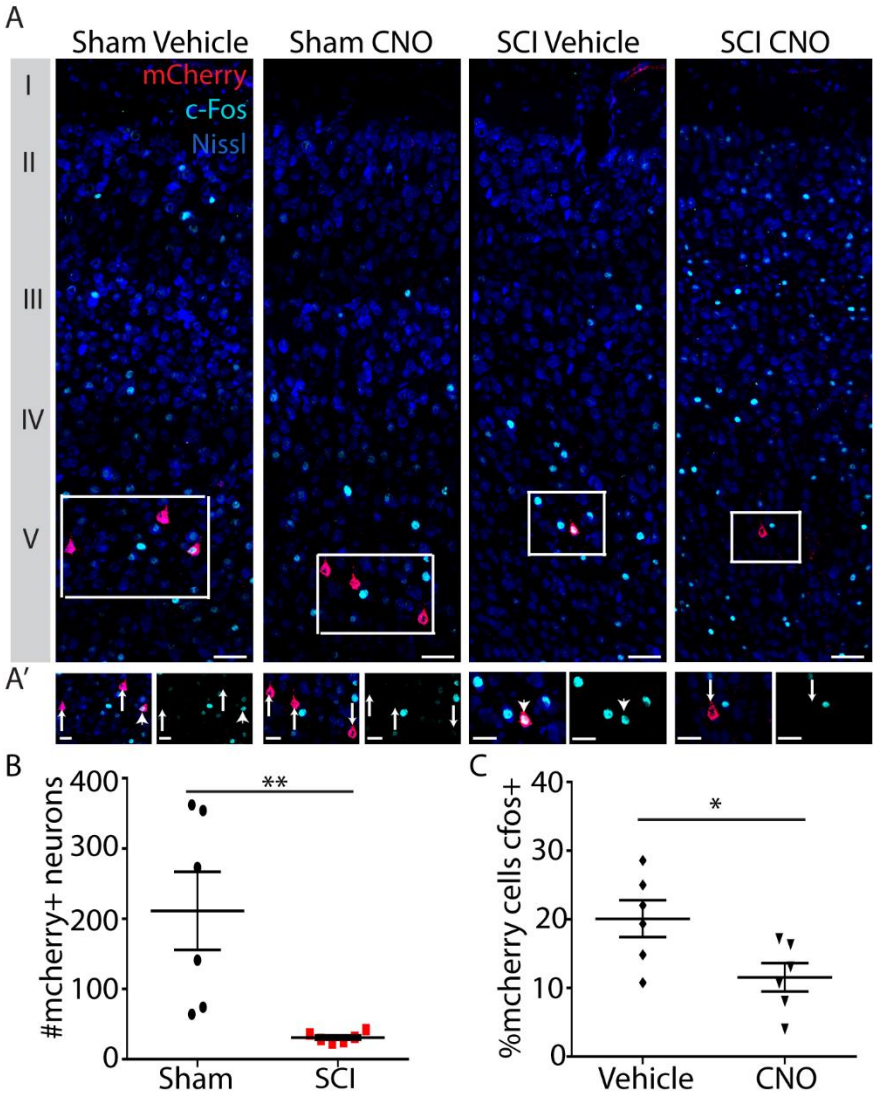
A
Sham Vehicle
Sham CNO
SCI Vehicle
SCI CNO
mCherry
c-Fos
Nissl
I
II
III
IV
V
A'
B
#mcherry+ neurons
400
300
200
100
0
**
Sham
SCI
C
%mcherry cells cfos+
40
30
20
10
0
*
Vehicle
CNO

Figure 4.8 Model of corticospinal plasticity following cervical spinal cord injury. I) In the uninjured adult mouse, ChR2 stimulation of layer V motor cortex evokes forelimb and hindlimb movement principally via the dCST and there is baseline skilled locomotion on the horizontal ladder task. II) Following C3/C4 dorsal column SCI, the dCST is interrupted (gray dashed line), resulting in depressed cortical motor output and a deficit in skilled locomotion. III) Chronically after C3/C4 SCI, cortical motor output is re-established and there is partial recovery in skilled locomotion, likely in part mediated by dlCST neurons (green). IV) When hM4Di is activated in dCST and dlCST neurons (red), there is a small but statistically significant change in skilled locomotion. V) When hM4DI is activated in dlCST neurons chronically in C3/C4 dorsal column SCI mice (red), there is an abrogation of spontaneous recovery and a greater deficit in skilled locomotion than in uninjured hM4Di activated mice as in IV despite similar dlCST silencing and no dCST silencing, representing a shift in function from the injured major dCST pathway to the uninjured minor dlCST pathway.

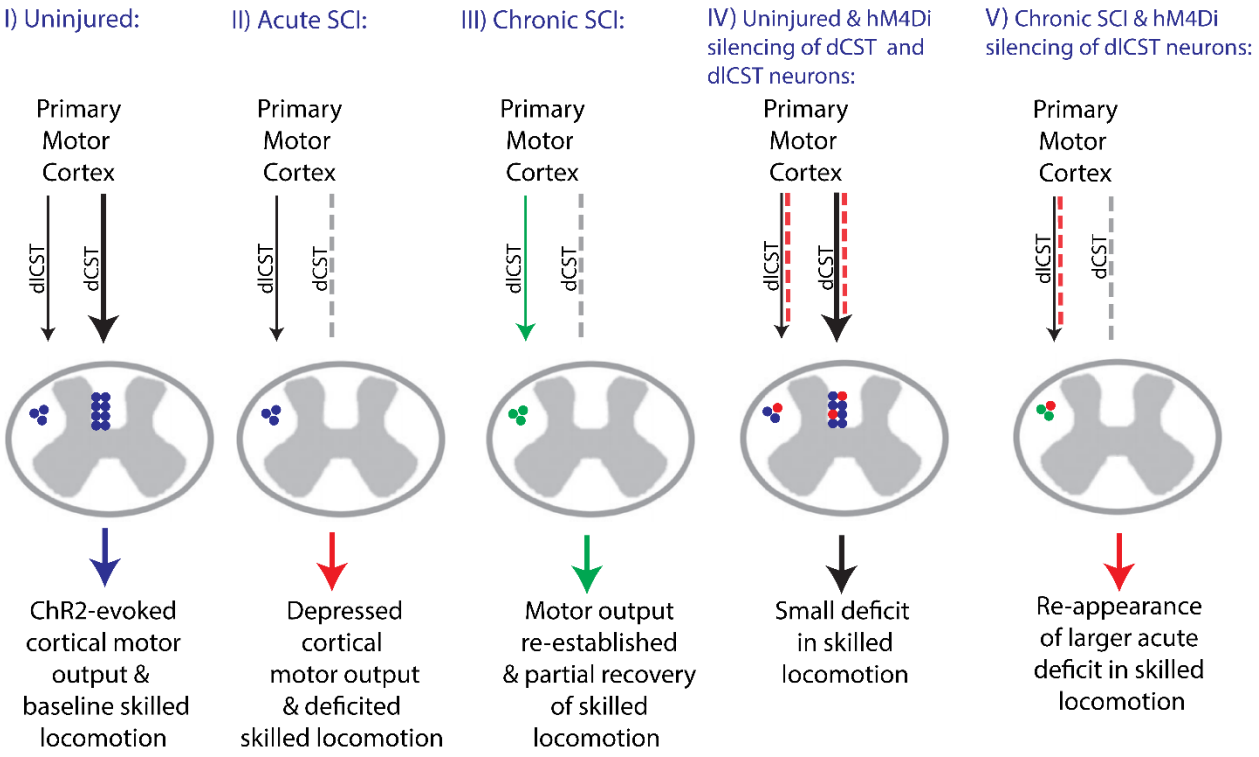
I) Uninjured:
II) Acute SCI:
III) Chronic SCI:
IV) Uninjured & hM4Di silencing of dCST and dlCST neurons:
V) Chronic SCI & hM4Di silencing of dlCST neurons:
Primary Motor Cortex
dlCST
dCST
ChR2-evoked cortical motor output & baseline skilled locomotion
Depressed cortical motor output & deficited skilled locomotion
Motor output re-established & partial recovery of skilled locomotion
Small deficit in skilled locomotion
Re-appearance of larger acute deficit in skilled locomotion

Chapter 5: Conclusions and future directions

The work conducted in this thesis demonstrates that there is an age-related decline in the capacity of adult mammalian central neurons to regenerate following axotomy. It also demonstrates that activity in a minor uninjured dorsolateral corticospinal pathway is necessary for spontaneous motor recovery following SCI that resulted in substantial corticospinal and sensory loss. Additionally, a new injury model that results in complete unilateral axotomy of the rubrospinal tract in adult mice was developed. Applying this injury model at the vertebral level C4 resulted in sustained forelimb motor deficits up to four weeks post-injury while applying it at vertebral level C6 lead to more transient deficits. In this chapter, I address the major hypotheses that drove this work, outline the significance of this work in light of other research findings, and highlight future directions for research into the regeneration and plasticity of descending motor pathways.

5.1 Hypothesis 1

Addressing the hypothesis that *C3/C4 dorsolateral funiculus crush injury results in deficits in adult mouse forelimb function up to 4 weeks post-injury*, I performed a battery of behavioural tests in adult mice subjected to this type of injury and made comparisons between mice injured at C3/C4, mice injured at C6/C7, and sham-operated mice (laminectomy only). By performing the same injury at the two different levels, we could assess the spinal level dependency of the motor deficit incurred. C3/C4 injury would interrupt communication of descending axons to C4/C5 and C5/C6, whereas C6/C7 injury would not. I found that when

injury was instigated at C3/C4, forelimb motor deficits were observed up to 4 weeks post-injury on a multitude of different tasks that assess forelimb function, including rearing, grooming, staircase pellet reaching, and horizontal ladder. However, when injury was instigated at C6/C7, deficits were relatively transient. This suggests that mid-cervical level circuitry encompassed in the dorsolateral funiculus is important for forelimb motor function, although it is possible that spontaneous recovery would occur at a time point later than 4 weeks (Hilton et al., 2016). Using CatWalk Gait Analysis, we also assessed multiple parameters of overground locomotion and the only difference following injury relative to pre-operatively was in stride length in mice that harboured injuries at C3/C4. This is consistent with previous work that has found that pathways descending in the ventrolateral funiculus are more important for locomotion than those in the dorsolateral funiculus (Schucht et al., 2002), and is very similar to the kind of effect on overground locomotion incurred following corticospinal tract (pyramidotomy) injury in adult mice (Starkey et al., 2005).

One important consideration for the development of preclinical injury models that can assess axon regeneration is the completeness of the injury. If an injury model does not completely axotomize a pathway of interest, then it is challenging to ascertain whether axons located distal to the injury site are regenerated, sprouted, or spared (Steward et al., 2003; Tuszynski and Steward, 2012; Steward and Willenberg, 2016). To assess this, we performed unilateral injections of the anterograde tracer BDA into the right red nucleus and comprehensively assessed whether axons were spared caudal to the injury site. We found no evidence of axon sparing, demonstrating that this injury model is suitable for the assessment of rubrospinal axon regeneration following treatment or molecular perturbation.

One outstanding question for further research is whether the motor deficits incurred from C3/C4 dorsolateral funiculus crush are a result of rubrospinal tract axotomy or not. Additional pathways involved in forelimb motor control, including the dorsolateral corticospinal tract (Steward et al., 2004) and fibers projecting from the reticular nucleus mdV (Esposito et al., 2014), will have been axotomized by this type of injury. Serotonergic and noradrenergic fibers will also be disrupted (Millan et al., 2002; Westlund et al, 1982) as will ascending spinocerebellar fibers that partially mediate proprioception (Jiang et al., 2015). Disruption of these pathways could also contribute to the behavioural deficits observed. Morris and colleagues have performed fractionated injuries of the dorsolateral funiculus in adult rats approximately confined to the area where rubrospinal axons project and demonstrated specific impairments in arpeggio movements during a skilled reaching task (Morris et al., 2011), but again such injuries are relatively non-specific and might result in forelimb deficits as a result of injury to other neural elements. To assess the role of the rubrospinal tract in forelimb motor control, a cre-dependent DREADD approach could be used as in Chapter 4. In this case, a virus encoding cre-dependent hm4Di (or a different neuronal activity inhibitory DREADD (Vardy et al., 2015)) could be targeted to the red nucleus and a retrograde virus encoding cre could be targeted to the dorsolateral funiculus, such that only rubrospinal neurons would be dual infected and thus silenced upon DREADD ligand administration (Park and Carmel, 2016). This approach would be useful in ascertaining the roles of many different projecting pathways in motor behaviour both in health and in disease or after injury.

5.2 Hypothesis 2

Addressing the hypothesis that *PTEN deletion in rubrospinal neurons promotes their axon regeneration following spinal cord injury but aging significantly diminishes this regeneration,* I assessed the regeneration of PTEN deleted rubrospinal neurons crush with AAV-Cre injection into $PTEN^{fl/fl}$ mice at 4 weeks or 7-8 months of age and dorsolateral funiculus crush injury at 8 weeks or 8-9 months of age. In both young and aged groups, PTEN deletion promoted axon growth rostral to the injury site, prevented the axotomy-induced decline in mTOR signalling based on p-S6 immunoreactivity, and prevented axotomy-associated cell body atrophy. However, in only the young group was regeneration caudal to the injury site observed. In addition to this data, the laboratory of Professor Binhai Zheng made the same finding in the corticospinal system (Geoffroy et al., 2016), suggesting that it has broad applicability.

The significance of this age-dependent decline is substantial. There is significant interest in developing axon regenerative therapies for many different disorders and diseases of the adult mammalian central nervous system. Hypothetically, such therapies would harbour the capacity to restore function following SCI, stroke, and a variety of neurodegenerative diseases. Animal models are frequently used to study axon regeneration and to define the molecular and cellular basis of its failure in the CNS. Often, studies utilize transgenic mice that are 2-3 months of age at the time of injury while the lifespan of the mouse is ~24 months. In contrast, many disorders and diseases of the adult mammalian CNS are related to

aging. Thus, studies that demonstrate axon regeneration in young adult animals should also assess whether the age at which treatment/molecular perturbation is initiated has an impact on the extent of regeneration observed.

One important avenue for further research will be to pinpoint causal mechanisms underlying the difference in regeneration observed between the young adult and middle-aged adult central nervous system. In this work, three key points of evidence suggest that PTEN knockout remains effective in promoting axon growth in middle aged adult mice. First, there was significantly more axon growth rostral to injury with PTEN knockout in 7-8 month aged mice relative to control, wildtype mice. Second, PTEN knockout remained effective in promoting mTOR signalling based on p-S6 immunoreactivity elevation in the red nucleus, and no difference in the p-S6 immunoreactivity was observed between young PTEN knockout and aged PTEN knockout mice. Third, PTEN knockout remained effective in preventing atrophy of rubrospinal neurons regardless of age, which has previously been associated with the promotion of regeneration-associated gene expression in rubrospinal neurons following SCI (Kobayashi et al., 1997). Therefore, PTEN knockout is likely effective in promoting axon growth independent of age in the adult mammalian CNS, except that with aging, additional factors intrinsic or extrinsic to neurons impede axon growth.

What could be these factors? We observed two key differences between young and aged mice following dorsolateral funiculus crush injury. The first was that there was heightened GFAP immunoreactivity in the vicinity of the lesion site in aged mice. GFAP is an

intermediate filament highly expressed in astrocytes and widely used to document astrogliosis and visualize spinal cord injury lesion sites. GFAP knockout is likely insufficient to promote axon regeneration but has been associated previously with axon growth and improved recovery when combined with knockout of the similar intermediate filament vimentin (Menet et al., 2003; Ribotta et al., 2004; Wilhelmsson et al., 2004). The difference in GFAP immunoreactivity between young and aged mice following injury suggests that astrogliosis may differ based on age. Reactive astrocytes likely form a physical barrier to axon growth through their construction of a dense wall that sequesters activated macrophages to the lesion epicentre. Reactive astrocytes are well characterized in their ability to form barriers to impede cellular migration and axonal growth (Cregg et al., 2014; Keough et al., 2016) and the enhanced GFAP immunoreactivity suggests that astrocytes may be more densely packed/enlarged with aging which may physically impede axon regeneration caudal to the injury site. Counterintuitively, recent high profile work has suggested that reactive astrocytes are actually permissive to axon regeneration (Anderson et al., 2016). Combining growth factors in hydrogel and conditioning lesions was shown to promote axon regeneration that was impeded by the prevention of astrocytic scar formation, suggesting that the astrocytic scar was an important factor in this regard. However, it is likely that preventing astrocytic scar formation resulted in substantive inflammation and deleterious axon loss that would make axon regeneration extremely difficult (Silver, 2016). Thus, it remains likely that the astrocytic scar is one of many scar-associated cells involved in axon regeneration failure. Importantly, a causal demonstration of astrocyte involvement in the age-dependent decline in axon regeneration in the adult mammalian central nervous system was not made by this work, and remains a hypothesis yet to be tested.

The second key difference we observed between young and aged mice following dorsolateral funiculus crush injury was an increase in rubrospinal axonal dieback in aged mice early after injury. In aged mice, rubrospinal axonal dieback was almost double (~400 μm) that observed in young adult mice (~200 μm). Intriguingly, the Zheng lab also observed a higher density of macrophages in the vicinity of the lesion site in aged mice relative to young adult mice following SCI (Geoffroy et al., 2016). Early after injury, activated macrophages mediate axonal dieback through physical contact interactions with axon tips and protease secretion (Horn et al., 2008; Busch et al., 2009; Busch et al., 2010; Gensel et al., 2015). With aging, it is possible that enhanced macrophage activation occurs which leads to greater axonal dieback and further impediment to regeneration. In aged mice, the balance between neurodegenerative M1 and neuroprotective M2 macrophages is altered following SCI towards a more M1-like state (Fenn et al., 2014; Zhang et al., 2015). Also, there is higher reactive oxygen species and NOX generation within macrophages following SCI in aged mice which leads to heightened oxidative stress (Zhang et al., 2016). Thus, the macrophage component of the inflammatory response to SCI changes with aging and this may be one factor underlying the age-dependent decline in axon regeneration. It will be interesting to assess how aging influences the inflammatory response to SCI and whether this is a major contributor to the increased inhibition of axon regeneration observed in middle aged mice.

5.3 Hypothesis 3

Addressing the hypothesis that *the motor cortex is able to re-establish output to the forelimb and hindlimb following C3/C4 ablation of the dorsal corticospinal tract*, I performed dorsal funiculus injuries in adult Thy1-ChR2 mice and assessed changes in motor cortical/limb connectivity longitudinally using optogenetic motor mapping. The corticospinal tract is an important descending pathway in the control of the forelimb, particularly for so-called skilled tasks that require the orchestration of timely movements of multiple muscles. Following SCI that results in substantial corticospinal axon loss, it is believed that the motor cortex has a capacity to remodel output projections to re-establish connectivity to the limbs. For example, plasticity of spared corticospinal neurons and rubrospinal neurons are both thought to be involved. To assess this, we performed optogenetic motor mapping in ChR2 expressing mice. Traditionally, the motor cortex is mapped using electrical approaches, which precludes both assaying how the motor cortex responds very early after injury as well as mapping longitudinally. Optogenetic mapping has the capacity to overcome these limitations of electrical approaches and to selectively activate the output layer of the motor cortex, layer V, which includes the cell bodies of corticospinal neurons.

Using optogenetic motor mapping, we found a substantial reduction in forelimb and hindlimb motor cortical output and map area after a C3/C4 dorsal column injury that ablated the dorsal corticospinal tract. In addition to abruption of the dorsal corticospinal pathway, the diminished cortical motor output observed early after C3/C4 dorsal column injury could also be in part due to spinal shock, which is the initial depression (hyporeflexia) or absence

(areflexia) of spinal reflexes that occurs following SCI. Given that this shock subsides in a few days following injury, it is unlikely that the deficits in motor output and map area observed 1-2 weeks post-injury relative to pre-injury are related to spinal shock.

The dorsal CST in adult mice is comprised of ~12500 corticospinal axons (at the cervical level) (Fink et al., 2015), representing 96% of all corticospinal axons. Very early after injury, the substantial deficits in motor cortical output and map area provide evidence that the dorsal CST provides most of the output to the limbs in the uninjured adult mouse. By mapping up to 4 weeks post-injury, we observed the re-establishment of motor cortical output and map area to parameters similar to baseline despite the substantial corticospinal loss invoked by this injury. It will be interesting to assess the anatomical and physiological basis of this. In addition to the spared corticospinal fibers (see below), layer V motor cortex also projects to brain stem motor nuclei and the red nucleus, which also project descending pathways involved in forelimb motor control (Brown, 1974b; Esposito et al., 2014). One possibility is that there is a plastic response involving increased output through these projections following interruption of corticospinal transmission, although this remains to be tested. This form of re-routing has been observed following administration of an axonal plasticity inducing therapy (Raineteau et al., 2001) but is not described to occur spontaneously following injury in the absence of treatment.

Soon after the publication of these results in *The Journal of Neuroscience* (Hilton et al., 2016), Edmund Hollis and colleagues from the laboratory of Yimin Zou published findings

using optogenetic mapping of motor cortex following SCI (Hollis II et al., 2016). In contrast to our mapping procedure, which involved the usage of non-invasive laser motion sensors to assay motor cortical output based on limb displacement and software driving stimulation of an array of cortical sites in semi-random order, Hollis and colleagues video-captured limb movements following fiber optic cable/cannulae stimulation of cortical sites after moving to these sites manually using a stereotaxic frame (Hollis II et al., 2016). An additional difference was that our dorsal column injury is at the C3 vertebral level whereas there's was at C5, sparing considerably more forelimb corticospinal circuitry. Despite these differences, the findings of forelimb reorganization of motor cortex were quite similar: a caudal displacement of the forelimb center of gravity was observed and over 4 weeks after injury, forelimb motor cortical reorganization occurred with stimulation of increasingly more cortical sites resulting in forelimb movement (Hollis II et al., 2016). Interestingly, one difference between our findings and theirs is that while we observed re-establishment of the hindlimb map, Hollis and colleagues did not. One possibility is that sub-threshold activation of hindlimb circuits occurred in their study that did not evoke hindlimb movements but were sufficient to activate forelimb circuitry above the threshold necessary for forelimb movement to occur, particularly since the laser ampltitude was chosen based on the minimum threshold necessary for forelimb movement to occur (Hollis II et al., 2016). In our study, laser amplitude was chosen based on the minimum level required to stimulate movement in each animal prior to injury and then kept consistent until end-point. Still, despite this minor disparity, the results of Hollis and colleagues are very complementary to those found in our study.

5.4 Hypothesis 4

Addressing the hypothesis that *spared, dorsolaterally projecting corticospinal neurons are necessary for spontaneous recovery following C3/C4 dorsal column spinal cord injury*, we established a transient silencing method specifically within dorsolaterally projecting corticospinal neurons using DREADD technology (Roth, 2016). Using a cre-dependent approach, we demonstrated the ability to selectively express hM4Di within dorsolateral corticospinal neurons in injured animals. Following hM4Di activation, spontaneous recovery was abrogated on the horizontal ladder task in a unilateral (left limb specific) manner. There was also a greater percentage change in forelimb horizontal ladder performance in injured mice versus uninjured mice, despite silencing of some dorsal projecting corticospinal neurons in uninjured mice and overall greater number of hM4Di positive corticospinal neurons in uninjured mice in total.

The dorsolateral corticospinal tract is comprised of about 400 axons (at the cervical level) in adult mice, representing 3% of the total number (Fink et al., 2015). That such a minor pathway is necessary for spontaneous recovery on a horizontal ladder task of forelimb motor recovery is perhaps the most important finding in this thesis, and is consistent with the re-establish of motor cortical output observed in Aim 3. The vast majority of SCIs are anatomically incomplete, and typically some axons are spared following injury. Our results suggest that anatomically minor descending pathways may be able to support substantial recovery following SCI, and understanding how this occurs is a key avenue for further research (Rasmussen and Carlsen, 2016). A detailed neurophysiological understanding of

how descending motor pathways help mediate recovery may be key to successfully translating activity-based and/or regeneration-based therapies, particularly since substantial regeneration of a large number of axons long distances past spinal sites of injury remains a formidable challenge (Tuszynski and Steward, 2012). That uninjured corticospinal neurons can help mediate such recovery has previously been suggested and experimentally evidenced by an association of the timeline of recovery on behavioural motor tasks with anatomical plasticity of corticospinal fibers following injury (Weidner et al., 2001; Rosenzweig et al., 2010). However, a direct causal demonstration of specific descending circuits following SCI had not occurred until our study, and such studies using transient silencing techniques will be of great use in determining the involvement of other descending pathways in recovery following SCI and other CNS diseases/disorders.

In conclusion, the results from this thesis constitute two major findings. First, I found that there is an age-related decline in the capacity of rubrospinal neurons to regenerate following SCI. Second, I found that activity in a minor corticospinal pathway is necessary for spontaneous recovery following SCI resulting in substantial corticospinal and sensory loss. The findings are representative of two different approaches to promoting repair of descending motor pathways: regenerating injured pathways versus promoting plasticity in spared or uninjured pathways. With greater knowledge of both, it may be possible in the future to promote lasting motor system recovery following SCI and other diseases/disorders of the nervous system.

References

Adler CE, Fetter RD, Bargmann CI (2006) UNC-6/Netrin induces neuronal asymmetry and defines the site of axon formation. Nat Neurosci 9:511-518.

Alstermark B, Pettersson L-G (2015) Skilled reaching and grasping in the rat: lacking effect of corticospinal lesion. Arm and Hand Movement: Current Knowledge and Future Perspective 5:118.

Alstermark B, Lundberg A, Norrsell U, Sybirska E (1981) Integration in descending motor pathways controlling the forelimb in the cat. Experimental Brain Research 42:299-318.

Anderson KD (2004) Targeting recovery: priorities of the spinal cord-injured population. Journal of neurotrauma 21:1371-1383.

Anderson KD, Gunawan A, Steward O (2007) Spinal pathways involved in the control of forelimb motor function in rats. Experimental neurology 206:318-331.

Anderson MA, Burda JE, Ren Y, Ao Y, O'Shea TM, Kawaguchi R, Coppola G, Khakh BS, Deming TJ, Sofroniew MV (2016) Astrocyte scar formation aids central nervous system axon regeneration. Nature 532:195-200.

Andrews EM, Richards RJ, Yin FQ, Viapiano MS, Jakeman LB (2012) Alterations in chondroitin sulfate proteoglycan expression occur both at and far from the site of spinal contusion injury. Exp Neurol 235:174-187.

Anenberg E, Arstikaitis P, Niitsu Y, Harrison TC, Boyd JD, Hilton BJ, Tetzlaff W, Murphy TH (2014a) Ministrokes in channelrhodopsin-2 transgenic mice reveal widespread deficits in motor output despite maintenance of cortical neuronal excitability. J Neurosci 34:1094-1104.

Anenberg E, Arstikaitis P, Niitsu Y, Harrison TC, Boyd JD, Hilton BJ, Tetzlaff W, Murphy TH (2014b) Ministrokes in channelrhodopsin-2 transgenic mice reveal widespread deficits in motor output despite maintenance of cortical neuronal excitability. The Journal of Neuroscience 34:1094-1104.

Arenkiel BR, Peca J, Davison IG, Feliciano C, Deisseroth K, Augustine GJ, Ehlers MD, Feng G (2007) In vivo light-induced activation of neural circuitry in transgenic mice expressing channelrhodopsin-2. Neuron 54:205-218.

Armbruster BN, Li X, Pausch MH, Herlitze S, Roth BL (2007) Evolving the lock to fit the key to create a family of G protein-coupled receptors potently activated by an inert ligand. Proceedings of the National Academy of Sciences 104:5163-5168.

Asante CO, Martin JH (2013) Differential joint-specific corticospinal tract projections within the cervical enlargement.

Ayling OG, Harrison TC, Boyd JD, Goroshkov A, Murphy TH (2009a) Automated light-based mapping of motor cortex by photoactivation of channelrhodopsin-2 transgenic mice. Nature methods 6:219-224.

Ayling OG, Harrison TC, Boyd JD, Goroshkov A, Murphy TH (2009b) Automated light-based mapping of motor cortex by photoactivation of channelrhodopsin-2 transgenic mice. Nature methods 6:219-224.

Backman SA, Stambolic V, Mak TW (2002) PTEN function in mammalian cell size regulation. Current opinion in neurobiology 12:516-522.

Badan I, Buchhold B, Hamm A, Gratz M, Walker L, Platt D, Kessler C, Popa-Wagner A (2003) Accelerated glial reactivity to stroke in aged rats correlates with reduced functional recovery. J Cereb Blood Flow Metab 23:845-854.

Baird AL, Meldrum A, Dunnett SB (2001) The staircase test of skilled reaching in mice. Brain research bulletin 54:243-250.

Ballermann M, Fouad K (2006) Spontaneous locomotor recovery in spinal cord injured rats is accompanied by anatomical plasticity of reticulospinal fibers. Eur J Neurosci 23:1988-1996.

Baker SN, Zaaimi B, Fisher KM, Edgley SA, Soteropoulos DS (2015) Pathways mediating functional recovery. Progress in brain research 218:389-412.

Bareyre FM, Kerschensteiner M, Misgeld T, Sanes JR (2005) Transgenic labeling of the corticospinal tract for monitoring axonal responses to spinal cord injury. Nature medicine 11:1355-1360.

Bareyre FM, Kerschensteiner M, Raineteau O, Mettenleiter TC, Weinmann O, Schwab ME (2004) The injured spinal cord spontaneously forms a new intraspinal circuit in adult rats. Nature neuroscience 7:269-277.

Barnabé-Heider F, Göritz C, Sabelström H, Takebayashi H, Pfrieger FW, Meletis K, Frisén J (2010) Origin of new glial cells in intact and injured adult spinal cord. Cell stem cell 7:470-482.

Barrett CP, Donati EJ, Guth L (1984) Differences between adult and neonatal rats in their astroglial response to spinal injury. Exp Neurol 84:374-385.

Barrett CP, Guth L, Donati EJ, Krikorian JG (1981) Astroglial reaction in the gray matter of lumbar segments after midthoracic transection of the adult rat spinal cord. Experimental neurology 73:365-377.

Baskin YK, Dietrich WD, Green EJ (2003) Two effective behavioral tasks for evaluating sensorimotor dysfunction following traumatic brain injury in mice. Journal of neuroscience methods 129:87-93.

Basso DM, Beattie MS, Bresnahan JC (1995) A sensitive and reliable locomotor rating scale for open field testing in rats. Journal of neurotrauma 12:1-21.

Basso DM, Beattie MS, Bresnahan JC (1996) Graded histological and locomotor outcomes after spinal cord contusion using the NYU weight-drop device versus transection. Experimental neurology 139:244-256.

Beattie MS, Salegio EA, Bresnahan JC, Sparrey CJ, Camisa W, Fischer J, Leasure J, Buckley J, Nout-Lomas YS, Rosenzweig E (2015) A Unilateral Cervical Spinal Cord Contusion Injury Model in Non-Human Primates (Macaca mulatta). Journal of neurotrauma.

Bender D, Holschbach M, Stöcklin G (1994) Synthesis of nca carbon-11 labelled clozapine and its major metabolite clozapine-N-oxide and comparison of their biodistribution in mice. Nuclear medicine and biology 21:921-925.

Bertelli JA, Mira J-C (1993) Behavioral evaluating methods in the objective clinical assessment of motor function after experimental brachial plexus reconstruction in the rat. Journal of neuroscience methods 46:203-208.

Bignami A, DAHL D (1976) The astroglial response to stabbing. Immunofluorescence studies with antibodies to astrocyte-specific protein (GFA) in mammalian and submammalian vertebrates. Neuropathology and Applied Neurobiology 2:99-110.

Blackmore MG, Wang Z, Lerch JK, Motti D, Zhang YP, Shields CB, Lee JK, Goldberg JL, Lemmon VP, Bixby JL (2012) Krüppel-like Factor 7 engineered for transcriptional activation promotes axon regeneration in the adult corticospinal tract. Proceedings of the National Academy of Sciences 109:7517-7522.

Boyden ES, Zhang F, Bamberg E, Nagel G, Deisseroth K (2005) Millisecond-timescale, genetically targeted optical control of neural activity. Nature neuroscience 8:1263-1268.

Bradbury EJ, Moon LD, Popat RJ, King VR, Bennett GS, Patel PN, Fawcett JW, McMahon SB (2002) Chondroitinase ABC promotes functional recovery after spinal cord injury. Nature 416:636-640.

Bradke F, Marin O (2014) Editorial overview: development and regeneration: nervous system development and regeneration. Curr Opin Neurobiol 27:iv-vi.

Bradke F, Fawcett JW, Spira ME (2012) Assembly of a new growth cone after axotomy: the precursor to axon regeneration. Nature Reviews Neuroscience 13:183-193.

Bretzner F, Liu J, Currie E, Roskams AJ, Tetzlaff W (2008) Undesired effects of a combinatorial treatment for spinal cord injury–transplantation of olfactory ensheathing cells and BDNF infusion to the red nucleus. European Journal of Neuroscience 28:1795-1807.

Brown LT (1974a) Rubrospinal projections in the rat. Journal of Comparative Neurology 154:169-187.

Brown LT (1974b) Corticorubral projections in the rat. Journal of Comparative Neurology 154:149-167.

Brus-Ramer M, Carmel JB, Chakrabarty S, Martin JH (2007) Electrical stimulation of spared corticospinal axons augments connections with ipsilateral spinal motor circuits after injury. The Journal of Neuroscience 27:13793-13801.

Busch SA, Silver J (2007) The role of extracellular matrix in CNS regeneration. Current opinion in neurobiology 17:120-127.

Busch SA, Horn KP, Silver DJ, Silver J (2009) Overcoming macrophage-mediated axonal dieback following CNS injury. The Journal of neuroscience 29:9967-9976.

Busch SA, Horn KP, Cuascut FX, Hawthorne AL, Bai L, Miller RH, Silver J (2010) Adult NG2+ cells are permissive to neurite outgrowth and stabilize sensory axons during macrophage-induced axonal dieback after spinal cord injury. The Journal of Neuroscience 30:255-265.

Byrne AB, Walradt T, Gardner KE, Hubbert A, Reinke V, Hammarlund M (2014) Insulin/IGF1 signaling inhibits age-dependent axon regeneration. Neuron 81:561-573.

Cafferty WB, Duffy P, Huebner E, Strittmatter SM (2010) MAG and OMgp synergize with Nogo-A to restrict axonal growth and neurological recovery after spinal cord trauma. The Journal of Neuroscience 30:6825-6837.

Cahoy JD, Emery B, Kaushal A, Foo LC, Zamanian JL, Christopherson KS, Xing Y, Lubischer JL, Krieg PA, Krupenko SA, Thompson WJ, Barres BA (2008) A transcriptome database for astrocytes, neurons, and oligodendrocytes: a new resource for understanding brain development and function. J Neurosci 28:264-278.

Caroni P, Schwab ME (1988) Two membrane protein fractions from rat central myelin with inhibitory properties for neurite growth and fibroblast spreading. The Journal of cell biology 106:1281-1288.

Carter LM, Starkey ML, Akrimi SF, Davies M, McMahon SB, Bradbury EJ (2008) The yellow fluorescent protein (YFP-H) mouse reveals neuroprotection as a novel

mechanism underlying chondroitinase ABC-mediated repair after spinal cord injury. J Neurosci 28:14107-14120.

Castillo-Ruiz MM, Campuzano O, Acarin L, Castellano B, Gonzalez B (2007) Delayed neurodegeneration and early astrogliosis after excitotoxicity to the aged brain. Exp Gerontol 42:343-354.

Caudle KL, Brown EH, Shum-Siu A, Burke DA, Magnuson TS, Voor MJ, Magnuson DS (2011) Hindlimb immobilization in a wheelchair alters functional recovery following contusive spinal cord injury in the adult rat. Neurorehabilitation and neural repair 25:729-739.

Chadborn NH, Ahmed AI, Holt MR, Prinjha R, Dunn GA, Jones GE, Eickholt BJ (2006) PTEN couples Sema3A signalling to growth cone collapse. Journal of cell science 119:951-957.

Chen MS, Huber AB, van der Haar ME, Frank M, Schnell L, Spillmann AA, Christ F, Schwab ME (2000) Nogo-A is a myelin-associated neurite outgrowth inhibitor and an antigen for monoclonal antibody IN-1. Nature 403:434-439.

Chow LM, Baker SJ (2006) PTEN function in normal and neoplastic growth. Cancer letters 241:184-196.

Christie KJ, Webber CA, Martinez JA, Singh B, Zochodne DW (2010) PTEN inhibition to facilitate intrinsic regenerative outgrowth of adult peripheral axons. The Journal of Neuroscience 30:9306-9315.

Chung K, Wallace J, Kim S-Y, Kalyanasundaram S, Andalman AS, Davidson TJ, Mirzabekov JJ, Zalocusky KA, Mattis J, Denisin AK (2013) Structural and molecular interrogation of intact biological systems. Nature 497:332-337.

Courtine G, Roy RR, Raven J, Hodgson J, Mckay H, Yang H, Zhong H, Tuszynski MH, Edgerton VR (2005) Performance of locomotion and foot grasping following a unilateral thoracic corticospinal tract lesion in monkeys (Macaca mulatta). Brain 128:2338-2358.

Courtine G, Song B, Roy RR, Zhong H, Herrmann JE, Ao Y, Qi J, Edgerton VR, Sofroniew MV (2008) Recovery of supraspinal control of stepping via indirect propriospinal relay connections after spinal cord injury. Nature medicine 14:69-74.

Courtine G, Bunge MB, Fawcett JW, Grossman RG, Kaas JH, Lemon R, Maier I, Martin J, Nudo RJ, Ramon-Cueto A (2007) Can experiments in nonhuman primates expedite the translation of treatments for spinal cord injury in humans? Nature medicine 13:561-566.

Cregg JM, DePaul MA, Filous AR, Lang BT, Tran A, Silver J (2014) Functional regeneration beyond the glial scar. Experimental neurology 253:197-207.

Cross DA, Alessi DR, Cohen P, Andjelkovich M, Hemmings BA (1995) Inhibition of glycogen synthase kinase-3 by insulin mediated by protein kinase B. Nature 378:785-789.

Cummings BJ, Engesser-Cesar C, Cadena G, Anderson AJ (2007) Adaptation of a ladder beam walking task to assess locomotor recovery in mice following spinal cord injury. Behavioural brain research 177:232-241.

Curt A, Van Hedel HJ, Klaus D, Dietz V (2008) Recovery from a spinal cord injury: significance of compensation, neural plasticity, and repair. Journal of neurotrauma 25:677-685.

Danilov CA, Steward O (2015) Conditional genetic deletion of PTEN after a spinal cord injury enhances regenerative growth of CST axons and motor function recovery in mice. Experimental neurology 266:147-160.

David S, Aguayo AJ (1981) Axonal elongation into peripheral nervous system" bridges" after central nervous system injury in adult rats. Science 214:931-933.

Davies SJ, Goucher DR, Doller C, Silver J (1999) Robust regeneration of adult sensory axons in degenerating white matter of the adult rat spinal cord. The Journal of neuroscience 19:5810-5822.

Davies SJ, Fitch MT, Memberg SP, Hall AK, Raisman G, Silver J (1997) Regeneration of adult axons in white matter tracts of the central nervous system. Nature 390:680-683.

De Ryck M, Van Reempts J, Duytschaever H, Van Deuren B, Clincke G (1992) Neocortical localization of tactile/proprioceptive limb placing reactions in the rat. Brain research 573:44-60.

Deisseroth K (2011) Optogenetics. Nature methods 8:26-29.

DeVivo MJ, Chen Y (2011) Trends in new injuries, prevalent cases, and aging with spinal cord injury. Arch Phys Med Rehabil 92:332-338.

Dickendesher TL, Baldwin KT, Mironova YA, Koriyama Y, Raiker SJ, Askew KL, Wood A, Geoffroy CG, Zheng B, Liepmann CD (2012) NgR1 and NgR3 are receptors for chondroitin sulfate proteoglycans. Nature neuroscience 15:703-712.

Dum RP, Strick PL (1991) The origin of corticospinal projections from the premotor areas in the frontal lobe. The Journal of neuroscience 11:667-689.

Dupraz S, Grassi D, Bernis ME, Sosa L, Bisbal M, Gastaldi L, Jausoro I, Caceres A, Pfenninger KH, Quiroga S (2009) The TC10-Exo70 complex is essential for membrane expansion and axonal specification in developing neurons. J Neurosci 29:13292-13301.

Engesser-Cesar C, Anderson AJ, Basso DM, Edgerton V, Cotman CW (2005) Voluntary wheel running improves recovery from a moderate spinal cord injury. Journal of neurotrauma 22:157-171.

Ertürk A, Mauch CP, Hellal F, Förstner F, Keck T, Becker K, Jährling N, Steffens H, Richter M, Hübener M (2012) Three-dimensional imaging of the unsectioned adult spinal cord to assess axon regeneration and glial responses after injury. Nature medicine 18:166-171.

Esposito MS, Capelli P, Arber S (2014) Brainstem nucleus MdV mediates skilled forelimb motor tasks. Nature 508:351-356.

Faulkner JR, Herrmann JE, Woo MJ, Tansey KE, Doan NB, Sofroniew MV (2004) Reactive astrocytes protect tissue and preserve function after spinal cord injury. The Journal of Neuroscience 24:2143-2155.

Fenn AM, Hall JC, Gensel JC, Popovich PG, Godbout JP (2014) IL-4 signaling drives a unique arginase+/IL-1β+ microglia phenotype and recruits macrophages to the inflammatory CNS: consequences of age-related deficits in IL-4Rα after traumatic spinal cord injury. The Journal of neuroscience 34:8904-8917.

Fernandes KJ, Fan DP, Tsui B, Cassar S, Tetzlaff W (1999) Influence of the axotomy to cell body distance in rat rubrospinal and spinal motoneurons: Differential regulation of GAP-43, tubulins, and neurofilament-M. Journal of Comparative Neurology 414:495-510.

Fetz EE (1968) Pyramidal tract effects on interneurons in the cat lumbar dorsal horn. Journal of neurophysiology 31:69-80.

Filli L, Zörner B, Weinmann O, Schwab ME (2011) Motor deficits and recovery in rats with unilateral spinal cord hemisection mimic the Brown-Sequard syndrome. Brain:awr167.

Filli L, Engmann AK, Zörner B, Weinmann O, Moraitis T, Gullo M, Kasper H, Schneider R, Schwab ME (2014) Bridging the gap: a reticulo-propriospinal detour bypassing an incomplete spinal cord injury. The Journal of Neuroscience 34:13399-13410.

Fink KL, Cafferty WB (2016a) Reorganization of intact descending motor circuits to replace lost connections after injury. Neurotherapeutics 13:370-381.

Fink KL, Cafferty WB (2016b) Reorganization of intact descending motor circuits to replace lost connections after injury. Neurotherapeutics:1-12.

Fink KL, Strittmatter SM, Cafferty WB (2015) Comprehensive Corticospinal Labeling with mu-crystallin Transgene Reveals Axon Regeneration after Spinal Cord Trauma in ngr1−/− Mice. The Journal of Neuroscience 35:15403-15418.

Fouad K, Pedersen V, Schwab ME, Brösamle C (2001) Cervical sprouting of corticospinal fibers after thoracic spinal cord injury accompanies shifts in evoked motor responses. Curr Biol 11:1766-1770.

Fournier AE, GrandPre T, Strittmatter SM (2001) Identification of a receptor mediating Nogo-66 inhibition of axonal regeneration. Nature 409:341-346.

Friedli L, Rosenzweig ES, Barraud Q, Schubert M, Dominici N, Awai L, Nielson JL, Musienko P, Nout-Lomas Y, Zhong H (2015) Pronounced species divergence in corticospinal tract reorganization and functional recovery after lateralized spinal cord injury favors primates. Sci Transl Med 7:302ra134-302ra134.

Galea MP, Darian-Smith I (1994) Multiple corticospinal neuron populations in the macaque monkey are specified by their unique cortical origins, spinal terminations, and connections. Cerebral Cortex 4:166-194.

Gao Y, Deng K, Hou J, Bryson JB, Barco A, Nikulina E, Spencer T, Mellado W, Kandel ER, Filbin MT (2004) Activated CREB is sufficient to overcome inhibitors in myelin and promote spinal axon regeneration in vivo. Neuron 44:609-621.

Gaub P, Tedeschi A, Puttagunta R, Nguyen T, Schmandke A, Di Giovanni S (2010) HDAC inhibition promotes neuronal outgrowth and counteracts growth cone collapse through CBP/p300 and P/CAF-dependent p53 acetylation. Cell Death & Differentiation 17:1392-1408.

Gaub P, Joshi Y, Wuttke A, Naumann U, Schnichels S, Heiduschka P, Di Giovanni S (2011) The histone acetyltransferase p300 promotes intrinsic axonal regeneration. Brain 134:2134-2148.

Geller HM, Fawcett JW (2002) Building a bridge: engineering spinal cord repair. Experimental neurology 174:125-136.

Gensel JC, Tovar CA, Hamers FP, Deibert RJ, Beattie MS, Bresnahan JC (2006) Behavioral and histological characterization of unilateral cervical spinal cord contusion injury in rats. Journal of neurotrauma 23:36-54.

Gensel JC, Wang Y, Guan Z, Beckwith KA, Braun KJ, Wei P, McTigue DM, Popovich PG (2015) Toll-like receptors and dectin-1, a C-type lectin receptor, trigger divergent functions in CNS macrophages. The Journal of Neuroscience 35:9966-9976.

Geoffroy CG, Zheng B (2014) Myelin-associated inhibitors in axonal growth after CNS injury. Current opinion in neurobiology 27:31-38.

Geoffroy CG, Hilton BJ, Tetzlaff W, Zheng B (2016) Evidence for an Age-Dependent Decline in Axon Regeneration in the Adult Mammalian Central Nervous System. Cell Reports.

Ghosh A, Sydekum E, Haiss F, Peduzzi S, Zörner B, Schneider R, Baltes C, Rudin M, Weber B, Schwab ME (2009) Functional and anatomical reorganization of the sensory-motor cortex after incomplete spinal cord injury in adult rats. The Journal of Neuroscience 29:12210-12219.

Ghosh A, Haiss F, Sydekum E, Schneider R, Gullo M, Wyss MT, Mueggler T, Baltes C, Rudin M, Weber B (2010) Rewiring of hindlimb corticospinal neurons after spinal cord injury. Nat Neurosci 13:97-104.

Gomis-Rüth S, Stiess M, Wierenga CJ, Meyn L, Bradke F (2014) Single-cell axotomy of cultured hippocampal neurons integrated in neuronal circuits. Nature protocols 9:1028-1037.

Göritz C, Dias DO, Tomilin N, Barbacid M, Shupliakov O, Frisén J (2011) A pericyte origin of spinal cord scar tissue. Science 333:238-242.

GrandPré T, Nakamura F, Vartanian T, Strittmatter SM (2000) Identification of the Nogo inhibitor of axon regeneration as a Reticulon protein. Nature 403:439-444.

Guertin DA, Sabatini DM (2007) Defining the role of mTOR in cancer. Cancer Cell 12:9-22.

Hamers FP, Koopmans GC, Joosten EA (2006) CatWalk-assisted gait analysis in the assessment of spinal cord injury. Journal of neurotrauma 23:537-548.

Harrison TC, Ayling OG, Murphy TH (2012) Distinct cortical circuit mechanisms for complex forelimb movement and motor map topography. Neuron 74:397-409.

Harrison TC, Silasi G, Boyd JD, Murphy TH (2013) Displacement of sensory maps and disorganization of motor cortex after targeted stroke in mice. Stroke 44:2300-2306.

He Z, Jin Y (2016) Intrinsic Control of Axon Regeneration. Neuron 90:437-451.

Heffner R, Masterton B (1975) Variation in Form of the Pyramidal Tract and Its Relationship to Digital Dexterity; pp. 188–200. Brain, behavior and evolution 12:188-200.

Heffner RS, Masterton RB (1983) The role of the corticospinal tract in the evolution of human digital dexterity. Brain, behavior and evolution 23:165-183.

Hilton BJ, Lang BT, Cregg JM (2012) Keratan sulfate proteoglycans in plasticity and recovery after spinal cord injury. The Journal of Neuroscience 32:4331-4333.

Hilton BJ, Assinck P, Duncan GJ, Lu D, Lo S, Tetzlaff W (2013) Dorsolateral funiculus lesioning of the mouse cervical spinal cord at C4 but not at C6 results in sustained forelimb motor deficits. J Neurotrauma 30:1070-1083.

Hilton BJ, Anenberg E, Harrison TC, Boyd JD, Murphy TH, Tetzlaff W (2016) Re-Establishment of Cortical Motor Output Maps and Spontaneous Functional Recovery via Spared Dorsolaterally Projecting Corticospinal Neurons after Dorsal Column Spinal Cord Injury in Adult Mice. The Journal of Neuroscience 36:4080-4092.

Hollis II ER, Ishiko N, Yu T, Lu C-C, Haimovich A, Tolentino K, Richman A, Tury A, Wang S-H, Pessian M (2016) Ryk controls remapping of motor cortex during functional recovery after spinal cord injury. Nature neuroscience.

Horn KP, Busch SA, Hawthorne AL, Van Rooijen N, Silver J (2008) Another barrier to regeneration in the CNS: activated macrophages induce extensive retraction of dystrophic axons through direct physical interactions. The Journal of Neuroscience 28:9330-9341.

Imagama S, Sakamoto K, Tauchi R, Shinjo R, Ohgomori T, Ito Z, Zhang H, Nishida Y, Asami N, Takeshita S (2011) Keratan sulfate restricts neural plasticity after spinal cord injury. The Journal of Neuroscience 31:17091-17102.

Jackson AB, Dijkers M, DeVivo MJ, Poczatek RB (2004) A demographic profile of new traumatic spinal cord injuries: change and stability over 30 years. Archives of physical medicine and rehabilitation 85:1740-1748.

Jaerve A, Kruse F, Malik K, Hartung HP, Muller HW (2012) Age-dependent modulation of cortical transcriptomes in spinal cord injury and repair. PLoS One 7:e49812.

Jankowska E (2001) Spinal interneuronal systems: identification, multifunctional character and reconfigurations in mammals. The Journal of physiology 533:31-40.

Jara JH, Genç B, Klessner JL, Özdinler PH (2014) Retrograde labeling, transduction, and genetic targeting allow cellular analysis of corticospinal motor neurons: implications in health and disease. Front Neuroanat 8.

Jara JH, Villa SR, Khan NA, Bohn MC, Özdinler PH (2012) AAV2 mediated retrograde transduction of corticospinal motor neurons reveals initial and selective apical dendrite degeneration in ALS. Neurobiol Dis 47:174-183.

Jiang J, Azim E, Ekerot CF, Alstermark B (2015) Direct and indirect spino-cerebellar pathways: shared ideas but different functions in motor control. Front Comput Neurosci 9:75.

Jones LL, Tuszynski MH (2002) Spinal cord injury elicits expression of keratan sulfate proteoglycans by macrophages, reactive microglia, and oligodendrocyte progenitors. The Journal of neuroscience 22:4611-4624.

Jones LL, Margolis RU, Tuszynski MH (2003a) The chondroitin sulfate proteoglycans neurocan, brevican, phosphacan, and versican are differentially regulated following spinal cord injury. Experimental neurology 182:399-411.

Jones LL, Margolis RU, Tuszynski MH (2003b) The chondroitin sulfate proteoglycans neurocan, brevican, phosphacan, and versican are differentially regulated following spinal cord injury. Exp Neurol 182:399-411.

Jones LL, Yamaguchi Y, Stallcup WB, Tuszynski MH (2002) NG2 is a major chondroitin sulfate proteoglycan produced after spinal cord injury and is expressed by macrophages and oligodendrocyte progenitors. The Journal of neuroscience 22:2792-2803.

Kakulas AB (1999) A review of the neuropathology of human spinal cord injury with emphasis on special features. The journal of spinal cord medicine 22:119-124.

Kanagal SG, Muir GD (2009) Task-dependent compensation after pyramidal tract and dorsolateral spinal lesions in rats. Experimental neurology 216:193-206.

Kandel ER, Schwartz JH, Jessell TM, Siegelbaum SA, Hudspeth A (2000) Principles of neural science: McGraw-hill New York.

Keough MB, Rogers JA, Zhang P, Jensen SK, Stephenson EL, Chen T, Hurlbert MG, Lau LW, Rawji KS, Plemel JR (2016) An inhibitor of chondroitin sulfate proteoglycan synthesis promotes central nervous system remyelination. Nature communications 7.

Kiehn O (2011) Development and functional organization of spinal locomotor circuits. Current opinion in neurobiology 21:100-109.

Kim J-E, Liu BP, Park JH, Strittmatter SM (2004) Nogo-66 receptor prevents raphespinal and rubrospinal axon regeneration and limits functional recovery from spinal cord injury. Neuron 44:439-451.

Kim J-E, Li S, GrandPré T, Qiu D, Strittmatter SM (2003) Axon regeneration in young adult mice lacking Nogo-A/B. Neuron 38:187-199.

Klaw MC, Xu C, Tom VJ (2013) Intraspinal AAV injections immediately rostral to a thoracic spinal cord injury site efficiently transduces neurons in spinal cord and brain. Molecular Therapy—Nucleic Acids 2:e108.

Kobayashi NR, Fan DP, Giehl KM, Bedard AM, Wiegand SJ, Tetzlaff W (1997a) BDNF and NT-4/5 prevent atrophy of rat rubrospinal neurons after cervical axotomy, stimulate GAP-43 and Talpha1-tubulin mRNA expression, and promote axonal regeneration. J Neurosci 17:9583-9595.

Kobayashi NR, Fan D-P, Giehl KM, Bedard AM, Wiegand SJ, Tetzlaff W (1997b) BDNF and NT-4/5 prevent atrophy of rat rubrospinal neurons after cervical axotomy, stimulate GAP-43 and Tα1-tubulin mRNA expression, and promote axonal regeneration. The Journal of neuroscience 17:9583-9595.

Krajacic A, Weishaupt N, Girgis J, Tetzlaff W, Fouad K (2010) Training-induced plasticity in rats with cervical spinal cord injury: effects and side effects. Behav Brain Res 214:323-331.

Küchler M, Fouad K, Weinmann O, Schwab ME, Raineteau O (2002) Red nucleus projections to distinct motor neuron pools in the rat spinal cord. Journal of Comparative Neurology 448:349-359.

Kullberg S, Ramirez-Leon V, Johnson H, Ulfhake B (1998) Decreased axosomatic input to motoneurons and astrogliosis in the spinal cord of aged rats. J Gerontol A Biol Sci Med Sci 53:B369-379.

Kwon BK, Oxland TR, Tetzlaff W (2002a) Animal models used in spinal cord regeneration research. Spine 27:1504-1510.

Kwon BK, Liu J, Messerer C, Kobayashi NR, McGraw J, Oschipok L, Tetzlaff W (2002b) Survival and regeneration of rubrospinal neurons 1 year after spinal cord injury. Proc Natl Acad Sci U S A 99:3246-3251.

Lang BT, Cregg JM, DePaul MA, Tran AP, Xu K, Dyck SM, Madalena KM, Brown BP, Weng Y-L, Li S (2015) Modulation of the proteoglycan receptor PTP [sgr] promotes recovery after spinal cord injury. Nature 518:404-408.

Laskowski CJ, Bradke F (2013) In vivo imaging: A dynamic imaging approach to study spinal cord regeneration. Experimental neurology 242:11-17.

Lawrence DG, Kuypers HG (1968) The functional organization of the motor system in the monkey. Brain 91:15-36.

Lee D-H, Luo X, Yungher BJ, Bray E, Lee JK, Park KK (2014) Mammalian target of rapamycin's distinct roles and effectiveness in promoting compensatory axonal sprouting in the injured CNS. The Journal of Neuroscience 34:15347-15355.

Lee JK, Geoffroy CG, Chan AF, Tolentino KE, Crawford MJ, Leal MA, Kang B, Zheng B (2010) Assessing spinal axon regeneration and sprouting in Nogo-, MAG-, and OMgp-deficient mice. Neuron 66:663-670.

Lemon RN (2008) Descending pathways in motor control. Annu Rev Neurosci 31:195-218.

Lemon RN, Griffiths J (2005) Comparing the function of the corticospinal system in different species: organizational differences for motor specialization? Muscle & nerve 32:261-279.

Lemon RN, Landau W, Tutssel D, Lawrence D (2012) Lawrence and Kuypers (1968a, b) revisited: copies of the original filmed material from their classic papers in Brain. Brain:aws037.

Lesche R, Groszer M, Gao J, Wang Y, Messing A, Sun H, Liu X, Wu H (2002) Cre/loxP-mediated inactivation of the murine Pten tumor suppressor gene. Genesis 32:148-149.

Lewandowski G, Steward O (2014) AAVshRNA-mediated suppression of PTEN in adult rats in combination with salmon fibrin administration enables regenerative growth of corticospinal axons and enhances recovery of voluntary motor function after cervical spinal cord injury. The Journal of Neuroscience 34:9951-9962.

Li S, Carmichael ST (2006) Growth-associated gene and protein expression in the region of axonal sprouting in the aged brain after stroke. Neurobiol Dis 23:362-373.

Li S, Overman JJ, Katsman D, Kozlov SV, Donnelly CJ, Twiss JL, Giger RJ, Coppola G, Geschwind DH, Carmichael ST (2010) An age-related sprouting transcriptome provides molecular control of axonal sprouting after stroke. Nat Neurosci 13:1496-1504.

Liang H, Paxinos G, Watson C (2012) The red nucleus and the rubrospinal projection in the mouse. Brain Structure and Function 217:221-232.

Lim DH, LeDue J, Mohajerani MH, Vanni MP, Murphy TH (2013) Optogenetic approaches for functional mouse brain mapping. Frontiers in neuroscience 7:54.

Lindner R, Puttagunta R, Di Giovanni S (2013) Epigenetic regulation of axon outgrowth and regeneration in CNS injury: the first steps forward. Neurotherapeutics 10:771-781.

Liu C-N, Chambers WW (1964) An Experimental study of the cortico-spinal system in the monkey (Macaca mulatta). The spinal pathways and preterminal distribution of degenerating fibers following discrete lesions of the pre-and postcentral gyri and bulbar pyramid. Journal of comparative neurology 123:257-283.

Liu K, Tedeschi A, Park KK, He Z (2011) Neuronal intrinsic mechanisms of axon regeneration. Annual review of neuroscience 34:131-152.

Liu K, Lu Y, Lee JK, Samara R, Willenberg R, Sears-Kraxberger I, Tedeschi A, Park KK, Jin D, Cai B, Xu B, Connolly L, Steward O, Zheng B, He Z (2010) PTEN deletion enhances the regenerative ability of adult corticospinal neurons. Nat Neurosci 13:1075-1081.

Liu Y, Kim D, Himes BT, Chow SY, Schallert T, Murray M, Tessler A, Fischer I (1999) Transplants of fibroblasts genetically modified to express BDNF promote regeneration of adult rat rubrospinal axons and recovery of forelimb function. The Journal of Neuroscience 19:4370-4387.

Lorenzana AO, Lee JK, Mui M, Chang A, Zheng B (2015) A surviving intact branch stabilizes remaining axon architecture after injury as revealed by in vivo imaging in the mouse spinal cord. Neuron 86:947-954.

Lu Y, Belin S, He Z (2014) Signaling regulations of neuronal regenerative ability. Curr Opin Neurobiol 27:135-142.

Ma XM, Blenis J (2009) Molecular mechanisms of mTOR-mediated translational control. Nat Rev Mol Cell Biol 10:307-318.

Maier IC, Baumann K, Thallmair M, Weinmann O, Scholl J, Schwab ME (2008) Constraint-induced movement therapy in the adult rat after unilateral corticospinal tract injury. The Journal of Neuroscience 28:9386-9403.

Massion J (1967) The mammalian red nucleus. Physiological Reviews 47:383-436.

McGee AW, Yang Y, Fischer QS, Daw NW, Strittmatter SM (2005) Experience-driven plasticity of visual cortex limited by myelin and Nogo receptor. Science 309:2222-2226.

McKenna JE, Prusky GT, Whishaw IQ (2000) Cervical motoneuron topography reflects the proximodistal organization of muscles and movements of the rat forelimb: a retrograde carbocyanine dye analysis. Journal of Comparative Neurology 419:286-296.

McKerracher Ld, David S, Jackson D, Kottis V, Dunn R, Braun P (1994) Identification of myelin-associated glycoprotein as a major myelin-derived inhibitor of neurite growth. Neuron 13:805-811.

McPhail LT, McBride CB, McGraw J, Steeves JD, Tetzlaff W (2004) Axotomy abolishes NeuN expression in facial but not rubrospinal neurons. Experimental neurology 185:182-190.

Meletis K, Barnabé-Heider F, Carlén M, Evergren E, Tomilin N, Shupliakov O, Frisén J (2008) Spinal cord injury reveals multilineage differentiation of ependymal cells. PLoS Biol 6:e182.

Menet V, Prieto M, Privat A, y Ribotta MG (2003) Axonal plasticity and functional recovery after spinal cord injury in mice deficient in both glial fibrillary acidic protein and vimentin genes. Proceedings of the National Academy of Sciences 100:8999-9004.

Millan MJ (2002) Descending control of pain. Progress in Neurobiology 66:355-474.

Miron VE, Boyd A, Zhao JW, Yuen TJ, Ruckh JM, Shadrach JL, van Wijngaarden P, Wagers AJ, Williams A, Franklin RJ, ffrench-Constant C (2013) M2 microglia and macrophages drive oligodendrocyte differentiation during CNS remyelination. Nat Neurosci 16:1211-1218.

Montoya C, Astell S, Dunnett S (1989) Effects of nigral and striatal grafts on skilled forelimb use in the rat. Progress in brain research 82:459-466.

Montoya C, Campbell-Hope L, Pemberton K, Dunnett S (1991) The "staircase test": a measure of independent forelimb reaching and grasping abilities in rats. Journal of neuroscience methods 36:219-228.

Moore DL, Blackmore MG, Hu Y, Kaestner KH, Bixby JL, Lemmon VP, Goldberg JL (2009) KLF family members regulate intrinsic axon regeneration ability. Science 326:298-301.

Morris R, Tosolini AP, Goldstein JD, Whishaw IQ (2011) Impaired arpeggio movement in skilled reaching by rubrospinal tract lesions in the rat: a behavioral/anatomical fractionation. Journal of neurotrauma 28:2439-2451.

Muir GD, Whishaw IQ (2000) Red nucleus lesions impair overground locomotion in rats: a kinetic analysis. European Journal of Neuroscience 12:1113-1122.

Murray H, Gurule M (1979) Origin of the rubrospinal tract of the rat. Neuroscience letters 14:19-23.

Murray KC, Nakae A, Stephens MJ, Rank M, D'Amico J, Harvey PJ, Li X, Harris RLW, Ballou EW, Anelli R (2010) Recovery of motoneuron and locomotor function after spinal cord injury depends on constitutive activity in 5-HT2C receptors. Nature medicine 16:694-700.

Nagel G, Brauner M, Liewald JF, Adeishvili N, Bamberg E, Gottschalk A (2005) Light activation of channelrhodopsin-2 in excitable cells of Caenorhabditis elegans triggers rapid behavioral responses. Current Biology 15:2279-2284.

Napieralski J, Banks R, Chesselet M (1998) Motor and somatosensory deficits following uni- and bilateral lesions of the cortex induced by aspiration or thermocoagulation in the adult rat. Experimental neurology 154:80-88.

Nathan P, SMITH MC (1955) Long descending tracts in man. Brain 78:248-303.

Nathan P, Smith MC (1982) The rubrospinal and central tegmental tracts in man. Brain: a journal of neurology 105:223-269.

Neumann S, Woolf CJ (1999) Regeneration of dorsal column fibers into and beyond the lesion site following adult spinal cord injury. Neuron 23:83-91.

Nishimura Y, Isa T (2009) Compensatory changes at the cerebral cortical level after spinal cord injury. The Neuroscientist 15:436-444.

Nishimura Y, Isa T (2012) Cortical and subcortical compensatory mechanisms after spinal cord injury in monkeys. Exp Neurol 235:152-161.

Norenberg MD, Smith J, Marcillo A (2004) The pathology of human spinal cord injury: defining the problems. Journal of neurotrauma 21:429-440.

Nudo RJ (2006) Mechanisms for recovery of motor function following cortical damage. Curr Opin Neurobiol 16:638-644.

Numakawa T, Suzuki S, Kumamaru E, Adachi N, Richards M, Kunugi H (2010) BDNF function and intracellular signaling in neurons. Histol Histopathol 25:237-258.

O'Callaghan JP, Miller DB (1991) The concentration of glial fibrillary acidic protein increases with age in the mouse and rat brain. Neurobiol Aging 12:171-174.

Onodera S, Hicks TP (2010) Carbocyanine dye usage in demarcating boundaries of the aged human red nucleus. PloS one 5:e14430.

Oudega M, Perez MA (2012) Corticospinal reorganization after spinal cord injury. The Journal of physiology 590:3647-3663.

Park HG, Carmel JB (2016) Selective manipulation of neural circuits. Neurotherapeutics 13:311-324.

Park JB, Yiu G, Kaneko S, Wang J, Chang J, He Z (2005) A TNF receptor family member, TROY, is a coreceptor with Nogo receptor in mediating the inhibitory activity of myelin inhibitors. Neuron 45:345-351.

Park KK, Liu K, Hu Y, Kanter JL, He Z (2010) PTEN/mTOR and axon regeneration. Experimental neurology 223:45-50.

Park KK, Liu K, Hu Y, Smith PD, Wang C, Cai B, Xu B, Connolly L, Kramvis I, Sahin M, He Z (2008) Promoting axon regeneration in the adult CNS by modulation of the PTEN/mTOR pathway. Science 322:963-966.

Planchon SM, Waite KA, Eng C (2008) The nuclear affairs of PTEN. Journal of cell science 121:249-253.

Plunet W, Kwon BK, Tetzlaff W (2002) Promoting axonal regeneration in the central nervous system by enhancing the cell body response to axotomy. Journal of neuroscience research 68:1-6.

Pompolo S, Harley VR (2001) Localisation of the SRY-related HMG box protein, SOX9, in rodent brain. Brain Res 906:143-148.

Popovich P, Guan Z, McGaughy V, Fisher L, Hickey W, Basso D (2002) The neuropathological and behavioral consequences of intraspinal microglial/macrophage activation. Journal of Neuropathology & Experimental Neurology 61:623-633.

Popovich PG, Wei P, Stokes BT (1997) Cellular inflammatory response after spinal cord injury in sprague-dawley and lewis rats. Journal of Comparative Neurology 377:443-464.

Prinjha R, Moore SE, Vinson M, Blake S, Morrow R, Christie G, Michalovich D, Simmons DL, Walsh FS (2000) Neurobiology: Inhibitor of neurite outgrowth in humans. Nature 403:383-384.

Raineteau O, Schwab ME (2001) Plasticity of motor systems after incomplete spinal cord injury. Nature Reviews Neuroscience 2:263-273.

Raineteau O, Fouad K, Noth P, Thallmair M, Schwab ME (2001) Functional switch between motor tracts in the presence of the mAb IN-1 in the adult rat. Proceedings of the National Academy of Sciences 98:6929-6934.

Ralston DD, Ralston HJ (1985) The terminations of corticospinal tract axons in the macaque monkey. Journal of Comparative Neurology 242:325-337.

Ramer LM, Ramer MS, Bradbury EJ (2014) Restoring function after spinal cord injury: towards clinical translation of experimental strategies. The Lancet Neurology 13:1241-1256.

Ramer LM, Au E, Richter MW, Liu J, Tetzlaff W, Roskams AJ (2004) Peripheral olfactory ensheathing cells reduce scar and cavity formation and promote regeneration after spinal cord injury. Journal of Comparative Neurology 473:1-15.

Ranvier L (1889) Traité technique d'histologie: A. Lahure.

Rasmussen R, Carlsen EM (2016) Spontaneous Functional Recovery from Incomplete Spinal Cord Injury. The Journal of Neuroscience 36:8535-8537.

Ribotta M, Menet V, Privat A (2004) Glial scar and axonal regeneration in the CNS: lessons from GFAP and vimentin transgenic mice. In: Mechanisms of Secondary Brain Damage from Trauma and Ischemia, pp 87-92: Springer.

Richardson P, Issa V (1984) Peripheral injury enhances central regeneration of primary sensory neurones.

Richardson P, McGuinness U, Aguayo A (1980) Axons from CNS neurones regenerate into PNS grafts.

Richardson P, Issa V, Aguayo A (1984) Regeneration of long spinal axons in the rat. Journal of neurocytology 13:165-182.

Rishal I, Fainzilber M (2010) Retrograde signaling in axonal regeneration. Experimental neurology 223:5-10.

Rizzolatti G, Luppino G, Matelli M (1998) The organization of the cortical motor system: new concepts. Electroencephalography and clinical neurophysiology 106:283-296.

Rogan SC, Roth BL (2011) Remote control of neuronal signaling. Pharmacol Rev 63:291-315.

Rosenzweig ES, Brock JH, Culbertson MD, Lu P, Moseanko R, Edgerton VR, Havton LA, Tuszynski MH (2009) Extensive spinal decussation and bilateral termination of cervical corticospinal projections in rhesus monkeys. Journal of Comparative Neurology 513:151-163.

Rosenzweig ES, Courtine G, Jindrich DL, Brock JH, Ferguson AR, Strand SC, Nout YS, Roy RR, Miller DM, Beattie MS (2010) Extensive spontaneous plasticity of corticospinal projections after primate spinal cord injury. Nature neuroscience 13:1505-1510.

Rossignol S, Dubuc R, Gossard J-P (2006) Dynamic sensorimotor interactions in locomotion. Physiological reviews 86:89-154.

Roth BL (2016) DREADDs for neuroscientists. Neuron 89:683-694.

Roth E, Park T, Pang T, Yarkony G, Lee M (1991) Traumatic cervical Brown-Sequard and Brown-Sequard-plus syndromes: the spectrum of presentations and outcomes. Paraplegia 29:582-589.

Sabelström H, Stenudd M, Réu P, Dias DO, Elfineh M, Zdunek S, Damberg P, Göritz C, Frisén J (2013) Resident neural stem cells restrict tissue damage and neuronal loss after spinal cord injury in mice. Science 342:637-640.

Sandhir R, Onyszchuk G, Berman NE (2008) Exacerbated glial response in the aged mouse hippocampus following controlled cortical impact injury. Exp Neurol 213:372-380.

Schallert T, Fleming SM, Leasure JL, Tillerson JL, Bland ST (2000) CNS plasticity and assessment of forelimb sensorimotor outcome in unilateral rat models of stroke, cortical ablation, parkinsonism and spinal cord injury. Neuropharmacology 39:777-787.

Schnell L, Schwab ME (1990) Axonal regeneration in the rat spinal cord produced by an antibody against myelin-associated neurite growth inhibitors. Nature 343:269-272.

Schucht P, Raineteau O, Schwab M, Fouad K (2002) Anatomical correlates of locomotor recovery following dorsal and ventral lesions of the rat spinal cord. Experimental neurology 176:143-153.

Schwab ME (2010) Functions of Nogo proteins and their receptors in the nervous system. Nature Reviews Neuroscience 11:799-811.

Schwab ME, Caroni P (1988) Oligodendrocytes and CNS myelin are nonpermissive substrates for neurite growth and fibroblast spreading in vitro. The Journal of neuroscience 8:2381-2393.

Seira O, Del Río JA (2014) Glycogen synthase kinase 3 beta (GSK3β) at the tip of neuronal development and regeneration. Molecular neurobiology 49:931-944.

Sekhon LH, Fehlings MG (2001) Epidemiology, demographics, and pathophysiology of acute spinal cord injury. Spine 26:S2-S12.

Shen Y, Tenney AP, Busch SA, Horn KP, Cuascut FX, Liu K, He Z, Silver J, Flanagan JG (2009) PTPσ is a receptor for chondroitin sulfate proteoglycan, an inhibitor of neural regeneration. Science 326:592-596.

Sherrington C (1910) The integrative action of the nervous system: CUP Archive.

Sidman RL, Angevine JB, Pierce ET (1971) Atlas of the mouse brain and spinal cord.

Siegel CS, Fink KL, Strittmatter SM, Cafferty WB (2015) Plasticity of intact rubral projections mediates spontaneous recovery of function after corticospinal tract injury. The Journal of Neuroscience 35:1443-1457.

Silasi G, Boyd JD, LeDue J, Murphy T (2013a) Improved methods for chronic light-based motor mapping in mice: automated movement tracking with accelerometers, and chronic EEG recording in a bilateral thin-skull preparation. Frontiers in neural circuits 7:123.

Silasi G, Boyd JD, LeDue J, Murphy TH (2013b) Improved methods for chronic light-based motor mapping in mice: automated movement tracking with accelerometers, and chronic EEG recording in a bilateral thin-skull preparation. Frontiers in neural circuits 7.

Silasi G, Xiao D, Vanni MP, Chen AC, Murphy TH (2016) Intact skull chronic windows for mesoscopic wide-field imaging in awake mice. Journal of neuroscience methods 267:141-149.

Silver J (2010) Much ado about Nogo. Neuron 66:619-621.

Silver J (2016) The glial scar is more than just astrocytes. Experimental Neurology.

Silver J, Schwab ME, Popovich PG (2015) Central nervous system regenerative failure: role of oligodendrocytes, astrocytes, and microglia. Cold Spring Harb Perspect Biol 7:a020602.

Simonen M, Pedersen V, Weinmann O, Schnell L, Buss A, Ledermann B, Christ F, Sansig G, van der Putten H, Schwab ME (2003) Systemic deletion of the myelin-associated outgrowth inhibitor Nogo-A improves regenerative and plastic responses after spinal cord injury. Neuron 38:201-211.

Singh A, Tetreault L, Kalsi-Ryan S, Nouri A, Fehlings MG (2014a) Global prevalence and incidence of traumatic spinal cord injury. Clin Epidemiol 6:309-331.

Singh B, Singh V, Krishnan A, Koshy K, Martinez JA, Cheng C, Almquist C, Zochodne DW (2014b) Regeneration of diabetic axons is enhanced by selective knockdown of the PTEN gene. Brain 137:1051-1067.

Smith PD, Sun F, Park KK, Cai B, Wang C, Kuwako K, Martinez-Carrasco I, Connolly L, He Z (2009) SOCS3 deletion promotes optic nerve regeneration in vivo. Neuron 64:617-623.

Soblosky JS, Song J-H, Dinh DH (2001) Graded unilateral cervical spinal cord injury in the rat: evaluation of forelimb recovery and histological effects. Behavioural brain research 119:1-13.

Soderblom C, Luo X, Blumenthal E, Bray E, Lyapichev K, Ramos J, Krishnan V, Lai-Hsu C, Park KK, Tsoulfas P (2013) Perivascular fibroblasts form the fibrotic scar after contusive spinal cord injury. The Journal of Neuroscience 33:13882-13887.

Song Y, Ori-McKenney KM, Zheng Y, Han C, Jan LY, Jan YN (2012) Regeneration of Drosophila sensory neuron axons and dendrites is regulated by the Akt pathway involving Pten and microRNA bantam. Genes & development 26:1612-1625.

Stachniak TJ, Ghosh A, Sternson SM (2014) Chemogenetic synaptic silencing of neural circuits localizes a hypothalamus→ midbrain pathway for feeding behavior. Neuron 82:797-808.

Stackhouse SK, Murray M, Shumsky JS (2008) Effect of cervical dorsolateral funiculotomy on reach-to-grasp function in the rat. Journal of neurotrauma 25:1039-1047.

Starkey ML, Barritt AW, Yip PK, Davies M, Hamers FP, McMahon SB, Bradbury EJ (2005) Assessing behavioural function following a pyramidotomy lesion of the corticospinal tract in adult mice. Experimental neurology 195:524-539.

Steeves J, Kramer J, Fawcett J, Cragg J, Lammertse D, Blight A, Marino R, Ditunno J, Coleman W, Geisler F (2011) Extent of spontaneous motor recovery after traumatic cervical sensorimotor complete spinal cord injury. Spinal Cord 49:257-265.

Sternson SM, Roth BL (2014) Chemogenetic tools to interrogate brain functions. Annual review of neuroscience 37:387-407.

Steward O, Willenberg R (2016) Rodent spinal cord injury models for studies of axon regeneration. Experimental Neurology.

Steward O, Zheng B, Tessier-Lavigne M (2003) False resurrections: distinguishing regenerated from spared axons in the injured central nervous system. Journal of Comparative Neurology 459:1-8.

Steward O, Zheng B, Ho C, Anderson K, Tessier-Lavigne M (2004) The dorsolateral corticospinal tract in mice: an alternative route for corticospinal input to caudal segments following dorsal column lesions. Journal of Comparative Neurology 472:463-477.

Storer JB (1966) Longevity and gross pathology at death in 22 inbred mouse strains. Journal of gerontology 21:404-409.

Strominger RN, McGiffen JE, Strominger NL (1987) Morphometric and experimental studies of the red nucleus in the albino rat. The Anatomical record 219:420-428.

Takeoka A, Vollenweider I, Courtine G, Arber S (2014) Muscle spindle feedback directs locomotor recovery and circuit reorganization after spinal cord injury. Cell 159:1626-1639.

Takeoka A, Jindrich DL, Muñoz-Quiles C, Zhong H, van den Brand R, Pham DL, Ziegler MD, Ramón-Cueto A, Roy RR, Edgerton VR (2011) Axon regeneration can facilitate or suppress hindlimb function after olfactory ensheathing glia transplantation. The Journal of Neuroscience 31:4298-4310.

Tedeschi A (2012) Tuning the orchestra: transcriptional pathways controlling axon regeneration. Frontiers in molecular neuroscience 4:60.

Tedeschi A, Nguyen T, Puttagunta R, Gaub P, Di Giovanni S (2009) A p53-CBP/p300 transcription module is required for GAP-43 expression, axon outgrowth, and regeneration. Cell Death & Differentiation 16:543-554.

Tetzlaff W, Alexander SW, Miller FD, Bisby MA (1991) Response of facial and rubrospinal neurons to axotomy: changes in mRNA expression for cytoskeletal proteins and GAP-43. The Journal of neuroscience 11:2528-2544.

Tetzlaff W, Kobayashi N, Giehl K, Tsui B, Cassar Sa, Bedard A (1994) Response of rubrospinal and corticospinal neurons to injury and neurotrophins. Progress in brain research 103:271.

Tuszynski MH, Steward O (2012) Concepts and methods for the study of axonal regeneration in the CNS. Neuron 74:777-791.

Vardy E, Robinson JE, Li C, Olsen RH, DiBerto JF, Giguere PM, Sassano FM, Huang X-P, Zhu H, Urban DJ (2015) A new DREADD facilitates the multiplexed chemogenetic interrogation of behavior. Neuron 86:936-946.

Vavrek R, Girgis J, Tetzlaff W, Hiebert G, Fouad K (2006) BDNF promotes connections of corticospinal neurons onto spared descending interneurons in spinal cord injured rats. Brain 129:1534-1545.

Wahl A, Omlor W, Rubio J, Chen J, Zheng H, Schröter A, Gullo M, Weinmann O, Kobayashi K, Helmchen F (2014) Asynchronous therapy restores motor control by rewiring of the rat corticospinal tract after stroke. Science 344:1250-1255.

Wang KC, Kim JA, Sivasankaran R, Segal R, He Z (2002a) P75 interacts with the Nogo receptor as a co-receptor for Nogo, MAG and OMgp. Nature 420:74-78.

Wang KC, Koprivica V, Kim JA, Sivasankaran R, Guo Y, Neve RL, He Z (2002b) Oligodendrocyte-myelin glycoprotein is a Nogo receptor ligand that inhibits neurite outgrowth. Nature 417:941-944.

Wang Z, Reynolds A, Kirry A, Nienhaus C, Blackmore MG (2015) Overexpression of sox11 promotes corticospinal tract regeneration after spinal injury while interfering with functional recovery. The Journal of Neuroscience 35:3139-3145.

Wannier-Morino P, Schmidlin E, Freund P, Belhaj-Saif A, Bloch J, Mir A, Schwab ME, Rouiller EM, Wannier T (2008) Fate of rubrospinal neurons after unilateral section of the cervical spinal cord in adult macaque monkeys: effects of an antibody treatment neutralizing Nogo-A. Brain research 1217:96-109.

Webb AA, Muir GD (2003) Unilateral dorsal column and rubrospinal tract injuries affect overground locomotion in the unrestrained rat. European Journal of Neuroscience 18:412-422.

Weidner N, Ner A, Salimi N, Tuszynski MH (2001) Spontaneous corticospinal axonal plasticity and functional recovery after adult central nervous system injury. Proceedings of the National Academy of Sciences 98:3513-3518.

Wells JE, Biernaskie J, Szymanska A, Larsen PH, Yong VW, Corbett D (2005) Matrix metalloproteinase (MMP)-12 expression has a negative impact on sensorimotor

function following intracerebral haemorrhage in mice. European Journal of Neuroscience 21:187-196.

Westlund KN, Bowker RM, Ziegler MG, Coulter JD (1982) Descending Noradrenergic Projections and their Spinal Terminations. Progress in Brain Research 57:219-238.

Whishaw IQ, Gorny B (1996) Does the red nucleus provide the tonic support against which fractionated movements occur? A study on forepaw movements used in skilled reaching by the rat. Behavioural brain research 74:79-90.

Whishaw IQ, Gorny B, Sarna J (1998) Paw and limb use in skilled and spontaneous reaching after pyramidal tract, red nucleus and combined lesions in the rat: behavioral and anatomical dissociations. Behavioural brain research 93:167-183.

Whishaw IQ, Pellis SM, Gorny B, Kolb B, Tetzlaff W (1993) Proximal and distal impairments in rat forelimb use in reaching follow unilateral pyramidal tract lesions. Behavioural brain research 56:59-76.

Wild JM, Cabot JB, Cohen DH, Karten H (1979) Origin, course and terminations of the rubrospinal tract in the pigeon (Columba livia). Journal of Comparative Neurology 187:639-654.

Wilhelmsson U, Li L, Pekna M, Berthold C-H, Blom S, Eliasson C, Renner O, Bushong E, Ellisman M, Morgan TE (2004) Absence of glial fibrillary acidic protein and vimentin prevents hypertrophy of astrocytic processes and improves post-traumatic regeneration. The Journal of neuroscience 24:5016-5021.

Windhorst U (2007) Muscle proprioceptive feedback and spinal networks. Brain research bulletin 73:155-202.

Woolf CJ (2003) No Nogo: now where to go? Neuron 38:153-156.

Xie Y, Chen S, Anenberg E, Murphy TH (2013) Resistance of optogenetically evoked motor function to global ischemia and reperfusion in mouse in vivo. Journal of Cerebral Blood Flow & Metabolism 33:1148-1152.

y Cajal SR (1928) Degeneration & regeneration of the nervous system: Oxford University Press, Humphrey Milford.

Yamada KM, Araki M (2001) Tumor suppressor PTEN: modulator of cell signaling, growth, migration and apoptosis. Journal of cell science 114:2375-2382.

Yang H-Y, Lieska N, Shao D, Kriho V, Pappas GD (1994) Proteins of the intermediate filament cytoskeleton as markers for astrocytes and human astrocytomas. Molecular and chemical neuropathology 21:155-176.

Yang L, Miao L, Liang F, Huang H, Teng X, Li S, Nuriddinov J, Selzer ME, Hu Y (2014) The mTORC1 effectors S6K1 and 4E-BP play different roles in CNS axon regeneration. Nat Commun 5:5416.

Yiu G, He Z (2003) Signaling mechanisms of the myelin inhibitors of axon regeneration. Current opinion in neurobiology 13:545-551.

Yiu G, He Z (2006) Glial inhibition of CNS axon regeneration. Nature Reviews Neuroscience 7:617-627.

Yizhar O, Fenno LE, Davidson TJ, Mogri M, Deisseroth K (2011) Optogenetics in neural systems. Neuron 71:9-34.

Ylera B, Ertürk A, Hellal F, Nadrigny F, Hurtado A, Tahirovic S, Oudega M, Kirchhoff F, Bradke F (2009) Chronically CNS-injured adult sensory neurons gain regenerative competence upon a lesion of their peripheral axon. Current Biology 19:930-936.

Zhang B, Bailey WM, Braun KJ, Gensel JC (2015) Age decreases macrophage IL-10 expression: implications for functional recovery and tissue repair in spinal cord injury. Experimental neurology 273:83-91.

Zhang B, Bailey W, McVicar A, Gensel J (2016) Age increases reactive oxygen species production in macrophages and potentiates oxidative damage after spinal cord injury. Neurobiology of Aging.

Zhang Y, Chen K, Sloan SA, Bennett ML, Scholze AR, O'Keeffe S, Phatnani HP, Guarnieri P, Caneda C, Ruderisch N, Deng S, Liddelow SA, Zhang C, Daneman R, Maniatis T, Barres BA, Wu JQ (2014) An RNA-sequencing transcriptome and splicing database of glia, neurons, and vascular cells of the cerebral cortex. J Neurosci 34:11929-11947.

Zheng B, Ho C, Li S, Keirstead H, Steward O, Tessier-Lavigne M (2003) Lack of enhanced spinal regeneration in Nogo-deficient mice. Neuron 38:213-224.

Zheng B, Atwal J, Ho C, Case L, He X-l, Garcia KC, Steward O, Tessier-Lavigne M (2005) Genetic deletion of the Nogo receptor does not reduce neurite inhibition in vitro or promote corticospinal tract regeneration in vivo. Proceedings of the National Academy of Sciences of the United States of America 102:1205-1210.

Zhou FQ, Snider WD (2005) Cell biology. GSK-3beta and microtubule assembly in axons. Science 308:211-214.

Zukor K, Belin S, Wang C, Keelan N, Wang X, He Z (2013) Short hairpin RNA against PTEN enhances regenerative growth of corticospinal tract axons after spinal cord injury. The Journal of Neuroscience 33:15350-15361.